# NANOBIO-APPROACHES
# FOR THE DETECTION OF BACTERIA BY SERS


# SERS İLE BAKTERİ TANISINDA
# NANOBİYO-YAKLAŞIMLAR


**FARZANEH MOGHTADER**


**PROF. DR. ERHAN BİŞKİN**

**Supervisor**


Submitted to Graduate School of Science and Engineering
of Hacettepe University as a Partial Fulfillment to the
Requirements for the Award of the Degree of Doctor of
Philosophy in Nanotechnology and Nanomedicine


**2019**

This work entitled **"Nanobio-Approaches for the Detection of Bacteria by SERS"** by **FARZANEH MOGHTADER** has been approved as a thesis for the Degree of **Doctor of Philosophy** in **Nanotechnology and Nanomedicine** by the Examine Committee Members mentioned below.

Prof. Dr. Adil DENİZLİ
Head

......................................................

Prof. Dr. Erhan BİŞKİN
Supervisor

......................................................

Prof. Dr. F. Yeşim EKİNCİ-KADIPAŞAOĞLU
Member

......................................................

Prof. Dr. Mustafa TÜRK
Member

......................................................

Assoc. Prof. Dr. Nelisa LAÇİN-TÜRKOĞLU
Member

......................................................

This thesis has been approved as a thesis for the Degree of Doctor of Philosophy in Nanotechnology and Nanomedicine by the Board of Directors of the Institute for Graduate Studies in Science and Engineering on …. /…/….

Prof. Dr. Menemşe Gümüşderelioğlu
Director of Institute of
Graduate School of Science and Engineering

*Sevgili annem Akram, babam Gholamali, abim Farzad ve kardeşim Farshid, hep vardınız uzakta da olsa hep yanımda içimde ...  siz yanımda olmadan buraya kadar gelmem mümkün değildi ... hep var olun inşallah ... Maryam ailemize hoş geldin ...*

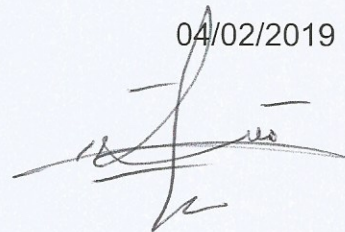*Tezimi size ithaf ediyorum ...*
*Lütfen kabul buyurun ...*

# ETHICS

In this thesis study, prepared in accordance with the spelling rules of Graduate School of Science and Engineering of Hacettepe University,

I declare that

- all the information and documents have been obtained in the base of the academic rules,

- all audio-visual and written information and results have been presented according to the rules of scientific ethics,

- in case of using others works, related studies have been cited in accordance with the scientific standards,

- all cited studies have been fully referenced,

- I did not do any distortion in the data set,

- and any part of this thesis has not been presented as another thesis as another thesis study at this or any other university.

04/02/2019

FARZANEH MOGHTADER

# YAYIMLAMA VE FİKRİ MÜLKİYET HAKLARI BEYANI

Enstitü tarafından onaylanan lisanüstü tezimin tamamını veya herhangi bir kısmını, basılı (kağıt) ve elektronik formatta arşivleme ve aşağıda verilen koşullarla kullanıma açna iznini Hacettepe Üniversitesi'ne verdiğimi bildiririm. Bu izinle Üniversiteye verilen kullanım hakları dışındaki tüm fikri mülkiyet haklarım bende kalacak, tezimin tamamının ya da bir bölümünün gelecekteki çalışmalarda (makale, kitap, lisans ve patent vb.) kullanım hakları bana ait olacaktır.

Tezin kendi original çalışmam olduğunu, başkalarının haklarını ihlal etmediğimi ve tezimin tek yetkili sahibi olduğumu beyan ve taahhüt ederim. Tezimde yer alan telif hakkı bulunan ve sahiplerinden yazılı izin alınarak kullanılması zorunlu metinleri yazılı izin alarak kullandığımı ve istenildiğinde suretlerini Üniversiteye teslim etmeyi taahhüt ederim.

Yükseköğretim Kurulu tarafından yayınlanan *"Lisansüstü Tezlerin Elektronik Ortamda Toplanması, Düzenlenmesi ve Erişime Açılmasına İlişkin Yönerge"* kapsamında tezim aşağıda belirtilen koşullar haricinde YÖK Ulusal Tez Merkezi / H. Ü. Kütüphaneleri Açık Erişim Sisteminde erişime açılır.

- ☐ Enstitü / Fakülte yönetim kurulu kararı ile tezimin erişime açılması Mezuniyet tarihimden itibaren ... yıl ertelenmiştir.

- ☐ Enstitü / Fakülte yönetim kurulu gerekçeli kararı ile tezimin erişime açılması mezuniyet tarihimden itibaren ... ay ertelenmiştir.

- ☐ Tezim ile ilgili gizlilik kararı verilmiştir.

04/02/2019

FARZANEH MOGHTADER

# ÖZET

## SERS İLE BAKTERİ TANISINDA
## NANOBİYO-YAKLAŞIMLAR

## Farzaneh MOGHTADER

**Doktora, Nanoteknoloji ve Nanotıp**
**Tez Danışmanı: Prof. Dr. Erhan BİŞKİN**
**Şubat 2019, 144 sayfa**

Besin ve su kaynaklı hastalıklar tüm dünyada çok ciddi ve maliyetli halk sağlığı sorunları arasındadır. Besin ve sularda patojenik bakteriyel kirliliğin izlenmesi/ erken tanısı global olarak en önemli öncelikli biridir. Bu doktora çalışmasının temel amacı patojenik bakterilerin tanısı/aydınlatılması için nanobiyo-esaslı protokolların geliştirilmesidir. *Escherichia coli (E.coli)* temel hedef bakteridir, ancak karşılaştırma yapmak üzere çalışmaya *Staphylococcus aureus* (*S.aureus*) and *Salmonella infantis* (*S.infantis*) de ilave edilmiştir. Bu bakteriler ve özgün bakteriyofajları Türkiye ve Gürcistan'daki (Eliava Institute, Tiflis) uzman enstitülerden/ laboratuvarlardan ve Amerikan Doku Kültür Kolleksiyonundan (ATCC) temin edilmiş, laboratuvarlarımızda çoğaltılmış, karakterize edilmiş ve kullanılmıştır. Bakteri kültürleri her çalışma günü için stoklardan taze olarak hazırlanmıştır. Bakteri ve fajları başlangıç konsantrasyonları tez kapsamındaki çalışmalarda, sırasıyla $10^8$ CFU/mL and $10^8$ PFU/mL dir. Optik sinyallerin zenginleştirilmesi için 3 farklı plasmonik nanopartikül - gümüş nanoküreler (AgNPs), altın nanoküre ve nanoçubuklar (AuNPs ve AuNRs) sentezlenmiştir. Farklı boyda nanopartikül üretmek için indirgeme ajanı ve nanoemülsiyonların kararlılığını artırmak için sitrat ve/veya CTAB kullanılan farklı yöntemler uygulanmıştır. Bunlar SEM/TEM, Zeta-Sizer, UV-spektrofotometre, LSPR ve AFM kullanılarak karakterize edilmiştir. Seçilen türler aşağıda verilen uygulamalarda kullanılmıştır. Bu tez kapsamında bakteri tanısı ve aydınlatılması amacıyla - temel olarak "Yüzey Zenginleştirilmiş Raman Spektroskopisi (SERS)" tekniği uygulanmıştır. Bakteriyofajların özgün biyoproblar ve nanopartiküllerin sinyal güçlendiriciler olarak yer aldığı bu

çalışmalarda alternatif uygulama protokolleri geliştirilmiştir. SERS çalışmaları önce farklı taşıyıcılar, cam slaytlar ve onların polidopamin kaplı formları ve silika kullanılmıştır. Platformlara ait SERS pikleri bakteri/faj piklerinin üzerini örtmediği silika slaytlar başarılı bulunmuş ve sonraki çalışmalarda yalnızca bu yüzeyler kullanılmıştır. İki grup tanı çalışması yapılmıştır. Birinci grupta önce nanopartiküller silika yüzeylere biriktirilmiş, daha sonra hedef bakteri/bakteriyofajlar yüzeye sırasıyla konularak SERS verileri toplanmıştır. Özellikle fajların konulmasından sonra spektrumlardaki değişimlerin çok belirleyici tanı protokolü oluşturulmasını sağladığı not edilmiştir. İkinci grupta, bakteriler önce süspansiyonda altın nanoçubuklar ile inkübe edilmiş ve nanoçubukların bakteri yüzeyine yığılmaları sağlanmıştır. Daha sonra bu karışım silika yüzeylere damlatılmış ve bakterilere odaklanarak SERS verileri toplanmıştır. Hedef bakterilerinin belirgin ve güçlü parmak izleri elde edilmiştir. Bu nanoçubuk yüklü bakterilerin bulunduğu slaytların üzerine özgün fajlar damlatılmış ve spektrumların zamanla değişimi izlenmiştir. Fajlara ait pikler güçlenirken bakteriye ait piklerin bir kısmı kaybolmuştur. Tek bir bakteri üzerine dahi hedefleme yapılarak tanımlayıcı belirgin spektral piklerin elde edilmesi mümkün olmuştur. Bu çok ilginç/yenilikçi bulgular burada uygulanan SERS protokolünün başarıyla kullanılabileceğini göstermiştir. Destekleyici olarak yapılan öncü çalışmalarda "Lokalize Yüzey Plazmon Resonans (LSPR) Spektroskopi" ve "Matriks Yardımcı Lazer Desorpsiyon/İyonizayon-Zaman/Uçuş Kütle Spektroskopi (MALDI-TOF MS)" tekniklerinin de kullanılabilirlikleri araştırılmıştır. LSPR çalışmaları polidopamin ile kaplanmış daha sonra AgNPs, AuNPs ve AuNRs lerin biriktirilmesi ile modifiye edilmiş cam slaytlar üzerinde gerçekleştirilmiştir. AuNPs - küresel şekilleri ve boyutları (yaklaşık 40 nm) nedeniyle en başarılı olarak bulunmuştur. Önce hedef bakteri (*E.coli*) yüzeylere damlatılmış ve LSPR verileri toplanmıştır. Daha sonra özgün faj taşıyıcı üzerine konmuş ve LSPR'de ki değişiklikler kaydedilmiştir. Bu değişimler hedef bakterileri tanısının LSPR ile başarıyla yapılabileceği gösterilmiştir. Özgün olmayan faj *E.coli* üzerinde çalışmamış, böylece bu çok basit LSPR tekniği ile özgün tanı yapılabileceği vurgulanmıştır. Son tanı grubunda bir profesyonel MALDI-TOF MS sistemi kullanılmıştır. Bu testler yine üç bakteri ve özgün fajları ve AuNPs kullanılarak gerçekleştirilmiştir. Farklı deney setleri uygulanmıştır. Bakteriler/fajları temsil eden çok ilginç pikler elde edilmiştir. Özgün fajların zaman kontrollu olarak ilavesi ile (piklerin zamanla değişimi izlenerek) özgün tanı yapılabileceği

gösterilmiştir. Bakteriyofajların hem depolamada hem de kullanımda hem aktivitelerini korumalarını hem de etkin kullanımlarını sağlamak için yapılan öncü çalışmalarda jelatin hidrojel mikrokürlere yüklenmeleri sağlanmıştır. Jelatin mikroküreler önce süspansiyonda jelleşme ile küresel formda hazırlanmış sonraki adımda "dehidrotermal" yöntemle çapraz bağlanmıştır. *E.coli* T4 fajı kuru jelatin mikrokürelere faj çözeltisi emdirilerek yüklenmiştir. Sulu ortamda salım hızları elde edilmiş ve karşılaştırılmıştır. Özellikle çok kolay hazırlanan çapraz bağlı stabil jelatin mikrokürelere yüklemenin hızlı ve kolay yapılabilmesi önemle not edilmiş ve devam eden sonraki çalışmalarda bu yaklaşımın kullanılmasına karar verilmiştir.

**Anahtar Kelimeler:** Patojenik bakteriler, Tanı, Bakteriyofajlar, Nanopartiküller, SERS, LSPR, MALDI-TOF MS, Gelatin hidrojel mikroküreler, Faj yükleme ve salım.

# ABSTRACT


## NANOBIO-APPROACHES
## FOR THE DETECTION OF BACTERIA BY SERS


**Farzaneh MOGHTADER**


**Doctor of Philosophy, Nanotechnology and Nanomedicine**
**Supervisor: Prof. Dr. Erhan BİŞKİN**
**February 2019, 144 Pages**

The main objective of this PhD thesis is to develop nanobio-based detection/identification protocols for pathogenic bacteria. *Escherichia coli (E.coli)* was the main target bacteria, *Staphylococcus aureus* (*S.aureus*) and *Salmonella infantis* (*S.infantis*) were included for comparison. Bacteria and their specific bacteriophages (used as specific bioprobes) were obtained from the expert laboratories and American Tissue Culture Collections (ATCC), and propagated, characterized and used by us. To enhance the optical signals, several plasmonic nanoparticles namely silver nanospheres (AgNPs), gold nanospheres and nanorods (AuNPs and AuNRs) were synthesized, characterized and the selected ones were used in the further studies described below. The SERS experiments were conducted in the following two different protocols: (i) The plasmonic nanoparticles were deposited on the carrier matrices, target bacteria were dropped and the SERS spectra were collected, then bacteriophages were added and changes in the spectral peaks were observed; (ii) the bacterial suspensions were mixed with the gold nanorod emulsions, then they were dropped on silica slides to collect the spectral data, then bacteriophages were added onto those surfaces and spectral changes with time were obtained. Especially the second protocol was very successful. The LSPR studies were performed on glass slides coated with polydopamine - carrying also the nanoparticles aggregates. We were able to follow a similar protocol that we applied in the SERS I experiments and changes in the LSPR spectra were used to describe the specific interaction of the target bacteria with their specific phages. Descriptive spectra for detection of three bacteria and

their respective phages using the AuNPs were also obtained with a MALDI-TOF MS system. Especially changes in the specific phage peaks with time were found very descriptive. In the final part of the studies, the cross-linked gelatin microbeads were prepared and T4 phages were loaded within these gelatin hydrogel microspheres by a very simple technique. The results of loadings and release studies were concluded as the proof of concept of improving storage and release characteristics in use of bacteriophages effectively.

# ACKNOWLEGEMENTS/TEŞEKKÜR

vi

# TABLE OF CONTENTS

# LIST OF FIGURES

xii

xiv

# SYMBOLS AND ABBREVIATIONS

AFM: Atomic Force Microscopy

Ag: Silver

$AgNO_3$: Silver nitrate

AgNPs: Silver nanoparticles

AR: Aspect ratio

ATCC: American Tissue Culture Collection

Au: Gold

AuNPs: Gold nanoparticles

AuNRs: Gold nanorods

CCD: Charge Coupled Detector

CDC: United States Centers for Disease Control and Prevention

CHCA: Alpha-cyano-4-hydroxycinnamic acid

CFU: Color Forming Units

CTAB: Hexadecyltrimethylammonium bromide

d: The adsorbed layer thickness

DHB: Dihydroxybenzoic acid

DI: Deionized

dsDNA: Double stranded DNA

dsRNA: Double stranded RNA

DTSP: Dithiobis succinimidyl propionate

*E.coli*: *Escherichia coli*

EF: Enhancement Factor

ELISA: Enzyme-Linked Immunosorbent Assay

ESI: Electrospray Ionization

EU: European Union

FAD: Flavin adenine dinucleotide

FT-MS: Fourier Transform-Mass Spectrometry

GA: Glutaraldehyde

GIT: Gastrointestinal Track

$HAuCl_4$: Tetrachloroauric acid

HUS: Hemolytic-Uremic Syndrome

$l_d$: The decay length of the electromagnetic field

IR: Infrared

LB: Luria Bertani

LSPR: Localized Surface Plasmon Resonance

**m**: The bulk refractive index

MALDI-TOF: Matrix-Assisted Laser Desorption/Ionization - Time of Flight

MRSA: Methicillin-resistant *S.aureus*

MS: Mass Spectroscopy

MUG: Methylumbelliferryl galactocide

$NaBH_4$: Sodium borohydride

NIH: National Institute of Health

NPs:  Nanoparticles

NS: Nanosilver

qRT-PCR: Quantitative Real-Time-PCR

OD: Optical density

ODNs: Oligonucleotides

PBS: Phosphate buffer solution

PCR:  Polymerase Chain Reaction

PDA: Polydopamine

PEI: Polyethylene imine

PEO: Polyethylene oxide

PFU: Plaque Forming unit

PhD: Doctor of Philosophy

PLE: Phage Loading Efficiency

PPO: Polypropylene oxide

PRC: People Republic of China

RS: Raman scattering

PVP: Polyvinylpyroliddone

RT-PCR: Real-Time PCR

*S.aureus*: *Staphylococcus aureus*

SD: Standard deviations

SDS: Sodium dodecyl sulphate

*S.enterica*: *Salmonella enterica*

SE: Surface Enhancement

SELDI: Surface-Enhanced Laser Desorption/Ionization

SEM: Scanning Electron Microscopy

SERS: Surface Enhanced Raman Spectroscopy

*S.infantis*: *Salmonella infantis*

SIF: Simulated intestinal fluid

SGF: Simulated gastrointestinal fluid

SPR: Surface Plasmon Resonance

ssDNA: Single stranded DNA

ssRNA: Single stranded RNA

SPR: Surface Plasmon Resonance

1    STEC: Shiga Toxin-producing *Escherichia coli*

t: Time

TEM: Transmission Electron Microscopy

TFA: Trifluoro acetic acid

TMV: Tobacco mosaic virus

TOF: Time-of-Flight

TSB: Tryptic soy broth

US: United States

USA: United States 0f America

UV: Ultra violet

VIS/NIR: Visible/Near Infrared

WHO: World Health Organization

3D: Three dimensions

$\Delta n$: the change in refractive index

$\Delta\lambda_{max}$: The scattering wavelength maximum

# 1. INTRODUCTION

Bacterial infections are among the most important health problems/concerns all over the world. WHO ("World Health Organization") has reported that millions of deaths occur each year as a result of food and water-borne bacterial infections and about 86% of these are children (WHO, 2017). Pathogens like *Escherichia coli* (especially O157:H7 and O104:H4 strains) and *Salmonella* species alone have resulted approximately 1.4 million cases in USA. *Campylobacter, Salmonella* and *Listeria* are among the number of pathogenic bacteria causing food/water borne bacterial infections close to 400,000 per year in Europe with (Mackenzie et al., 1994; EFSA, 2009; Garcia et al., 2010).

Fresh meat, chicken, milk, cheese, and even vegetables are potential sources/ carriers of pathogenic bacteria (Wells et al., 1983; Batz et al., 2005). Even very low (~10 bacteria) contaminations may cause severe infection problems. It should be noted that the number of bacterial strains with rather high drug-resistivity is getting higher every year. Pathogenic bacteria are easily carried with human, animals and other living creatures. It is afraid of that those pathogens can easily be used as extremely dangerous/effective warfare agents which may be distributed by contamination of food and water. Therefore, pathogenic contaminations in the food and water that we use daily should be carefully followed/monitored which one of the most leading priority and safety health issues globally.

There are several microbiological analysis approaches - rather traditional methodologies - applied almost routinely every day worldwide include in the expert laboratories (Singh, Poshtiban and Evoy, 2013; Brown and Smith, 2016): (i) Classical microbiology techniques (bacterial cultures); and rather modern molecular techniques (ii) methods using "Polymerase Chain Reaction - PCR" approach and (iii) methods using antibodies, for instance "Enzyme-Linked Immunosorbent Assay - ELISA".

Microbiological techniques are the oldest, but they are still considered as the most accurate approaches. Here, the target bacteria are grown in defined culture media, followed by counting and morphological analysis by microscopic techniques. More

complex biochemical analysis should be applied for strain level characterization. All these tests usually take several days even much longer (few weeks) - which are time-consuming, laborious and expensive especially for strain level tests. More modern/molecular based approaches such as immunological or nucleic acid-based techniques typically are much faster - may take few hours to complete. However, highly experienced experts are needed, sample preparation (which also takes hours to days) is time consuming, expensive and highly developed infrastructure is required. In addition, they are not real-time detection methods. Development of alternative approaches for sensitive, selective, accurate and fast detections are required which should also be miniaturized/portable automated therefore cost effective - that allows much wider use and on-site applications.

Diagnostic test kits and related array technologies (for multiple detections) are in use to describe the presence of target bacteria. Here, interaction of bioprobes which recognize the target specifically are interacted with the target (here bacteria) in the sample usually on a proper platform and the respond - positive or negative is reached quite fast. Biosensors are also based on these specific interactions between the bioprobe and the target. They are very heavily studied as alternative strategies to overcome the problems dictated in classical pathogen detection approaches described above (Singh, Poshtiban and Evoy, 2013). Biosensors are analytical devices which have a sensor platform carrying the bioprobes, i.e., oligonucleotides, oligopeptides, antibodies, antibody fragments, and bacteriophages - are immobilized, and the signal coming out from those interactions are monitored/recorded. In contrary to diagnostic test kits and array technologies, biosensors can give quantitative results - the amount/number of the target within the unit volume (mass) of the sample to be analysed.

**The main objective** of this PhD thesis is to investigate nanobio-based methodologies and to develop new protocols for pathogenic bacteria detection/ identification. *Escherichia coli (E.coli)* was selected as the main target bacteria while *Staphylococcus aureus* (*S.aureus*) and *Salmonella infantis* (*S.infantis*) were also included in some group of studies for comparison. These bacteria and their respective/specific bacteriophages were either obtained from the expert institutions in Turkey and Georgia (Eliava Institute, Tbilisi) or bought from ATCC. Both bacteria and their specific bacteriophages were propagated in our studies,

usually freshly in each test group and used. Three different plasmonic nanoparticles, silver and gold nanospheres and gold nanorods, AgNPs, AuNPs and AuNRs, respectively synthesized by several procedures described in the related literature, the ones with proper properties (size, size distribution, absorbance spectra and charge) were selected and used in the detection protocols. SERS was the main methodology used in different formats. In addition, LSPR spectroscopy and MALDI-TOF MS were also applied to collect the supportive information and comparison. Some preliminary studies aiming to prevent activity lost of bacteriophages in storage and use we have also investigated immobilization of phages into gelatin based microhydrogel beads, gelatin - as a follow up approach to our previous studies in which alginate based carriers have been used (Moghtader, Egri and Piskin, 2017).

# 2. LITERATURE SURVEY

## 2.1. Target Bacteria: *Escherichia Coli*

### 2.1.1. Definitions and Properties

*Escherichia coli* (*E. coli*) is a member of family *Enterobacteriaceae.* It is a gram-negative/anaerobic/rod-shaped bacteria which cannot sporulate (Figure 2.1A) (Lewin, 1987; Kaper, Nataro and Mobley, 2004; Croxen et al., 2013; Kotloff et al., 2013; Gomez et al., 2016; *E.coli* facts sheet, 2016). It was discovered in 1885 by Theodor **Escherich**, a German - Austrian paediatrician - bacteriologist (Figure 2.1B) - he was an academician at the universities in Austria and able to isolate/identify 19 different bacteria from the infant's intestinal flora - one of them was *Bacterium coli* commune - which was re-named as ***Escherichia*** *coli* after him for his honour (Escherich, 1988; Shulman, Friedmann and Sims, 2007; Joan and Slonczewski, 2017).
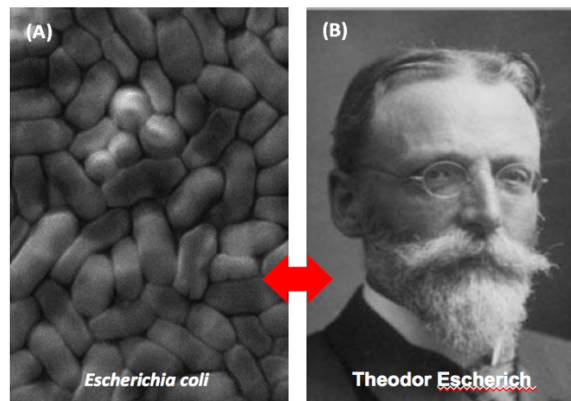


Figure 2.1.   (A) A representative SEM picture of *Escherichia coli*; and (B) Theodor Escherich who discovered *E.coli* (Shulman, Friedmann and Sims, 2007).

Several family members of *E.coli* are present in the lower intestinal micro flora of warm-blooded organisms - such as human and mammals (animals) and therefore easily contaminate the feces. There are hundreds of different strains. Some strains are highly pathogenic as described below - however some of them are normal habitants in human intestinal flora where they do help food breakdown/ absorption/waste processing and in the same time they do contribute positive

reactions such as vitamin K production. *E.coli* has been considered/widely used in the recombinant DNA technology as the cloning host - which is another important note - positive part of this very versatile bacteria. *E.coli* strains do grow at human body temperature - 37°C as expected - they can easily be destroyed at higher temperature - for instance in boiling water - in other words sterilization is easy by classical sterilization methods - like steam sterilization.

Some strains - which usually produce "Shiga-like toxins" may be quite dangerous - severely pathogenic - mainly come from food that we consume daily such as milk and milk products (yogurt, cheese, etc.), meat (especially raw meat or not well-cooked meat products such as hamburgers, sausages, etc.), raw vegetables (salads, lettuce, spinach, coleslaw, etc.) and in water that we drink or use and may cause severe - deadly diseases (Lewin, 1987; Mckeinzie et al., 1994; Kaper, Nataro and Mobley, 2004; Gomez et al., 2016). The *E.coli* strains producing "Shiga-like toxin" - called as STEC - are harmful/pathogenic and responsible of foodborne diseases especially affecting children and elderly people. *E.coli* O157:H7 is a typical STEC - well-studies because it was main cause in the bacterial outbreaks - especially in North America, while *E.coli* O104:H4 is another important STEC which was one of the main pathogen caused outbreaks in Europe in 2011 (Buchholtz et al., 2011).

In the patients contaminated with STEC, fewer, abdominal cramps, vomiting and diarrhoea - even bloody diarrhoea - called as haemorrhagic colitis - are observed (WHO, 2017). The recovery period is about 10 days, however the infections may go to more severe phases and cause deadly renal diseases/failure such as haemolytic uremic syndrome (HUS). It has been reported that about 10% of patients carrying STEC may develop HUS - which is a quite important percentage. HUS may result other important neurological and other complications in the young/older patients - like stroke and coma (Qadri et al., 2005). Some of the *E.coli* strains are resistive to almost all known antibiotics and - even worse - these isolates are found all around us (mainly in hospitals) (Blair et al., 2015; Khalil et al., 2016; Bassetti et al., 2017).

Millions of people get affected by gastrointestinal diseases annually worldwide (WHO, 2012). The problems are severe and mortalities are high in some countries

like in South Asia (especially in India) and sub-Saharan Africa as indicated in the World Map (WHO) (Figure 1.2). "Centers for Diseases Control and Prevention" (CDC) - USA reports that there are about 300,000 cases of the STEC infections are reported each year only in the United States - about 36% of these due to *E. coli* O157 - 3,600 US hospitalizations and 30 deaths among 3,600 hospitalized patients each year (CDC - 2019). These are quite high numbers in a developed country - and gives the clue the extend of *E.coli* infections and potential outbreaks that may occur in the developing and undeveloped countries.
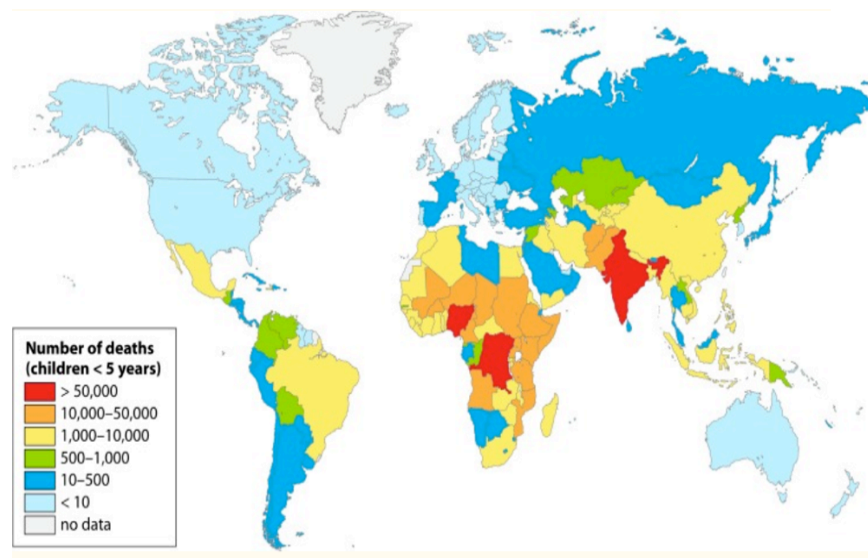


Figure 2.2.    *E.coli* infections/dead in the World (WHO, 2012).

Pathogenic *E.coli* is transmitted to human mainly by consumption of food (mentioned above) and water (drinking and recreational) contaminated with feces (Figure 2.3) (Croxen et al., 2013). Cross-contaminations between humans (face to face contacts) and animals (both domestic and wild) are also possible due to direct contact. Cattle is the main animal carrying those pathogenic *E.coli*, however others such as sheep, goat, pigs, horses, deer, rabbits, several birds, may carry them and therefore potential candidates for bacterial infections by cross-transmissions. The scenario is highly complex - therefore difficult to prevent outbreaks which are directly associated all these kind of transmission routes especially use of contaminated food and water - not only in not well-developed societies but also in the developed communities as shown in Figure 2.3.
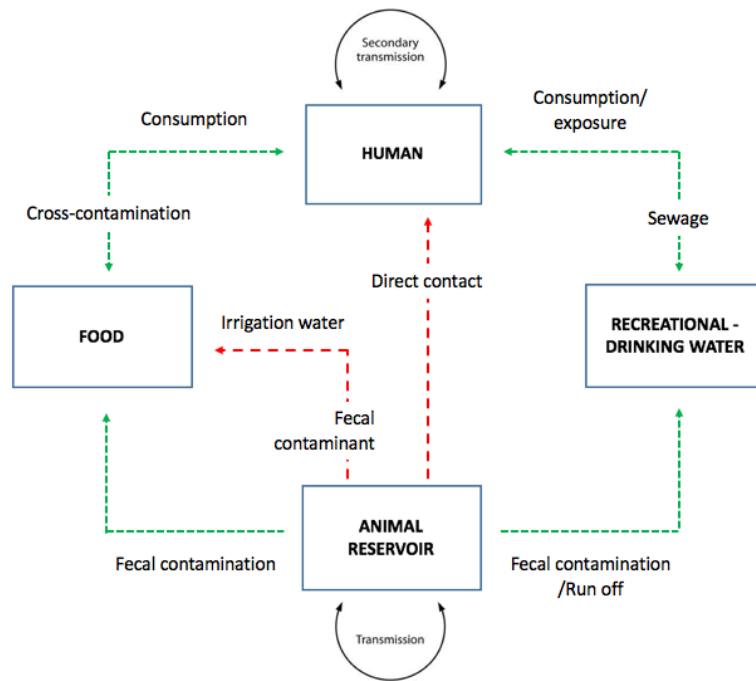
Figure 2.3.    *E.coli* reservoirs/infection/transmission routes.Adapted from literature
(Croxen et al., 2013).

## 2.1.2. Traditional Microbial Analysis

There are several rather traditional microbiological techniques for identification/ detection of bacteria. Sampling and sample preparation are the first and important part of bacterial detection. Collecting samples from water and air are rather easy. Water samples can be transferred to testing labs or bacterial contaminations in the environmental water reservoirs can be directly examine at site by using portable devices. If the level of contaminations are rather low, extra enrichment steps may be needed. Physical techniques like centrifugation and filtration may be used. However, they are not specific - many other compound/species in addition to the target bacteria are precipitated/collected in the precipitates or on the filters that may inhibit the selectivity/sensitivity of the technique to be used in the further step.

Magnetic particle-based separation using specific ligands allows more specific separation of the target bacteria from others (Croxen et al., 2013). Magnetic particles are composed of mainly a paramagnetic core and specific affinity ligands (lectines, antibodies, peptides, bacteriophages, etc.) on their surfaces (Figure 2.4A). Lectines are polysaccrides - not very specific and the particles may form

aggregates. Antibodies - especially monoclonal antibodies - proteins (poly-peptides) are very selective but rather expensive bioligands and they are temperature sensitive, could lost easily their 3D structures/activities - therefore special care should be taken in their storage and use. Due to easer synthesis/ production and low cost peptides (oligopetides) have been also attracted a great attention especially in resent years as bioligands - most probably we will see more in the market for microbial detection/identification. Immunogenic separation was first patented in 2000 (Bisconte De Saint Julien, 2000). It was then become an important selection methodology it was adapted to modern methodologies both increase the specificities of the detection and reduce negative findings (Benoit and Donahue, 2003) as schematically demonstrated in Figure 2.4B.

The success of this approach depends the specificity of the bioligand immobilized onto magnetic particles, there may be a number of cross-reactions that decreases specificity. The extra cost and time should be carefully considered.
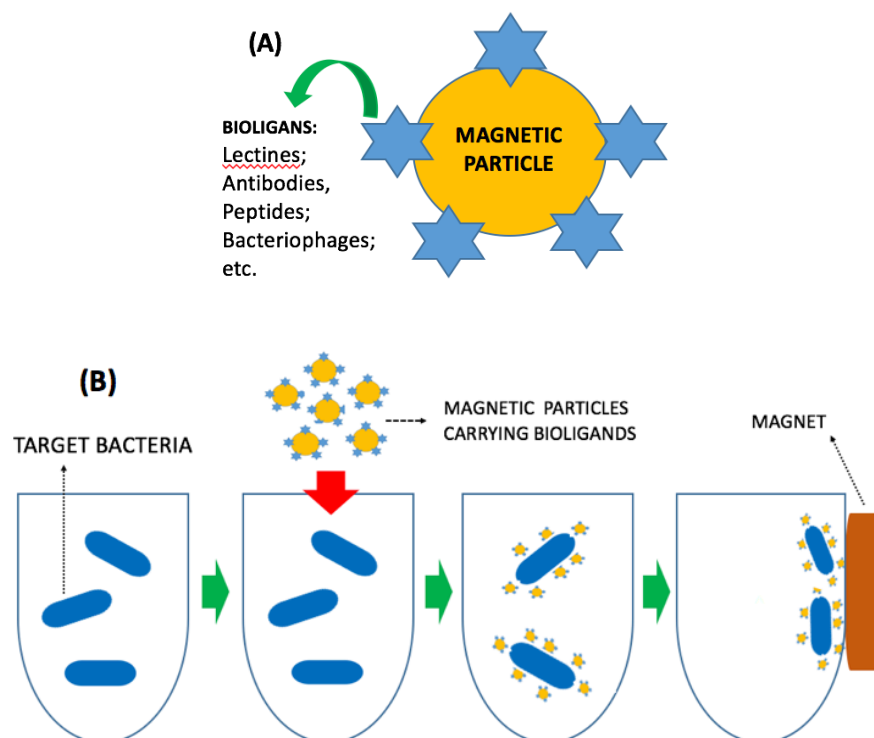


Figure 2.4.    (A) Magnetic particles carrying bioligands; (B) Separation of bacteria selectively with bioligand carrying magnetic particles using a simple magnet.

Bacteriophages have also been proposed as specific bioligands as an alternative to antibodies for separation of their host bacteria quite specifically by using magnetic separation approach (Benett et al., 1997; Sun, Brovko and Griffiths, 2001). High specificity and low cost of bacteriophages are important advantages to be used as bioaffinity ligands, however, bacteria captured may be destructed (lysed) and further compounds coming out from the bacteria may further contaminate the sample and effect the measurements. In further studies bacteriophage-derived ligands (enzymes, the tail peptides, etc.) have been also studied by some improved properties with promising results (Kretzer et al., 2007).

Bacteria can be collected from air - simply using bacterial dishes containing proper media that are placed within the area for inspection (like hospitals). Bacteria in air just settle down from the air in the media then they are carried to microbiology labs for screening tests. There are portable devices - called air collectors in which air in the room is circulated through the device continuously with a controlled rate and measured, bacteria are capture on petri dishes or on specially design filters attached/placed to the device and dishes/filters are carried to microbiology labs for further testing.

In contrary to water and air samples/sampling, solid/semi-solid/liquid matrices (like food, feces, clinical tissues, blood, urine, etc.) contaminated with bacteria are not easy to handle. The matrices may vary significantly in microbial content and diversity, chemical composition and physical properties - they are heterogeneous; target bacteria contaminations may be low and hiding in anywhere in the matrix. The matrices should be homogenized, disintegrated, suspended, centrifuged, filtered, etc. to bring them in the forms that samples can be taken and plated on specific medium for formation of bacterial colonies - which means extra time and cost to the detection protocol.

In the typical culture technique, the sample is put/plated in a growth-permitting medium which may be non-selective; selective (containing specific agents that allows better the target bacterial growth and inhibits the others - such as antibiotics, salts, acids); or differential, and incubated to reach desired concentrations depending on the analytical technique to be applied for detection at optimum growth conditions for proper time periods - may be few days even weeks.

Selection and screening may be employed at the same time of the culturing process, for instance acid producing bacteria can be distinguished (selection and screening simultaneously) from the non-acid producing ones by using pH indicators (change in the color) in proper media such as carbohydrate containing agar. Very simple test that may be applied for initial screening of contaminated water samples to differentiate between *E. coli*. and the total coliforms. These specific substrates are added to the water sample to be analysed - if the water contains total coliform - the colour turns to yellow - as a result of beta galactocidase activity of those microorganisms. However, if the medium contains a proper substrate like methylumbelliferryl galactocide (MUG) which is cleaved by specific enzymes of *E.coli* and a fluorescence blue color appears that indicates its presence in the sample. These indicators based assays have been further studied/modified for bacterial identification/detection including *E. coli*. Several specific substrates including 4-aminophenyl-β-D-galactopyranoside, methylumbelli ferrylgalactocide, 8-hydroxyquinoline glucuronide and 4-nitrophenyl β-D-glucuronide have been used. They are hydrolyzed with enzymes expressed by *E.coli* - e.g., β-D-galactosidase and β-D-glucuronidase - which are considered as as specific markers - which yield formation of optically active compounds (such as fluorogenic compounds - 4-methylum belliferone). These compounds are followed by colorimetric or fluorometric measurements using typical microplate readers and/or fluorimeters/fluorescence detectors (Wildeboer et al., 2010; Jackson, Tyler and Millar, 2013; Hesari et al., 2016).

Interaction of substrates and *E.coli* enzymes may also lead to electrochemically active compound production which can be measured in a microbial fuel cell (Kim and Han, 2013). It should be noted that these measurements not only show the presence of *E.coli* within the medium but also may give quantitative data. However, there are also serious drawbacks of these rather simple tests. For example, there may be negative findings - there may be some indication even if the indicator organisms are absent (Gerba, 1996; Straub and Chandler, 2003). It was also reported that a high percentage *E. coli* strains do not cleave the substrates, therefore they cannot be detected by these indicator assays (Straub and Chandler, 2003).

After culturing, the number of colonies formed may be counted by light microscopy which allows also morphological identification of bacterial cells/ colonies using also specific staining agents which is rather routine procedure in microbiology labs. More detailed - sub-cellular morphological characterization can be performed by using electron microscopy images. Cell morphology including colony shape, dimension, pigmentation, etc. which is observed under microscopy. These microscopic cell morphology observations give important information that includes if they are gram positive or negative, their shape and organization, flagellation, etc. - which may allow phenotyping with certain level of specificity. However, it should be noted that strain level characterizations cannot be reached by these microscopy techniques.

A large number of biochemical analysis may be needed to describe the type of bacteria. Several enzyme activities - including catalyse, nitrate reductase, oxidase, ß-galactosidase, amylase, thermo nuclease and urease activities should be studied (Sneath, 2005). The carbohydrate utilizations are followed in these assay for identification. Growth of bacteria at different conditions like at different pH, temperature and using various salts with concentrations are monitored for identification. Testing antimicrobial substances (antibiotics) gives also information about the type of the bacteria. Note that about 200-300 hundred even more tests are needed/done in the biochemical and physiological analysis (Brown and Smith, 2016). There are commercially available kits, even microarrays and highly developed software for multiplex tests which decreases the test time, however it should be note that these number of tests reflects only 5-20% of the bacterial genome potential - means that even with those tests it is very difficult to identify the bacterial contaminations clearly within complex samples. It means that even only this part of identification is time consuming, costly and not reliable.

For identification of bacteria and also grouping phenotypes may be achieved with the experiments targeting their morphology, physiological and biochemical properties (Brenner, Krieg and Staley, 2005). It should be stress on once again that these culturing and microscopic evaluations are limited characterization tools, time-consuming and laborious for type of bacteria including pathogenic *E.coli* detection. Considering rapid development of outbreaks - it is clear that this is very

critical limitation - diagnosis should be very quick and sharp to prevent/stop the disease transmission/spread.

It should be noted also that in many cases biotyping including genotyping is a very important step in identification which may be achieved with the following two molecular techniques described briefly below: (A) Immunological and (B) genetic (Henchal et al., 2001; Myers et al., 2006; Struelens, 2006Zourob et al., 2008).

### 2.1.3. Immunological Techniques for Microbiological Analysis

Immunological techniques for bacterial identification and detection are molecular approaches based on quite specific antibody-antigen interactions (Yolken et al., 1997; Hubner et al., 1992; Brenner et al., 2005; Xi et al., 2005; Wang, He and Shi, 2007; Zourob et al., 2008; Nurliyana et al., 2018). Antibodies are used as the specific bioligands and specific antigens of the bacterial cells are the targets.

Immune-based approaches are used in serological analysis at various levels as common bacterial identifications tools in which antibody/antigen reactions - here the antibody is a very specific bioligand and the antigen is the specific /characteristic target usually on the bacterial cell wall. The antibody-antigen reactions the target bacteria are followed by several observations including agglutination or precipitation in the test, or color (Kreig, 2005). There may be several surface antigens of the bacterial cells that are used as target markers. For instance; "Somatic (O) antigens" are exist in gram negative bacteria more than gram positive. For instance, 173 O-antigen, 56 H-antigen and 103 K-antigen are descriptive markers for *E.coli* for serotyping. Serological tests are successfully applied for serotypings today, however, they may be quite costly because of the ingredients (antibodies, staining markers, medium, etc.) used, and needs rather long assay times. In addition, some negative results could be observed. For instance, Nataro et al. have investigated *E. coli* 0157:H7 serotypes by somatic and flagella - but the other serotypes that were excluded were found to be caused similar disease symptoms (Nataro et al., 2007).

Enzyme-linked immunosorbent assay have been widely used for all kind of antigen detection (Carpenter, 2007; Lam and Mutharia, 1994). Figure 2.5 illustrates schematically a sandwich ELISA tests. Here, the specific - usually monoclonal

antibody is immobilized onto a substrate - for instance on the surface of magnetic particles as specific bioligand - as given in Figure 2.4, or on the surfaces of simple tubes or 96 well plates for multiple detections. When the sample is added within the medium, the target antigen (on the surface of the bacteria) is interacted with the antibody immobilized onto surface. A second antibody carrying the label (which is an enzyme here) is then added that finds the target captured by the surface antibodies and attach to the target forming of a sandwich. In the final step, when a chromogenic substrate - specific for the enzyme linked to the second antibody on the surface is added within the medium - the enzymatically catalysed reactions occur which results a change in the colour that is the positive respond - showing the presence of the target bacteria within the medium. There are several ELISA kits in different forms are commercially available.
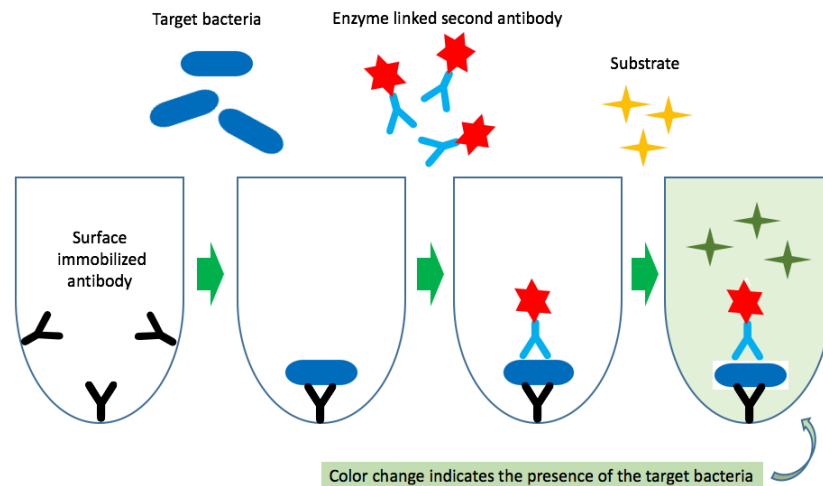


Figure 2.5.    Schematically description of an ELISA test for bacterial detection/ identification.

ELISA like tests are also conducted in bacterial suspension (in the tubes) using magnetic spheres carrying antibodies are used instead of the classical ELISA plates similar to the ones demonstrated in Figure 2.4. Sensitivity of these type of ELISA kits may be around $10^5$-$10^7$ cells/mL (Kim et al., 1999; Chou et al., 2001). Nonspecific antibody-antigen binding has been considered a limitation but may be overcome using simultaneous steps (e.g., separation and then identification) (Gehring et al., 2004). Interesting approaches have been studied, for instance, Phyle et al. have reported detection of *E.coli* O157:H7 in food and water directly by

using magnetic particles carrying specific fluorescein-labelled antibodies were used for separation and detection with a solid-phase laser cytometry (Pyle, Broadaway and McFeters, 1999).

### 2.1.4. Genetic Techniques for Microbiological Analysis

Genetic identification/detection methodologies have become rather traditional techniques for genotyping of target bacteria. PCR have been been used in microbial analysis in which DNA fragments of the target bacteria are amplified *in vitro* by using enzymatic replications and identified. PCR was developed first by K.B. Mullis in 1983 - who has received the Nobel Prize in Chemistry later in 1993 (Mullis, 2018).

PCR is conducted in a Thermo cycler. Figure 2.6 describes schematically the main steps in a PCR cycle which are: (i) "**Denaturation**" - in which the complementary strands of the DNA are separated by breaking the hydrogen bonds (called also as "DNA unzipping" or "melting"); (ii) "**Annealing"** - in which the primers do attach the specific sites on the DNA template. Thermophile DNA polymerase then works for replication; and (iii) finally the DNA strands zip back up upon cooling to complete the cycle which may be repeated several times to reach the necessary amplification - thousand-million copies can be produced. These fragments are separated by electrophoresis and fluorescent stained DNA bands are analysed for identification.
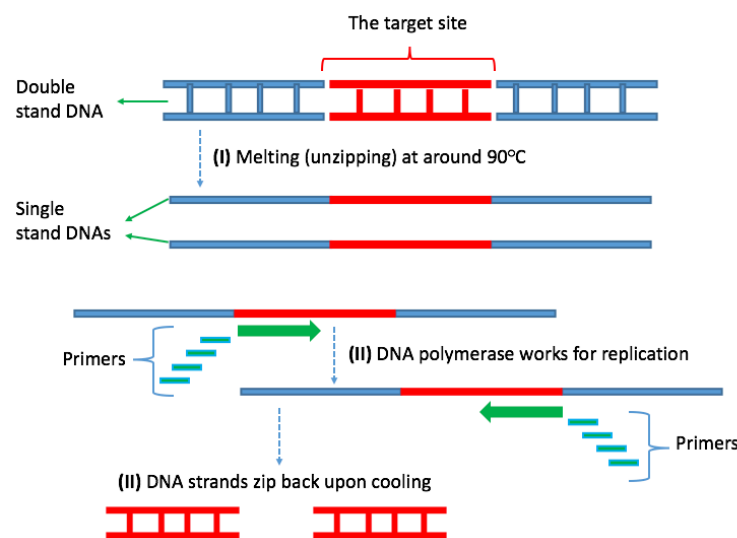


Figure 2.6. Schematically description of PCR technique.

There are a variety of PCR techniques including "Conventional", "Multiplex-PCR", "Nested-PCR", "Real-Time-PCR" (RT-PCR), "Quantitative Real-Time-PCR" (qRT-PCR), etc. (Atlas and Bej, 1994; Belgrader et al., 1999; Winter, 2005; Nolte and Caliendo, 2007). The multiplex PCR used multiple pathogens detection by using multiple primers sets. The Nested-PCR is especially used for more sensitive pathogen detection. The RT-PCR is based on using reverse transcriptase that converts RNA to cDNA. The qRT-PCR uses fluorescence dyes (e.g., Syber green) or fluorescence containing DNA probes (e.g. TagMan) that allow quantification of the replicates during the cycling process. Almost all of these different PCR techniques have also been applied for detection of pathogenic *E. coli* (Olsvik and Strockbine, 1993; Fratamico, Bagi and Pepe, 2000; Holland et al., 2000; Fortin, Mulchandani and Chen, 2001; Li and Drake 2001; Daly et al., 2002; Ibekwe et al., 2002; Ibekwe and Grieve, 2003; Maki et al., 2003; Ferreira et al., 2004; O'Sullivan et al., 2006; Italia et al., 2012; Soto-Muñoz et al., 2014).

With the new versions, PCR is an excellent molecular technique for identification of pathogenic bacteria at genomic level. It is rather expensive and needs personal highly expertise in this field. The cost may be accepted considering the importance of identification of pathogenic bacteria having a chance for out-breaks. The main drawback is the inhibition of the process due to several components - PCR inhibitors/facilitators should be considered carefully, DNA polymerases should be selected properly, etc. for a successful PCR (Rossen et al., 1992: Abu Al-Soud and Rådström, 1998; Abu Al-Soud and Rådström, 2001; Rådström et al., 2003)

In the DNA-based genetic approaches, characteristic sequences of the target bacterial genome are looked for identification. PCR and its modified forms are applied today. It is rather sophisticated and needs expert - manpower for testing. In addition, chemicals/biochemicals are quite expensive to run the test. It is of course much faster than culturing techniques - but still need heavy pre-enhancement/concentration steps to perform the test at reliable detection limits in small size sample volumes. Several multiplex PCR techniques have been studies for simultaneous identification of multiple target genes in one test which have made the analyser life much better - reduce the test time very significantly (Fagan et al., 1999). However, the cost of a test is still high and even higher. Separating the PCR amplification products classically electrophoresis that are performed on

agarose gels seems limitations in accuracy for describing the amplicon sizes. It should be noted that some of these limitations have been overcome by using real-time PCR. One of the main drawbacks in the PCR analysis is the inhibition by the matrix components - extreme purification may be possible but expensive and time consuming. One of the most reliable pathogen identification technique is the 16S rRNA gene sequencing - primers for highly conservative regions are available, by using universal primers the complete gene can be amplified. However, it is not easy to implements this approach into routine test labs - it is expensive and time consuming and still needs in expensive protocols with better automated devices.

## 2.4.2. Bacteriophages

### 2.4.2.1. General Properties

Viruses have been first described as "particles smaller then bacteria and causes also diseases". They are rather simple nanosize structures/species - noncellular - composed of a nucleic acid genome (single or double strand DNA or RNA) and several proteins. Tobacco mosaic virus (TMV) was one of the first viruses described. The structure of TMV is given in Figure 2.7 - which is typical in almost all other viruses - in which the nucleic acid genome is packed in a protein coat – which is called as "capsid".
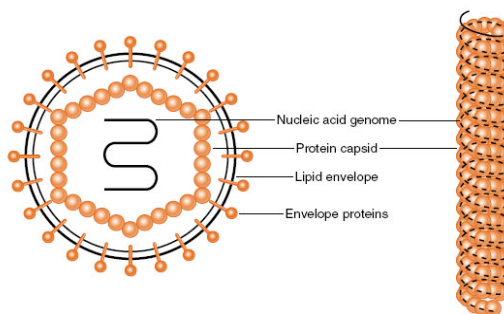


Figure 2.7.    Typical structure of Tobacco mosaic virus (TMV) (Slide Share, 2016).

There are a variety of viruses with different sizes, shapes and structures as exemplified Figure 2.8. Viruses do infect almost all species - living creatures including human, other vertebrates, invertebrates, plants, fungi, bacteria, etc., as shown in Figure 2.9 and may cause severe health problems which is one of the most important issues globally today and bringing human being in a very

16

dangerous/sensitive situation - they are **our enemies** getting stronger every day - we have to find much better strategies **to detect** them and fight to protect us.
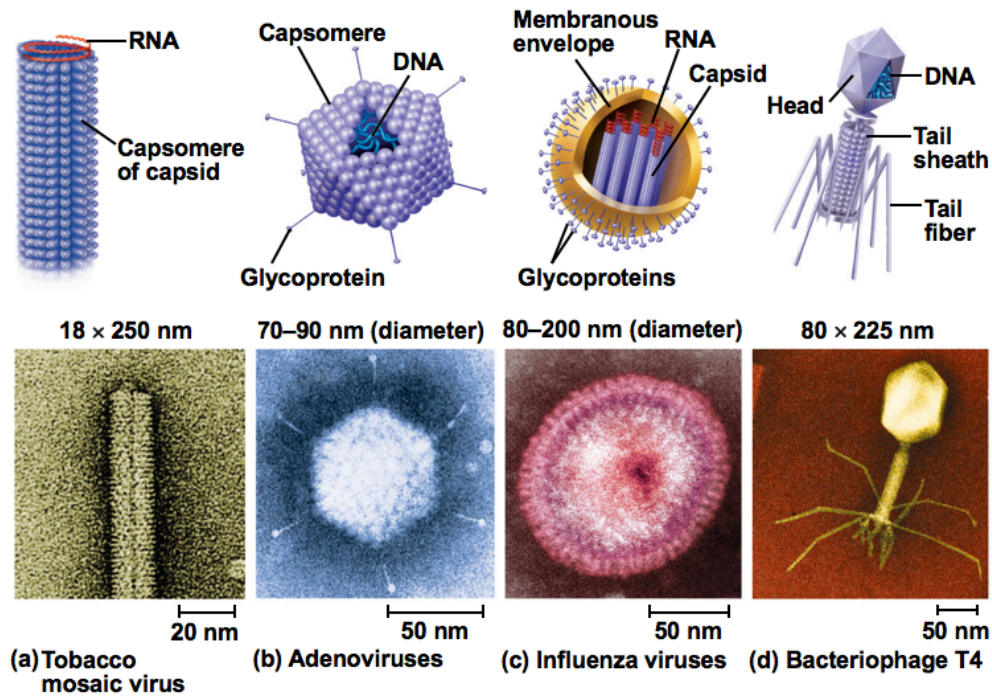


Figure 2.8.    Some examples to viruses (Napa Valley, 2016).
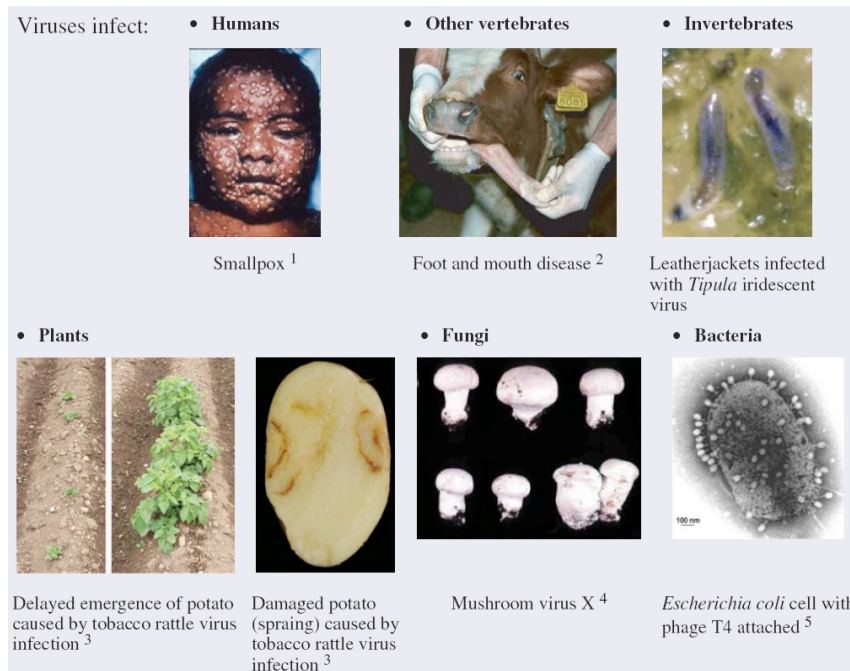


Figure 2.9.    Viruses do infect almost any type of living creatures (Encyclopaedia Britannica, 2016; World Press, 2016a).

Bacteriophages (**phages**), are the most abundant living organism in the world - are typical viruses. They do quite specifically infect and may kill/destroy ("**eat**") their target bacteria. The name comes from an old Greek word "**phagein**" means "**to eat**". They do specifically infect bacteria and are known as harmless for humans - no side effects have been described which means that they are actually **our friends** and therefore are used as antibacterial agents - as an important alternative to antibiotics - for the therapy of many kind of bacterial infections.

Frederick W. Twort - a bacteriologist in England - was the first who described bacteriophages in 1915 (Twort, 1915) (Figure 2.10). Felix D'Herelle (a French-Canadian) observed also lysis of *Shigella* at the Pasteur Institute in Paris in 1917 (D'Herelle, 1917). After his exiting discovery, Twort stopped working on these new agents and continued in other areas. However, D'Herelle has spent almost all his scientific life on bacteriophages and their possible use in the treatment of several bacterial infections, the so-called "phage therapy". He was the one who named these species a "bacteriophage" (D'Herelle, 1918). He has also supported development of phage therapy in the Soviet Union with George Eliava (founder of Eliava Institute in Tbilisi-Georgia where F. Moghtader also had chance to work).



**Frederick W. Twort** given first credit for phages

**Felix D' Herelle** naming of the "bacteriophages"

**Elena Makashvili, Felix D'Herelle,** and **George Eliava** (left to right),founded the Eliava Institute in Tbilisi - Georgia

Figure 2.10. Frederick W. Twort (an English-on the left) and Felix d'Herelle (A French-Canadian-on the right) were two scientist discovered bacteriophages. Elena Makashvili, Felix D'Herelle and George Eliava (left to right) at the Eliava Institute (Twort, 1915; D'Herelle, 1917).

More detailed information about the early history of phage therapy and also the current status has been reviewed in a number of publications (Summers, 2001; Sulakvelidze and Kutter, 2005; Hausler, 2006; Housby and Mann, 2009). Historically, there were many criticisms of phage therapy in earlier studies/reports however, it is changing rapidly - their safety and efficacy have been discussed/ demonstrated even in clinical studies. It is clear that phage therapy will be strategically a very important alternative in medicine especially in the case of drug (antibiotic) resistance cases. It seems/clear that there will be much more products based on phages available not only for therapy but also diagnosis (detection) of bacteria to follow and protect us (including animals, plants, etc.) from bacterial attacks.

Bacteriophages are non-self-replicating - cannot reproduce and survive on their own, must take over host cell (i.e., bacteria) - therefore they usually defined as non-living organisms - they do neither have a cytoplasm nor cellular organelles. Note that there is usually more than one phage for every bacterium. They can be found almost everywhere - in any every environment, in the biosphere. They are very specific even at strain level as mentioned before (i.e., usually infect only the targeted bacterial species). They do replicate at the site of infection forming new virions in a very rapid process that is explained below.

Bacteriophages are different in morphology and nucleic acid properties. They may be in different 3D structures such as contractile tails; noncontractile tails; tailless; filamentous or head shapes and their genome can be dsDNA; ssDNA; dsRNA or ssRNA (Figure 2.11A). Vast majority of phage has dsDNS. The first electron micrograph of a T2 phage was taken in 1942 by Luria and Anderson which is given in Figure 2.11B. Some representative SEM micrographs of different type - well known - of phages are given in Figure 2.12.

Bacteriophages have two life styles: (A) Lytic (e.g., T4) and (B) Lysogenic (e.g., Lambda). Figure 2.13 shows schematically the six steps in a typical lytic cycle (i.e., for *E.coli* as an example which is the main bacteria that was also used in this PhD thesis) which are briefly described below:
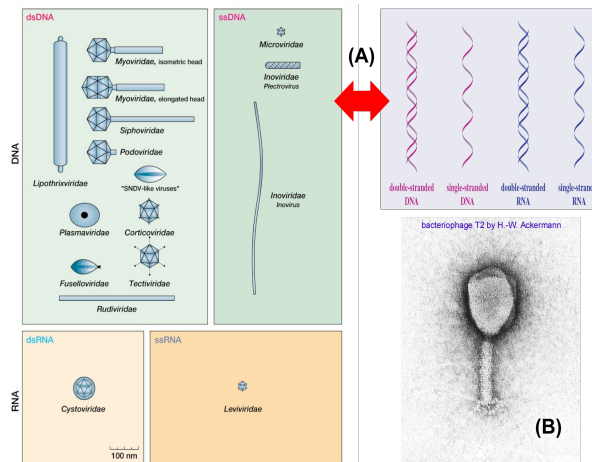
Figure 2.11. Bacteriophages: (A) classification; and (B) the first electron micrograph of a T2 phage was taken in 1942 by Luria and Anderson (Slide Share, 2016).
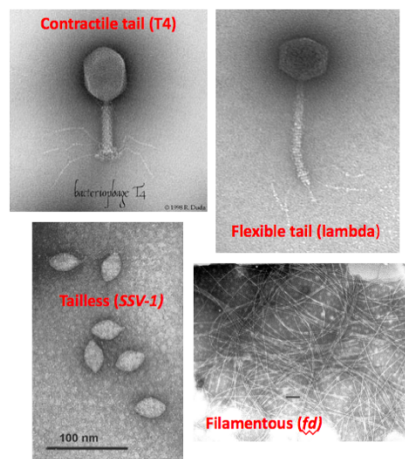


Figure 2.12. Representative SEM micrograph of four different type of bacteriophages (ASM Org, 2016; Britannica, 2016; Study Blue, 2016).

**Step 1. Attachment**: They do find and attach the receptors (such as proteins; lipopolysaccharides; carbohydrates; teichoic acids, etc.) on the bacterial membrane surfaces - quite specifically. Thus this phase of the infection is specific for the virus - it can only infect those cells that have the complimentary receptor sites - host specificity. Also, since the target attached are mostly proteins, it also makes the viruses sensitive to environmental factors such as heat - heat sensitivity.

20

**Step 2. Penetration**: Following attachment phage DNA is inserted into the cell - by tail contraction (T4), by a simple injection or unknown mechanisms. The viral capsid stays outside the host cell and while only the nucleic acid is found within the host.

**Step 3. Transcription**: Phage DNA is transcribed and phage mRNA is translated to phage proteins - using host RNA polymerase including viral enzymes are synthesized using the cells energy and raw materials.

**Step 4. Replication of DNA and protein synthesis**: Proteins of the phage coat and DNA/RNA are produced and the host DNA is degraded.

**Step 5. Assembly**: Phage components are brought together to form the mature virions.

**Step 6. Release**: The bacterial cell is destructed (lysis) and new born babies (virions) are released from the host. Many phages lyse their host by destructing the bacterial wall or while some phages (e.g., filamentous phages) are released without lysing the host cell.
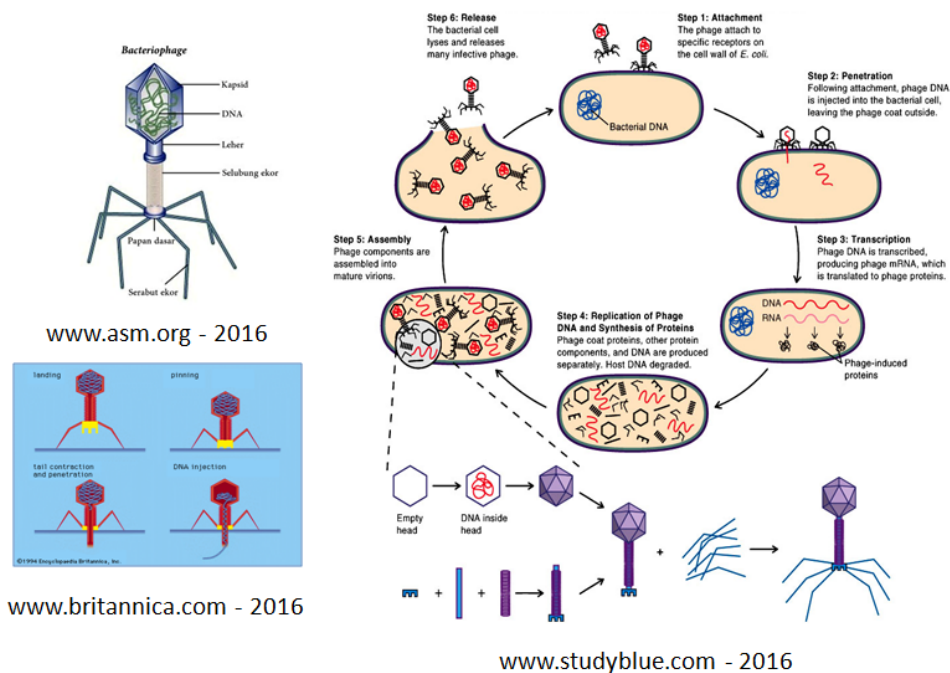


Figure 2.13. T4 phage structure (upper left); T4 attachment and DNA injection (lower left); and a typical -six steps- lytic cycle for *E.coli* (right) (ASM Org, 2016; Britannica, 2016; Study Blue, 2016).

There are two processes: Lytic and lysogenic which are described schematically in in Figure 2.14 for comparison. In contrast to lytic pathway in lysogeny, the viral genome ("prophage") is integrated into the host DNA for some period of time and may switch to the lytic cycle at some later time which is called "**induction".** Lambda phages are typical "**Lysogenic phages".** Most bacteriophages are temperate indicating that this life strategy is advantageous. One T4 phage = 300 new phages (may exterminate hosts, while lambda phage infects one host and host produces 1000 daughter cells (can live with hosts), means that Lambda emerges with 100 phages per cell = 100,000 new phages. There are a series of Tphages - T1, T2, etc. They are nano in size, latent periods are 13-40 mins (including all phases of bacterial infection and phage growth) and burst size (the number of virions - babies) may reach 300.
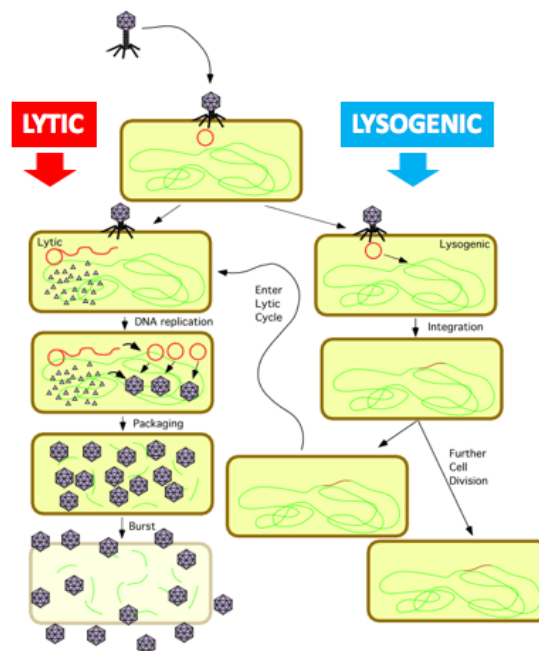


Figure 2.14. Comparison of "Lytic" and "Lysogenic" processes (World Press, 2016b).

### 2.4.2.2. Bacteriophages Immobilization

As mentioned several parts of this thesis, bacteriophages a promising alternative bioprobes for specific detection of target bacteria. In all these applications one of the most important criteria is "oriented immobilization" (head down-tail up) of the phage onto the support ("carrier") matrix/platform (Figure 2.15). The tails of the

phages carry several proteins as biospecific recognition elements which recognize and specifically bind to the target bacterial cell wall (Kutter and Sulakvelidze, 2004), then the genetic element (DNA/RNA) is then injected into the bacteria for propagation as explain in the previous parts above. It means that immobilization of these types of phages correct immobilization is via the head. Note that the head of phages is negatively and the tail is positively charged. Therefore, they can be immobilized in a correct orientation onto the positively charged surfaces means tails will be free to interact with the target bacteria (Serwer and Hayes, 1982).

Phages have been immobilized on several surfaces by simple physical adsorption (onto positively charged surfaces by electrostatic interaction) or chemical bonding by different chemistries (Balasubramanian et al., 2007; Lakshmanan et al., 2007a; Lakshmanan et al., 2007b; Nanduri et al., 2007; Handa et al., 2008; Shabani et al., 2008; Singh et al., 2009; Cademartiri et al., 2010; Handa et al., 2010; Anany et al., 2011; Arya et al., 2011). It was proposed that chemical immobilization is more stable and more suitable in sensor applications. Much higher adsorption densities have been reported on the gold platforms via covalent bonding via amino group (Singh et al., 2009). Self-assembled monolayer have been also created to immobilize phages onto gold surfaces covalently in an oriented form (Arya et al., 2011).

Silane chemistry have been used to immobilize phages onto for silicon based platforms for *Salmonella* detection (Handa et al., 2008; Handa et al., 2010). Electrochemical oxidation has been used to generation functional groups on the carbon surfaces T4 phages immobilization and for further *E.coli* capture (Shabani et al., 2008). Immobilization of phages in highly oriented form may be achieved by using biotin-streptavidin couple (Gervais et al., 2007; Tolba et al., 2010). Figure 2.16 shows an example of phage immobilization onto a sensor surface using this couple. Phages are covalently immobilized onto the sensor surfaces, while the proteins on the head are biotinylated and therefore oriented immobilization phages onto biosensing platforms are achieved by interaction of biotin-streptavidin. High and active phage immobilization has also been reported (Gervais et al., 2007). However, these protocol consist of multistep processes and expensive chemicals that limit economical uses of this approach.
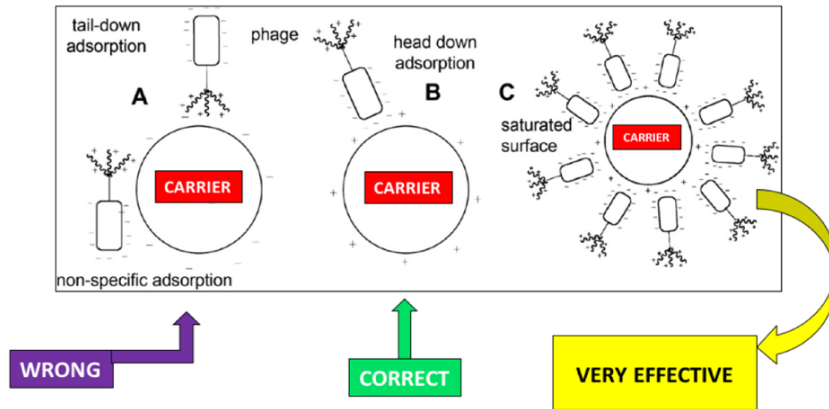
Figure 2.15. Phage immobilization onto surfaces. Adapted/modified from the related literature.
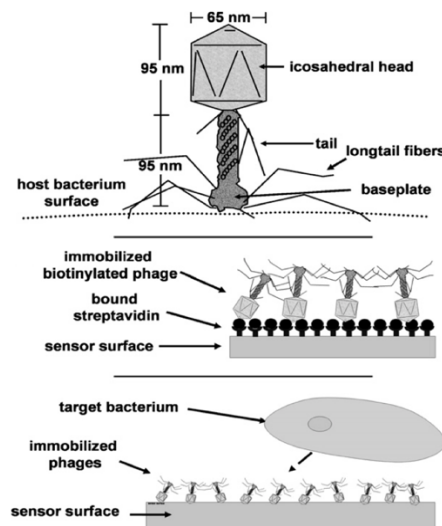


Figure 2.16. Oriented immobilization of phages using biotin-streptavidin couple onto bio-sensing platforms (Gervais et al., 2007).

Attaching phages onto surfaces by physical means is a very simple and in expensive approach. Surfaces may be replenished easily and reused. However, surface density of the phages initially will be relatively low and may be less predictable. It should be noted that in bio-sensing applications, when the phages on the surfaces are interacted with the target bacteria, their number will increase very rapidly after infection therefore the signal will increase (enhanced) significantly and reach to detectable levels.

24

Phages should be highly pure for a good immobilization protocol. Phages are propagated in the host bacterial cultures, therefore bacterial proteins, lipids and carbohydrates contaminate severely which in turn cause many problems in any kind of applications of those phages. Several methods for phage purification have been proposed including precipitation-gradient centrifugation using usually poly(ethylene glycol), ultrafiltration, ultra-high speed centrifugation, size exclusion chromatography and chromatofocusing (Humphrey et al., 1997; Singh et al. 2009; Naidoo and Lindsay, 2010). For the purity to be reached, both cost and difficulty of applications should be considered. Here **in this PhD thesis** after several preliminary studies we have decided to use first ultrafiltration (membranes with about 0.22 μm) which was followed by centrifugation around 12000g in which effective and healthy phages were obtained and used for further applications, as also described in the later parts of this section.

There are wild-type phages for potential use in bacterial detection. However, the followings have been considered as their main drawbacks. There may be loss of signal after lysis (Singh et al, 2009; Singh et al, 2011). Possible enzymatic activity of the phages against certain bacterial receptors may lead to inconsistent signals - which may be due to detachment of bacteria from the surface (Lindberg et al., 1978). Phages on the substrate surfaces may dry, collapse and lose their recognition ability to the host bacteria. These are all considered in our studies presented **in this PhD thesis.**

### 2.4.2.3. Quantification of Bacteriophages

One of the most widely used quantification technique of bacteriophages is the "**Plaque assay**" which was also applied **in this PhD Thesis** (Brown and Smith, 2016). A typical virus (including bacteriophages) plaque assays is schematically described in Figure 2.17. Typically, the host cell culture is mixed with a dilution of the phages suspension and the mixture added on the surface of culture media plates.  As the host cells grow and form lawns on the plate surface the plaques showing the bacterial cell destruction by the phages become visible and can be counted to quantitate the phage in the suspension (Plaque assay, 2018).
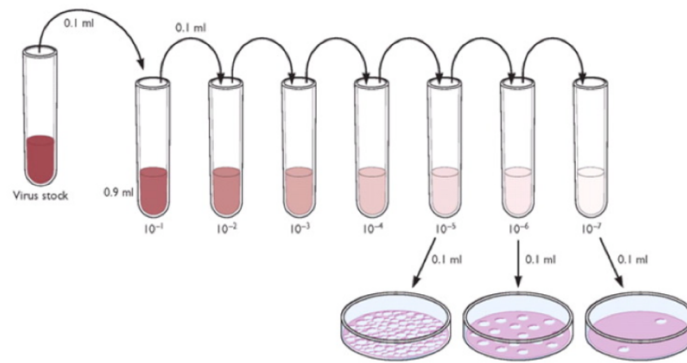
Figure 2.17. A typical Plaque assay (Plaque assay, 2018).

## 2.3. Plasmonic Metallic Nanoparticles

In recent year due to the "size and shape-dependent" properties metallic nanoparticles have been extensively studied (Figure 2.18) (Rosi and Mirkin, 2005; Boken et al., 2017). Particularly AuNPs and AgNPs been studied/applied very extensively in wide variety of fields/applications including medical imaging/sensing/ therapy. The followings make them excellent materials also for bio-based applications: (i) Excellent and variable optical properties. They do have strong plasmon band that make them excellent candidates as "optical signal enhancers" - that is one of main objectives **in this PhD thesis** for detection of pathogenic bacteria; (ii) small size/high surface area; (iii) forming stable nanoemulsion; (iv) can be easily sterilised by sterile filtration which is critical for medical applications; (v) easy to be uptaken by the cells and organelles; and (vi) they exhibit (especially AgNPs) very strong antibacterial properties.

### 2.3.1. Gold Nanoparticles

Gold nanoparticles are being attracted huge and increasing attention in nanomedicine due to nanoparticle properties mentioned above and - in addition – inertness in biological system (in the body) (Figure 2.19) (Boisselier and Astruc, 2009; Dreaden et al., 2012). The bulk gold reflects light, but in contrary gold nanoparticles do absorb, transfer, and convert light into energy (heat). The gold nanoparticles - in more historical terms - the "gold colloids" are ruby red when transmitting light, while green in reflecting.
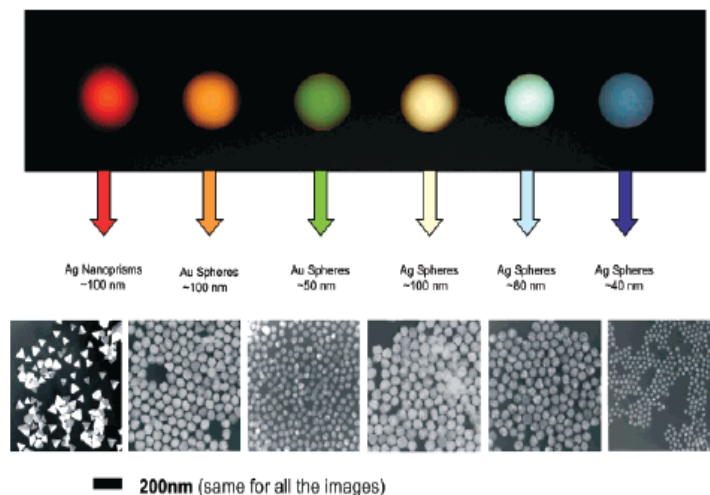
Figure 2.18.  Optical properties of AuNPs and AgNPs with different size and shape (Rosi and Mirkin, 2005).
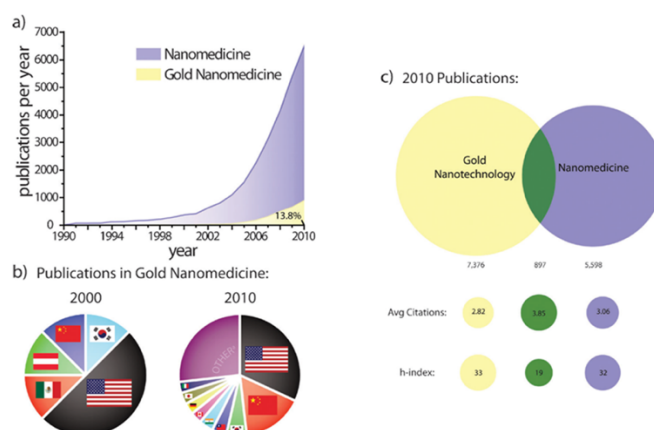


Figure 2.19.  Interest in gold nanoparticles in "Nanomedicine" (Dreaden et al., 2012).

Several techniques have been proposed in preparation of AuNPs. One of the successful approaches is the "Brust-Schiffrin" method. Here, $Au^{+3}$ ions are reduced by $NaBH_4$ (Figure 2.20) (Daniel and Astruc, 2004). The color of the organic phase is orange at the beginning but turns to deep brown after addition of the reducing agent ($NaBH_4$). The Brust-Schiffrin method for synthesis of AuNPs was first presented in the beginning of 1990s, and became one of the most successful techniques to produce stable AuNPs nanoemulsions with controlled size in the range of 1.5 and 5.2 nm.
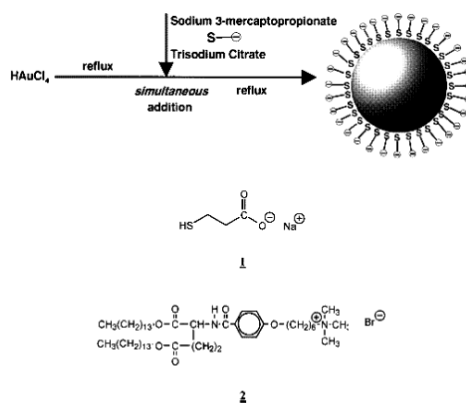
Figure 2.20.  The "Brust-Schiffrin" method for production of AuNPs (Daniel and
Astruc, 2004).

One of the classical methods for synthesis of AuNPs is the "Turkevich-Frens"
method in which AuNPs are produced in aqueous solutions from the reduction of
$Au^{+3}$ ions using several reducing agents (e.g., citric acid and ascorbic acid) and
others water-soluble polymers and chemicals as surfactants, capping agents, etc.
(Daniel and Astruc, 2004). Irradiation or heating are also applied for further control
the reduction rate, therefore the size of the AuNPs. Nanoparticles in a wide range
the size are produced by this classical method even today. Several factors
including the followings control the size and size distribution: (i) type, content and
aging time of the seed solution; (ii) surfactants types and concentrations; (iii) type
and amount of the ingredients (e.g., $AgNO_3$, ascorbic acid); and (iv) temperature.

One of the important procedures for AuNPs synthesis - worthy to include here -
has been developed by Sakai and Alexandridis who have presented that
poly(ethyleneoxide)-poly(propyleneoxide) (PEO-PPO) block copolymers (commer-
cially available Pluronics or Poloxamers) can act as very efficient reductants and
stabilizers. Here - AuNPs with different sizes are synthesized in a single-step by
using these block copolymers gold salts at room temperature (Figure 2.21) (Sakai
and Alexandridis, 2005). Nanoemulsions carrying AuNPs are-highly stable for
several years. AuNPs with different shapes (e.g., spheres, plates, prisms) can be
produced by controlling/ changing the PEO-PPO composition, molecular weight,
and concentration.

Many nice and detail synthesis protocols to produce gold nanoparticles/structures
with different size/shape have already been presented/established in the related

literature as exemplified in Figure 2.22 (Boisselier and Astruc, 2009). UV-spectra are usually used to demonstrate the optical (plasmonic) properties of nanoparticles. Figure 2.23 shows typical UV-spectra of both spherical and rod-shaped nanoparticles. There is only one single peak for nanospheres and it shifts depending on the size (the maximum peak, $\Delta\lambda_{max}$ shifts to right when the particles size gets bigger). Nanorods have two peaks - one small which belongs to the diameter and one large demonstrates the length. When the aspect ratio (AR: the ratio of length to diameter) increases the $\Delta\lambda_{max}$ shifts to right - to the red zone in electromagnetic waves. Note that $\Delta\lambda_{max}$ values are typical to describe the particle size and shape.
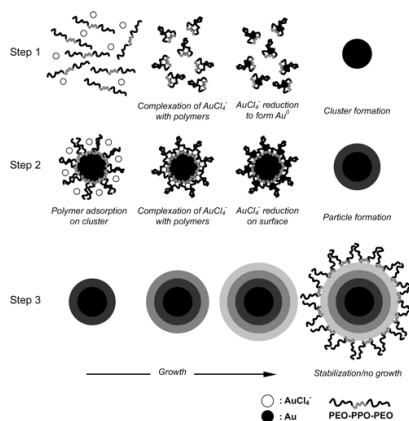


Figure 2.21.  Synthesis of AuNPs by using PEO-PPO block copolymers for reduction and stability (Sakai and Alexandridis, 2005).



Small (A) and large (B) nanospheres, (C) nanorods, (D) sharpened nanorods, (E) nanoshells, (F) nanocages/frames, (G) hollow nanospheres, (H) tetrahedra octahedra/cubes /icosahedra, (I) rhombic dodecahedra, (J) octahedra, (K) concave nanocubes, (L) tetrahexahedra (M) rhombic dodecahedra, (N) obtuse triangular pipyramids (O) Trisoctahedra and (P) nanoprisms.
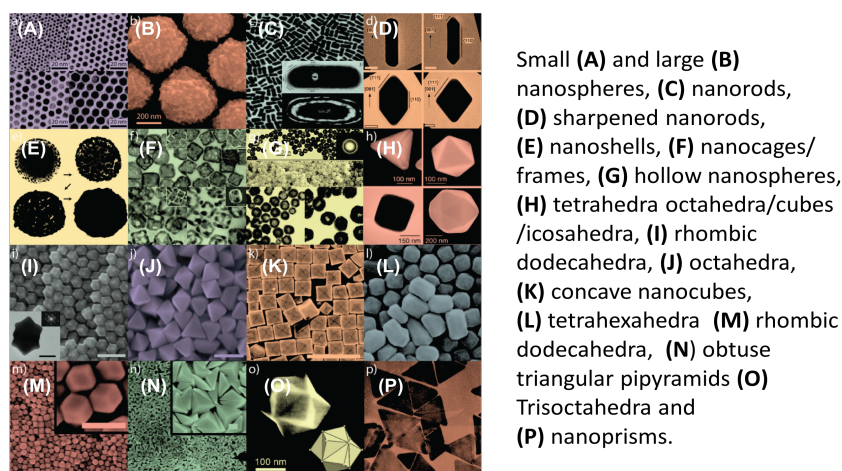
Figure 2.22.  Gold nanoparticles/structures with different size/shape (Boisselier and Astruc, 2009).

## 2.3.2. Silver Nanoparticles

Silver nanoparticles (AgNPs) have attracted a great attention as antibacterial agents for diverse applications including nanomedicine. They are incorporated in clothing (such as socks effecting the odour-forming bacteria); various food contact materials (packaging), storage bags, device (such as refrigerator) surfaces, etc.
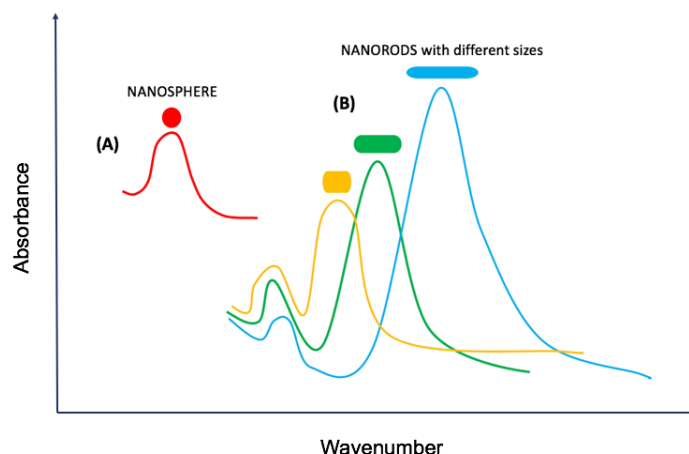


Figure 2.23.  Representative UV-absorbance spectra of: (A) Nanospheres and (B) nanorods with different sizes.

There are several synthesis protocols - each method has its own advantages/ disadvantages. The mean nanoparticle size and size distribution, shape, stability, capping (coating layers), and the presence of impurities are dependent on both the recipe and production protocol. Most commonly, AgNPs are obtained by reduction of silver nitrate using either a reducing agent or photo-reduction using UV-source. Several synthetic and biological approaches for preparation of silver nanoparticles can be found in the related literature. In synthetic methods several reducing and capping (for stability) agents, such as citrate, SDS, PVP are used to prevent agglomeration of NPs acting as surfactants. Microorganisms, plants, etc. are used in the biological approach. The molecules present in the microbial supernatant reduce $Ag^+$ to nanoparticle form. The obvious drawback of this method is the purification of AgNPs contaminated with several molecules coming from the extract that may cause problems in medical use.

There are many applications of AgNPs, most of them are related to their antibacterial properties on pathogenic bacteria as demonstrated in Figure 2.24 schematically (Moghtader et al., 2014). Figure 2.25 summarizes medical uses of AgNPs. Their excellent plasmonic properties have made them attractive nanostructures for enhancing optical signals in many biosensor applications.
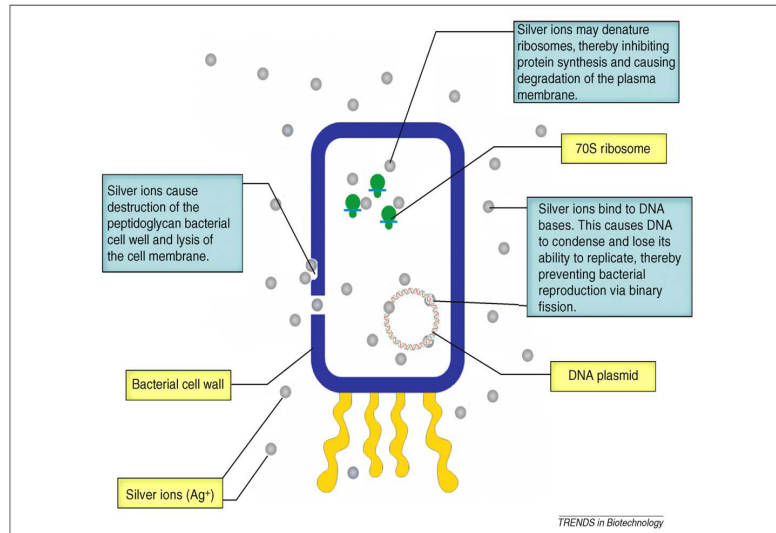


Figure 2.24.  Antibacterial effect of AgNPs on pathogenic bacteria (Chaloupka et al., 2010).
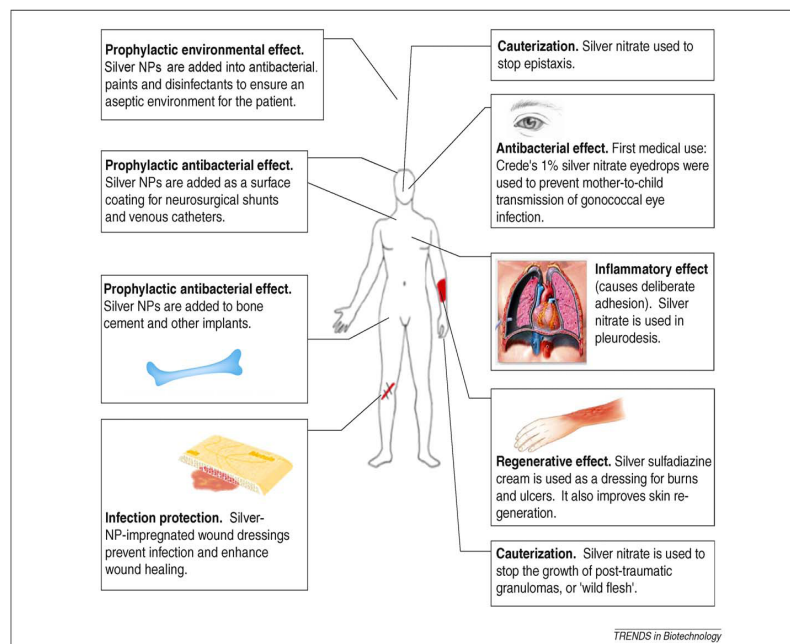


Figure 2.25. AgNPs in medical uses (Chaloupka et al., 2010).

## 2.4. Biosensors

### 2.4.1. Basic Definitions

Biosensors are analytical devices which are usually composed of a sensor platform and bioprobes (bio-recognition elements/entities) which are attached/ immobilized preferentially-covalently on those platforms (Figure 2.26). Bioprobes interact specifically with the target on the platform and a measurable signal is generated, which is amplified and measured. It is possible to measure the target concentration (amount) in the medium also which is the main difference between biosensors and diagnostic test kits that are much simpler systems and give only an information about the target if it is present or not - not quantitative results.

Biosensors may be evaluated in two main groups: (i) detection of changes differences in mass and chemical composition, heat, optical properties, without using a label; and (ii) using labels such as optical labels (fluorescent dyes, etc.), enzymes or electrochemically active labels, etc. Figure 2.27 exemplifies both approaches in which antibodies are used as bioprobes just for demonstration here. Almost all technologies described schematically in this figure are being utilized for bacterial detection using bacteriophages as specific bioligands/bioprobes (Olsen et al., 2006; Shen et al., 2009; Li et al., 2010; Tawil et al., 2012; Singh et al., 2012; Singh et al., 2013)
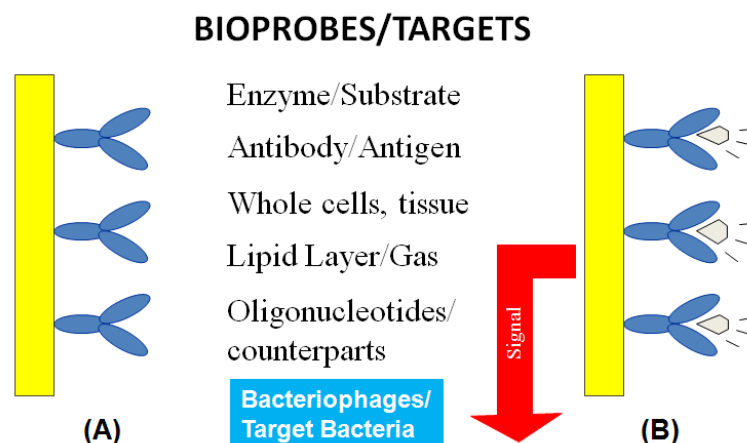


Figure 2.26. Biosensors: (A) Bioprobes/targets (example: antibody/antigen); and (B) generation of the signal after interaction on the platform surfaces.

In the context of **this PhD thesis** three optical based label-free techniques have been studied - which are: (i) "Surface Enhanced Raman Spectroscopy (SERS) which is applied as the main technique; the other two were included to contribute these studies - which are (ii) Localized Surface Plasmon Resonance (LSPR) spectroscopy; and (iv) Matrix Assisted Laser Desorption/Ionization - Time to Flight Mass Spectroscopy (MALDI-TOF MS). More detail general information about these approaches are given in the following sections separately.
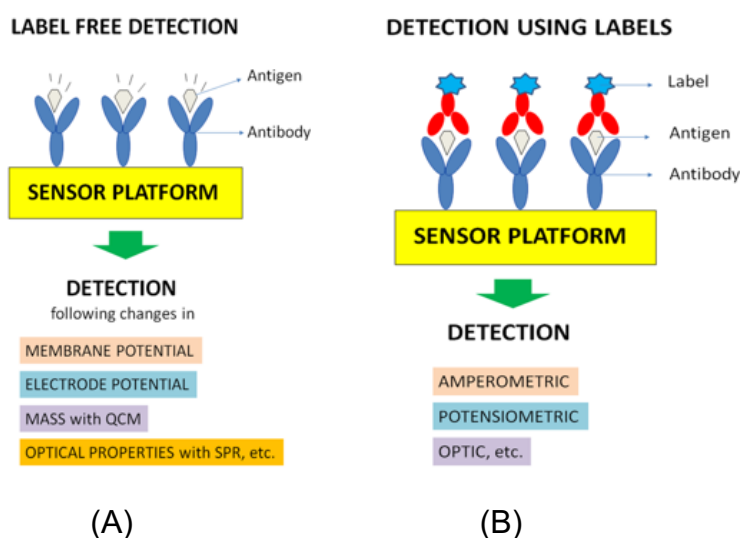


Figure 2.27. Classification of biosensors by detection technologies (the antibody/ antigen couple is used here as an example): (A) label free; and (B) using labels.

## 2.4.2. Bioprobes

A number of biological recognition elements ("bioprobes") have been studied for sensitive detection of pathogenic bacteria. Similar to nucleic acid-based test systems, oligonucleotides have been used as bioprobes in which detection is based on interaction of two complementary oligos (i.e., the probe and target) (Figure 2.28A). There are already commercial products based on nucleic acid (as bioprobes) sensor technology for pathogen detection - but with still several significant limitations - as also discussed in the previous sections given above (Mothershed and Whitney, 2006; Singh et al., 2013). The purity of the probe-nucleic acid produced by PCR-based amplification methods may not high enough which results false positive findings. The template nucleic acid may be degraded which results false negative indications. It is not possible to observe the viability of

the bacteria and cannot be applied for detection of bacterial toxins which are important limitations.

ELISA which is a rather conventional/most widely applied technique based on antibody-antigen specific interactions and has been also successfully used in biosensor platforms for diverse applications including for pathogen detection and monitoring (see aslo Section 2.1). There are several/successful antibody immobilization techniques onto surfaces to create biosensor platforms. They do recognize the target bacteria from the surface groups (as seen in Figure 2.28B) with quite high specificity. Both antibodies and oligopeptides have been studied/ used as specific bioligands/probes for bacterial detection and also their pathogenic spores and toxins.



(A)                                              (B)
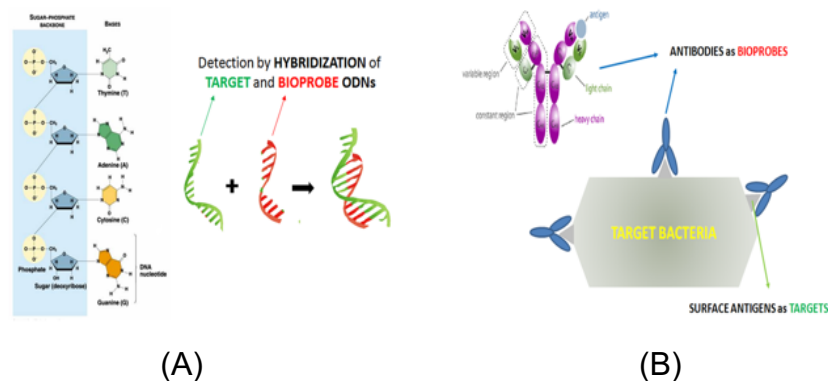
Figure 2.28. Classical bioprobes: (A) Oligonucleotides (ODNs); and (B) antibo-
dies. Adapted/modified from the related literature.

These bioprobes exhibit quite high specific affinity towards their target, but they exhibit also quite significant drawbacks as follows: (i) Antibodies are proteins - therefore sensitive to temperature, pH, several chemical and enzymatic attacks - and lose their 3D active forms irreversibly; (ii) they are temperature sensitive therefore should be kept in the refrigerator and should be transported in cold-chain. Their shelf life may be short which limits their application; (iii) polyclonal antibodies have several recognition epitopes. They are inexpensive but they are not very specific as monoclonal antibodies, one should be careful to use those polyclonal ones; and (iv) antibody production is difficult, animals are needed which is difficult and brings also ethical issues. There are several extensive and nice reviews about these immunobased sensors explaining advantages and limitations also (Perelle et al., 2004; Byrne et al., 2009; Singh et al., 2013).

As described in the previous sections in detail, bacteriophages recognize bacteria very specifically even strain level and therefore have been received great attention (rapidly increasing) as bioprobes for pathogen detection. Bacteriophages, shortly called as "phages", are viruses that infect bacteria specifically (Figure 2.29) (Microbiology Society, 2013; Nature, 2016). Phages do use their bacterial hosts for propagation. As explain more in detail in the next chapter **in this thesis**, phages find and bind to their specific bacteria, inject their DNA via bacterial cell wall, propagate in the bacteria to produce new virions.  In the case of lytic-phages they lyse (kill the bacteria) and come out. However, some other types - lysogenic phage after infection of the host bacteria they do integrate their DNA genome into the bacterial genome. They do stay silent there until a stimulation, then they do also propagate and new virons come out. Recently Singh *et al.* has extensively/nicely reviewed use of bacteriophages in biosensors as specific bioprobes for bacterial detection (Singh et al., 2012; Singh et al., 2013). The main advantages of using bacteriophages over other bioligands (e.g., oligonucleotides and antibodies) are as follows, **which are the main rational using phages as bioprobes in this PhD thesis**: (i) most phages are very specific they do recognize bacteria at even strain level specifically; (ii) they recognize only living bacteria which is very critical issue (others do not); (iii) their number increase after invasion of target bacteria which means even one bacteria may be detected (very high sensitivity); (iv) there are about $10^{31}$ phages exist in the world means a huge potential for detection/therapy.
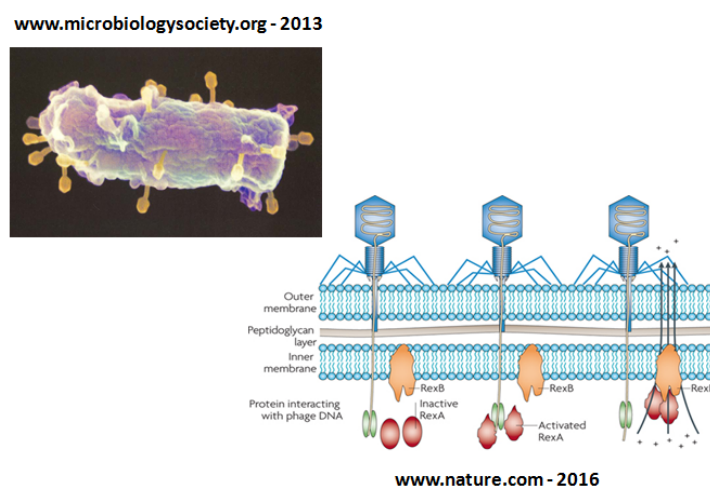


Figure 2.29.  Bacteriophages as bioprobes for specific detection of the target pathogenic bacteria (Microbiology Society, 2013; Nature, 2016).

### 2.4.3. Raman Spectroscopy

### 2.4.3.1. General Definition

Spectroscopy deals with interactions between electromagnetic radiation and matter. The incident light (the electromagnetic radiation) is absorbed, emitted or scattered which is followed by different techniques to measure/detect for analyzing the target substances/molecules. There are a variety of very successful spectroscopic techniques, including different "Optical Spectroscopies"; "Nuclear Magnetic Resonance Spectroscopy", "Mass Spectroscopy", etc., (Gauglitz and Vo-Dihn, 2003). Infrared absorption (IR) and Raman scattering (RS) are the most widely used - complementary and competitive - optical spectroscopy techniques which are both based on detecting vibrations in molecules. IR and RS spectra represents the chemical structure of the target substances - they are also called "fingerprints". It is also possible to analyze molecules quantitatively/semi - quantitatively in different media - solids, liquids or vapors by these techniques. IR is more widely used technique however RS is getting also very popular. Recently a number of portable RS systems with quite low costs, but with high enough sensitivities have been developed/commercialized in which the main problems such as fluorescence shading and sample degradation are reduced significantly.

Especially in recent years, "Surface Enhancement (SE)" techniques have been proposed in which plasmonic properties of nanoparticles and nanostructures are utilized to increase the intensity of the signals (Moskovits, 1985; Hanlon et al., 2000; Cotton, Kim and Chumanov, 1991; Haynes, McFarland and Van Duyne, 2005; Bocklitz et al., 2009; Han et al., 2009; Bocklitz et al., 2011; Rodriguez-Lorezoa, Fabrish and Alvarez-Pueblaa, 2012). It should also be noted that RS spectra can be obtained in aqueous solutions, samples in the original packages and without any sample preparation steps which have resulted a huge interest in the RS system.

**Discovery of Raman Spectroscopy**. In 1928, an Indian Physicist C. Venkata **Raman** described Raman scattering by molecules and changes ("shifts") in frequencies of the scattered beams depending on the chemical structure of those molecules (Figure 2.30) (Raman and Krishnan, 1928). These are the first definitions to develop Raman spectroscopy that we are using today for specific detection of numerous molecules/structures. He has awarded by the Nobel Prize

in Physics in 1930. In his "Nobel Price Lecture - The Molecular Scattering of Light" on December 11, 1930 in the first part - "color of the sea" (which was also published as a note in *Nature*), he has described that "the color of the ocean independent of sky reflection or absorption but it is due to Raman scattering".
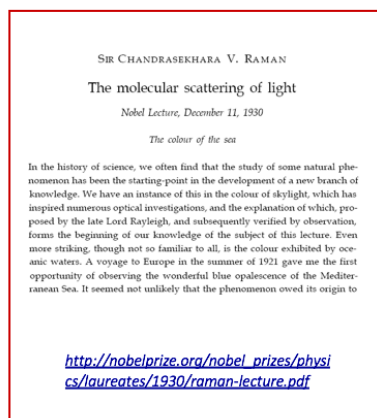


Figure 2.30.  C. Venkata Raman - an "Indian Physicist" - who discovered Raman scattering - awarded with a Nobel Prize.

Two types of scattering occur when electromagnetic radiation (EMR) interacts with a molecule (Figure 2.31): (i) Elastic scattering ("Rayleigh scattering"), which is very intense and most probable (the green arrows); and (ii) inelastic scattering ("Raman scattering") which is rather very weak (the red arrow). Most of the incident photons are elastically scattered by the molecule in which the energy of the incident photons equal to the energy of the scattered photons. While only a very small fraction is scattered inelastic and the energies of the emitted light is different than that of the incident light which is the so-called "Raman scattering".

In this case the energy is absorbed and the molecules go to an exited vibrational state ("virtual state from the ground state") which is followed by the simultaneous emission of Raman scattered photons. In Figure 2.32 the horizontal lines are the vibrational energy levels. The difference in length between upward arrows ("the excitation light") and down arrows ("the Raman scattered light") is the molecular vibration frequency.
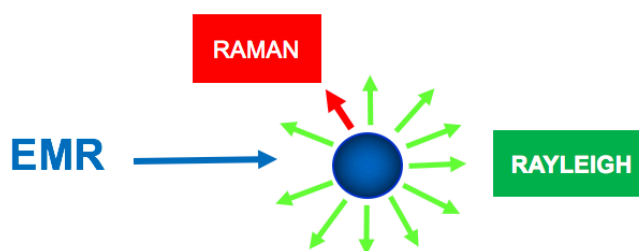
Scattering when electromagnetic radiation
(**EMR**) – an incident photon interacts with a
molecule: (i) **RAYLEIGH** and (ii) **RAMAN**

Figure 2.31. Scattering when electromagnetic radiation "an incident photon" interacts with a molecule. Adapted/modified from the related literature (Moskovits, 1985; Gauglitz and Vo-Dihn, 2003).

One of the important drawbacks in the earlier Raman spectroscopy studies/ devices - as also mentioned above - is the spectral interference especially by fluorescence which should be minimized or even eliminated. It should be noted that - in the Raman systems - the incident light can be in the excitation range from UV to near-IR. Almost the same change in vibrational energy is observed in all cases. This means that any of those incident lights can be used to form the Raman scattering. The light frequencies in fluorescence and Raman scattering are similar which means that an intense fluorescence background is observed when visible excitation is applied in Raman systems - that is of course not desirable. However, near-IR light and UV excitations are too low to excite fluorescence, means that Raman scattered light frequency is much higher than the fluorescence light frequency. This means that Raman spectra should be obtained in the near-IR region of the spectrum or in the UV region (usually below 270 nm), in order to reduce the fluorescence background.

As seen in Figure 2.32, the radiation can be either higher (Anti-stokes) or lower energy (Stokes) levels comparing to the incident light. Note that the Stokes shifted Raman is the most common due to higher probability. Due to the Boltzmann distribution we see Stokes lines with a much greater intensity than Anti-stokes in which the ground state is more populated at room temperature.
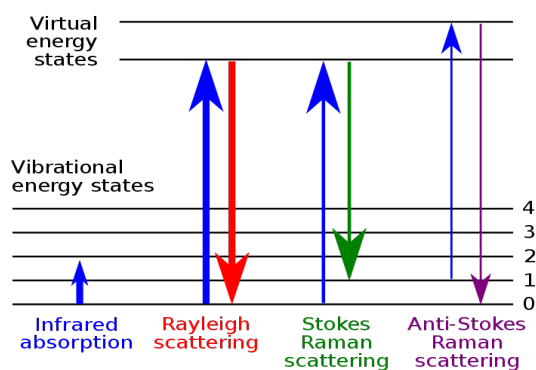
Figure 2.32.  Comparison of Rayleigh and Raman scatterings. Adapted/modified from the related literature (Moskovits, 1985; Gauglitz and Vo-Dihn, 2003).

The Raman spectra are presented as the changes in the scattered light intensity with changes in frequency ("Raman shift" - in wavenumber - $cm^{-1}$). The Raman spectrum of each molecule is consist of a series of characteristic peaks ("bands") corresponding the characteristic vibrational frequencies, which are also so-called "fingerprints" (Hanlon et al., 2000). In many of the related reviews/books the Raman spectrum of cholesterol is used for demonstration - which is also included here and given in Figure 2.33. Some characteristic/representing peaks (i.e., the fingerprints of the cholesterol molecule) in this spectrum are the peak at 1440 $cm^{-1}$ which represents the $CH_2$ and $CH_3$ deformation vibrations and the peak at 1670 $cm^{-1}$ corresponds to C=C stretching vibrations.
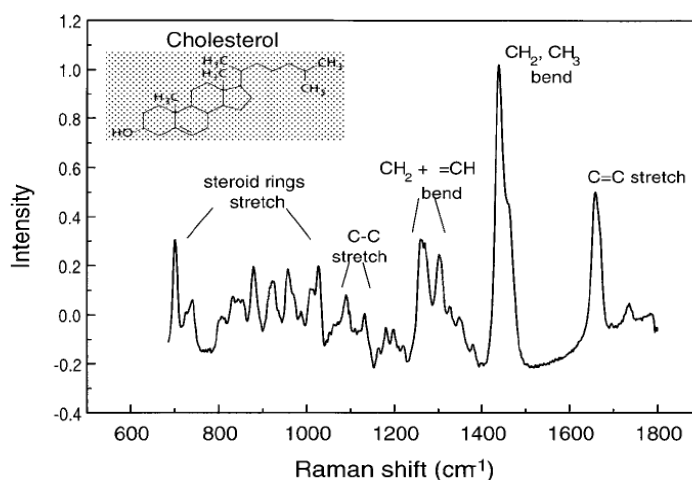


Figure 2.33.  A typical Raman spectrum - "Fingerprints" of cholesterol (Hanlon et al., 2000).

39

A typical Raman spectroscopy system are constructed bring together several typical components as schematically shown in Figure 2.34. Lasers, spectrometers, optics and detectors are used. The laser excitation frequency is one of the main characteristics of the Raman spectrometers. Both continuous and pulsed lasers are used. Filters are used to remove the Rayleigh scattered photons. If the Rayleigh light is allowed to enter the spectrograph un-attenuated, it will cover (depress) all or part of the much weaker Raman spectrum. Then, the Raman scattered light is dispersed into its component frequencies for detection. Photomultipliers were the standard detectors used until recently. The "Charge Coupled Detector (CCDs)" are now more commonly used.
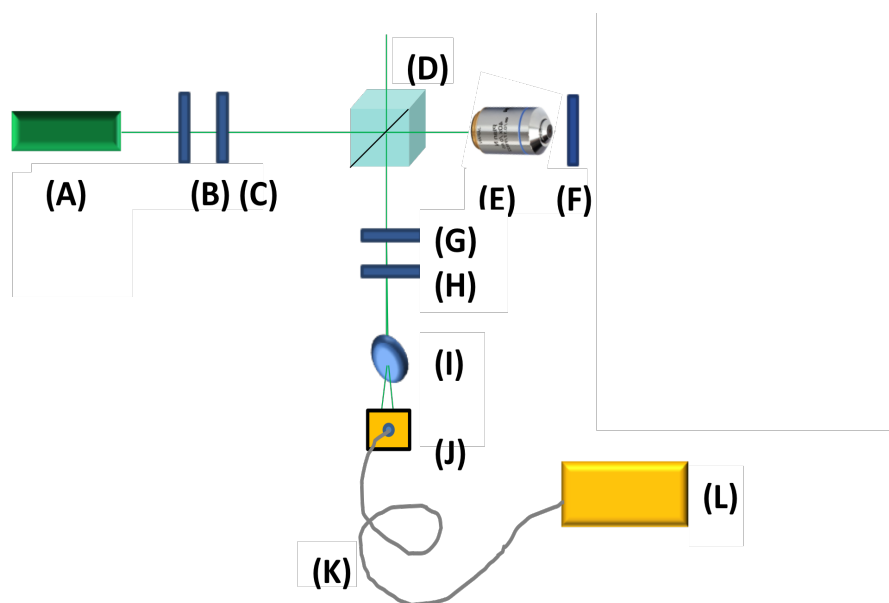


Figure 2.34. A typical Raman spectroscopy system: (A) A laser (532 nm and/or 735 nm); (B) laser line; (C) low pass filter (<750nm); (D) beam splitter; (E) objectives (10x-100x); (F) sample holder; (G) high pass filter (>550 nm); (H) notch filter; (I) lens; (J) collimator; (K) fiber optic cable; and (L) spectrometer.

Raman spectroscopy are being used in diverse/wide range of applications including material characterization/analysis, medical imaging and sensing/ detection/identification of molecules, cells, tissues both healthy and diseased. The advantages of Raman over other optical spectral systems can be summarized as follows: (i) Sample preparation is usually not required; (ii) measurements can be done in aqueous media without any further treatment - because scattering due to water is quite low; (iii) it is a non-destructive and non-invasive approach means

can be applied both *in vitro* and *in vivo* quite safely and effectively. Today Raman endoscopy is considered as an important technique for medical imaging; (iv) since Molecules can be can be identified quite specifically using Raman spectral data with related libraries; (v) Raman spectra exhibit usually "cleaner/sharper" peaks than IR spectra; (vi) Raman spectra of both organic and inorganic molecules can be obtained; (vii) peaks corresponding to the symmetric linkages like "-S-S-, -C-S-, and -C=C-" are weak in the IR region however they can be measured by RS; (viii) information about 3D structural changes such as orientation and confirmation can be followed; (ix) information about intermolecular interactions can be obtained; (x) label free detection is possible and (xi) RS measurements can be conducted at different temperature, pressure, etc.

However, there are also disadvantages which include the followings: (i) Further improvements are needed because about 1 million incident photons can only generate one Raman scattered photon; (ii) expensive lasers, detectors and filters are needed for systems with higher resolution; (iii) weak signals are due to extremely small cross section about 10-30 $cm^2$ in non-resonant Raman case (15 orders of magnitude lower than fluorescence excitation); (iv) intensity enhancement is required for quantitative measurement. It should be noted that especially sensitivities of today's systems have been very successfully increased by using "Surface Enhanced Raman Spectroscopy (SERS)" which is briefly described below.

### 2.4.3.2. Surface Enhanced Raman Spectroscopy (SERS)

Surface Enhanced Raman Spectroscopy has recently emerged as a very popular field of research - especially over the recent years, we have observed tremendous impressive interest and related advances in this field, in which RS signals are enhanced by several orders where plasmonic nanoparticles and nanostructured metal surfaces are applied (Moskovits, 1985; Hanlon et al., 2000; Cotton, Kim and Chumanov, 1991; Haynes, McFarland and Van Duyne, 2005; Bocklitz et al., 2009; Han et al., 2009; Bocklitz et al., 2011; Rodriguez-Lorezoa, Fabrish and Alvarez-Pueblaa, 2012). In order to collect Raman spectra with sharp/clea peaks, signals should be enhanced significantly by using nanoparticles/nanostructures with plasmonic properties in the case of SERS that allows also molecular trace analysis.

SERS can be a resulted of two mechanisms, i.e. chemical and electromagnetic mechanisms (Haynes, McFarland and Van Duyne, 2005). In the chemical mechanism, the laser excites new electronic states as a result of chemisorption which yields a resonance condition. It is a short range effect (1-5 Å) and contributes "Enhancement Factor" ("EF") about $10^2$-$10^4$. However, electromagnetic mechanism is based on LSPR, which induces large electromagnetic fields at nanostructured surfaces where molecules are adsorbed. In contrast to chemical mechanism it is a long range effect which is about 2-4 nm, affected by all factors determining LSPR, and its contribution to EF is usually larger than $10^4$.

As also discussed in the previous section, nanoparticle aggregation may produce Raman enhancements quite significantly ($10^{14}$-$10^{15}$) even making single molecule detection possible (Kneipp et al., 1998). This enhancement in intensity is a result of the highly localized fields of plasmons. There is a huge and very detailed literature in which nanosize entities (particles and surfaces) with different material (mainly silver and gold), shape, size, orientation, porosity, etc. have been used (Moskovits, 1985; Hanlon et al., 2000; Haynes, McFarland and Van Duyne, 2005; Stiles et al., 2008; Bocklitz et al., 2009; Han et al., 2009; Bocklitz et al., 2011; Rodriguez-Lorezoa, Fabrish and Alvarez-Pueblaa, 2012; Srivastava et al., 2015).

Several SERS based-biosensors have been for detection of very different substances (Herne, Ahern and Garrrell, 1991; Vo-Dinh, Houck and Stokes, 1994; Weldon and Morris, 2000; Cavalu at al., 2001; Sundram et al., 2013). SERS was also considered as an emerging/powerful methodology for microbial including bacterial detection with high sensitivity (Singh et al., 2012; Singh, Poshtiban and Evoy, 2013; Jarvis and Goodacre, 2004; Jarvis, Brooker and Goodacre, 2004; Zeiri et al., 2004; Sengupta, Mary and Davis, 2005; Zeiri et al., 2005; Gaus, et al., 2006; Sengupta, Mirna and Davis, 2006; Goeller and Riley, 2007; Griffiths and Evoy, 2007; Liu et al., 2009; Meisel et al., 2012; Stöckel et al., 2012a and b; Blattel et al., 2013; Meisel et al., 2014)

## 2.4.4. Surface Plasmon Resonance (SPR) Spectroscopy

### 2.4.4.1. General Descriptions

In the "Surface Plasmon Resonance" ("SPR") spectroscopy, adsorption of molecules/biomolecules from liquid onto planar films/surfaces - usually glass slides coated with a thin gold layer or other metallic (silver, copper, etc.) layers having with plasmonic properties are monitored. The principle is based on the excitation of surface propagating electromagnetic waves called surface plasmons which interact with the molecules on the surface that results the SPR signal, as schematically described in Figure 2.35. Here, the polarized laser beams from a laser source passing through a prism are reflected at the gold-glass interface (a total internal reflection). The incident light interacts with the gold atoms and excite surface plasmons which are basically strong electromagnetic waves on the metal surfaces. There is almost complete attenuation - a dip for that specific incidence angle ("SPR angle") is produced. The refractive index of the surface layer changes if there are molecules adsorbed onto the gold surface. A slight angle shifts is observed which depends the amount of the molecules adsorbed.

SPR sensors are label-free sensors not only to detect the targets but also allow to follow real-time interaction on the substrate surfaces to obtain the kinetics and equilibrium binding constants as schematically demonstrated in Figure 2.36. As seen in a typical experiment performed an SPR biosensor in which the target is first bind to the bioprobe on the surface, the target can be dissociated from the surface using different stimuli (by changing pH, ionic strength, etc.) - surface is regenerated and therefore could be used in repeated experiments. Both association and dissociation kinetics can be monitored.

Bacteriophages have been used as specific bioprobes on SPR sensors carrying bacteriophages as specific bioprobes have been used for bacterial detection. Balasubramanian et al. have studied *S.aureus* detection by using its specific phages as bioprobe on SPR platforms (Balasubramanian et al., 2007). Arya et al. have immobilized T4-bacteriophage chemically onto sensor surfaces and detected the target bacteria, i.e., *E.coli* by SPR, quite specifically (Arya et al., 2011). Tawil et al. presented detection of both *E.coli* O157:H7 and methicillin-resistant *S.aureus* (MRSA) with SPR in which sensor surfaces carrying bacteriophages were used to recognize those bacteria quite specifically (Tawil et al., 2012). The detection limits

in these studies were in the range of $10^2$-$10^3$ CFU/mL. The receptor binding proteins of bacteriophages have also been proposed as bioprobes for bacterial detection. *Salmonella* and *Campylobacter jejuni* have been detected by using gold coated substrates carrying genetically engineered receptor binding protein by SPR with a detection limit of around $10^3$ CFU/mL (Singh et al., 2011).
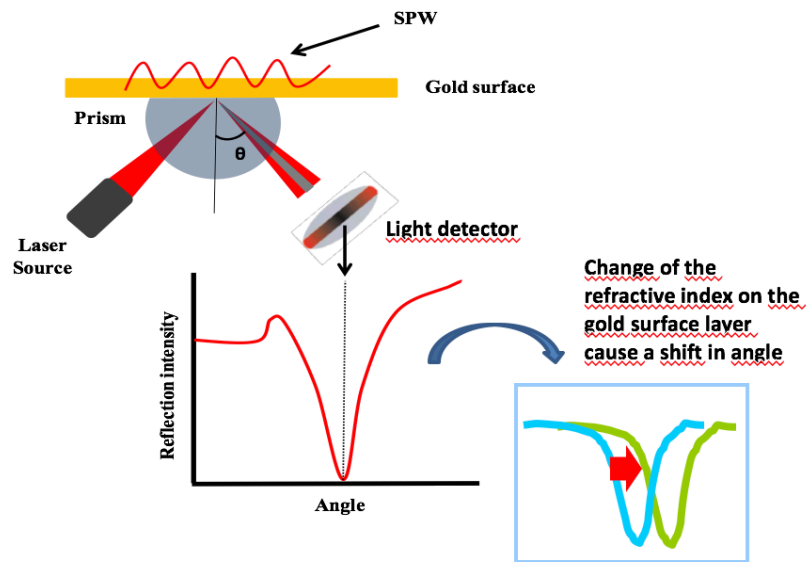


Figure 2.35. A typical SPR system. The refractive index on the gold surface layer changes due to adsorption of any substances that cause a shift in angle. Adapted/modified from the related literature.
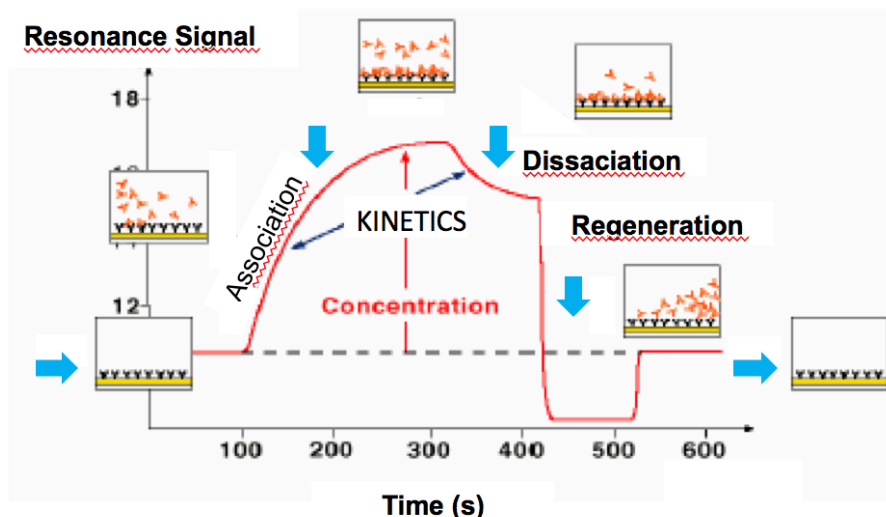


Figure 2.36. A real time SPR signal demonstrating the kinetics of interaction of bioprobe immobilized on the gold SPR slide surface and the target within the medium. Adapted/modified from the related literature.

SPR spectroscopy as a sensor platform have many advantages including: (i) It is a - label free - optical detection system; (ii) adsorption processes can be followed in real time with high sensitivity down to few seconds for measurement of binding kinetics; (iii) the method is surface sensitive and based on the changes the refractive index within about hundred nanometer of the sensor surface; (iv) different detection modes (angle and/or wavelength shift and imaging) could be applied; (v) lateral resolution could go down to few microns for using SPR imaging mode; and (vi) several SPR systems with different resolutions and prices are commercially available.

## 2.4.4.2. Localized Surface Plasmon Resonance (LSPR) Spectroscopy

"Localized Surface Plasmon Resonance" ("LSPR") is observed when an electromagnetic wave is interacted with the surface electrons of metallic/plasmonic nanoparticles (e.g., gold and silver) (Csaki, Stranik and Fritzsche, 2018). The distance between the particles should be smaller than the wave length in order to observe the LSPR effect as depicted in Figure 2.37 (Bohren and Huffman, 1983; Stiles et al., 2008). The followings affect the resonant frequency of the localized plasmon oscillations: (i) The distance between the particles; (ii) dielectric environment; and (iii) particle composition, size and shape. LSPR of the noble metals e.g., Ag and Au are observed in the visible wave range due to the energy levels of d-d transitions (Liz-Marsan, 2006; Willets and Van Duyne, 2007). The LSPR spectral shift detected in the LSPR based sensors (the scattering wavelength maximum - "$\Delta\lambda_{max}$") may be calculated from the following expression (Willets and Van Duyne, 2007). This equation is used to explain in the LSPR assays - probe-target interactions at the surface of nanostructures.

$$\Delta\lambda_{max} = m\ \Delta n\ [1\text{-exp}\ (\ \text{-}2d\ /\ l_d\ ) \qquad\qquad 2.1$$

In which, **m**: the bulk refractive index of the NPs; **Δn:** the change in the refractive index; **d:** the adsorbed layer thickness (nm); and **$l_d$**: the decay length of the electromagnetic field (nm).

Both gold and silver are used as plasmonic materials. The LSPR bands of silver are sharper and more intense than those of gold. However, gold nanostructures are chemically more stable and thiol containing molecular bioprobes could be easily immobilized (even in oriented forms) onto these nanoparticles/structures for biosensing - therefore it is used more often than silver.
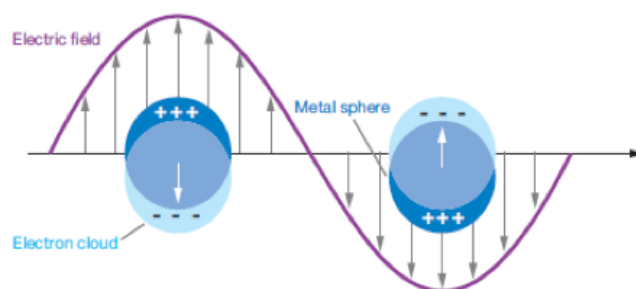
Figure 2.37. "Localized surface plasmon resonance" occurs as a result of the interactions between the light wave and surface electrons of metallic nanoparticles (Stiles et al., 2008).

The incident photons are either absorbed or scattered when the light beam interacts with metallic nanostructure. The LSPR extinction significantly enhances both absorption and scattering. This is (especially scattering) the basis of several LSPR-optical spectroscopy systems.

LSPR based sensor can be classified in the following two categories: (i) "*aggregation*" based; and (ii) "*refractive index*" based. The first category is based on near-field electromagnetic coupling which occurs when the incident light interacts with the nanoparticle aggregates that results clear color changes. Strong LSPR peaks are observed if the distance between two nanoparticles in the aggregates is smaller than the particle dimensions (Figure 2.38) (Willets and Van Duyne, 2007). For instance, when two different NPs carrying two different complementary molecules comes together they do interact specifically which results aggregation of the NPs that in turn causes color changes due to LSPR that is monitored.

Figure 2.39 describes schematically preparation of a refractive index based sensor platform in which the steps are as follows: (A) Preparation of a substrate (surface cleaning, etc.); (B) deposition of NPs with a predesign structure usually by nanolithography techniques; (C) bioprobe immobilization onto the NPs surfaces; (D) interaction of the bioprobe with the target on the substrate surface; which results a change in the refractive index that is observed as an LSPR shift (E) (Sepulveda et al., 2009).
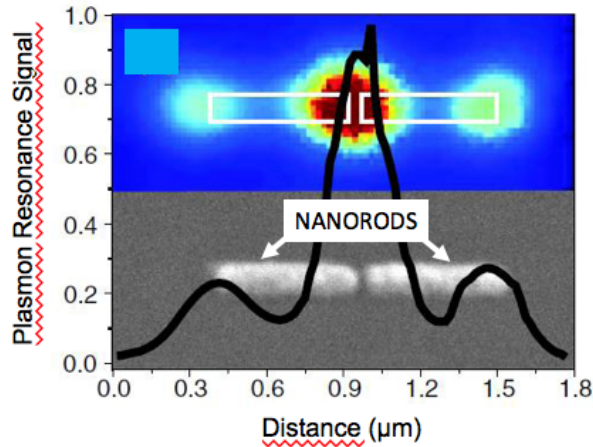
Figure 2.38. Aggregation based LSPR sensors. Strong LSPR signals are observed when the distance between the particles is smaller than the particle diameter (Willets and Van Dune, 2007).
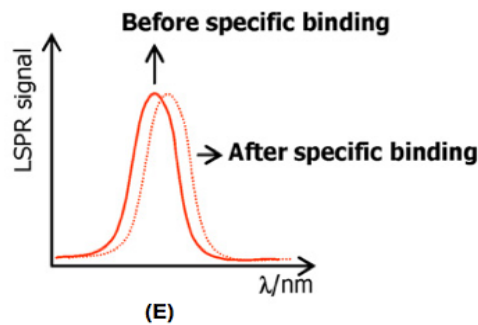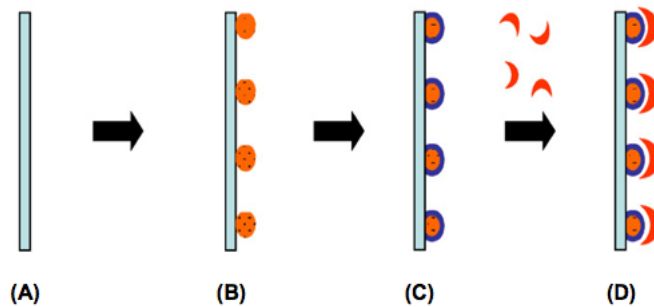


Figure 2.39. Preparation of a LSPR biosensor using nanoparticles and a typical response - change in the refractive (Sepulveda et al., 2009).

The surface polarization - therefore spectral properties of the nanoparticles - changes depending on both size and shape. Figure 2.40 - taken from the related literature - nicely demonstrates these relations (Lu et al., 2009). As a summary, it can be said that NPs having different LSPR spectra with different peak intensities

may be designed/produced to work in a wide electromagnetic wave region from visible to infrared regions.

Both the refractive index sensitivities and the characteristic electromagnetic field decay lengths ($l_d$) of the SPR and LSPR sensors are significantly different. The refractive index sensitivity of SPR sensors is large (~$2x10^6$ nm/RIU) (Jung et al., 1998) in comparison to a LSPR nanosensor (~$2x10^2$nm/RIU) (Malinsky et al., 2001). This means that SPR sensors are much more sensitive than LSPR sensors. However, the "$l_d$" of LSPR sensors is about 5-15 nm - this value is 200-300 nm for SPR sensors - that means high sensitivities are also achieved in LSPR systems (Jung et al., 1998).

Experimentally, SPR sensing requires at least an area of 10x10 μm spot size. This spot size for LSPR sensing is much lower, because high surface is of the NPs which allows high number of bioprobe immobilization that results enough signal strength even in very small sensing spots (McFarland and Van Duyne, 2003). The pixel size can be minimized down to 100 nm in LSPR therefore similar information could be obtained as the SPR. The other differences between two systems are temperature control. Due to lower refractive index specificity no temperature control is needed in LSPR while temperature should be controlled in the SPR systems. The difference in the cost between the two systems of LSPR and SPR is also an important issue.

Recently, LSPR spectroscopy progresses have made it excellent and sensitive tool, for detecting biological molecule interactions - the first LSPR as biosensing system was reported by Englebienne (Englebienne, 1998). Use of LSPR technique in nanobiotechnology has been published in a number of good papers. Van Duyne and co-workers were one of the first groups to investigate biological sensors based on metal nanoparticles using LSPR and SERS (Haynes, McFarland and Van Duyne, 2005). The detection of several biomolecules, such as streptavidin, anti-biotin, concanavalin, Alzheimer disease bio-markers, and others have been reported (Haes and Van Duyne, 2002; Riboh et al., 2003; Yonzon et al., 2004; Dahlin et al., 2005).
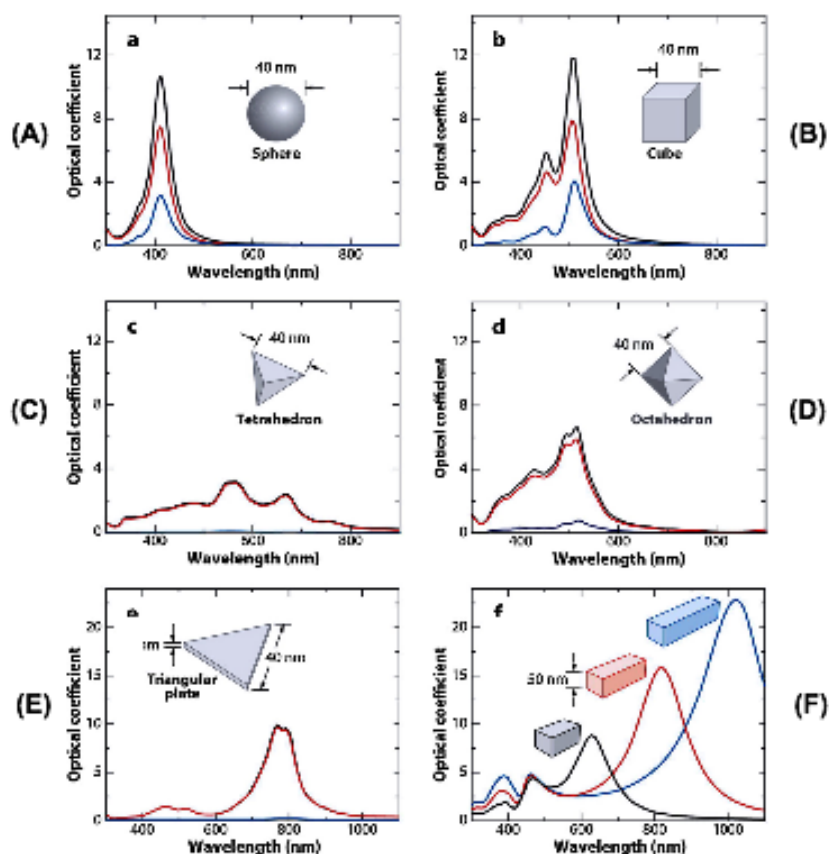
Figure 2.40. Typical spectra for AgNPs with different shapes: (A) A sphere; (B) a cube; (C) a tetrahedron; (D) an octahedron; and (E) a triangular plate. The extinction, absorption, and scattering spectra are black, red and blue - respectively; and (F) Extinction spectra of rectangular bars with different aspect ratios of 2, 3 and 4 - black), red and blue - respectively (Lu et al., 2009).

### 2.4.5. Mass Spectroscopy

Mass spectrometry (MS) is one of the most important technique for molecular level of analysis of biological. A typical mass spectrometer is composed of the following three parts: (i) An ionization unit in which sample is ionized to form ions; (ii) a mass analysis unit in which the mass-to-charge ratio (**m/z**) of those ions in the gas phase are measured, and (iii) a detector that register/counts the number of ions at each **m/z** value.

There are two main techniques desorption/ionization of large biomolecules such as proteins for MS analysis, namely "Electrospray Ionization (ESI)" and "Matrix-

Assisted Laser Desorption/Ionization (MALDI)" (Karas and Hillenkamp, 1988; Tanaka et al., 1988; Fenn et al., 1989; Horneffer et al., 2001; Aebersold and Mann, 2003). In the ESI, the molecules are first pre-separated in a unit such as a liquid-chromatography and than they are vaporized/ionized. However, in MALDI the molecules mixed/dried with a matrix on a platform are sublimated/desorbed/ ionized by using a pulsed laser as depicted in Figure 2.41.

There are two inventors of MALDI. The first one is the researchers of a Japanese company (the Shimadzu Corp.). They have reported analysis of several molecules (e.g., carboxypeptidase) - with high mass ions - first in 1987 at the symposium organized in Takarazuka, Japan and then published the results in 1988 (Tanaka et al., 1988). Michael Karas and Franz Hillenkamp (University of Muenster, Germany) have developed a matrix-assisted technique for detection of molecular ions with high mass (e.g., albumin) almost at the same time which was presented at an international meeting in France in 1988, and then published (Karas and Hillenkamp, 1988).
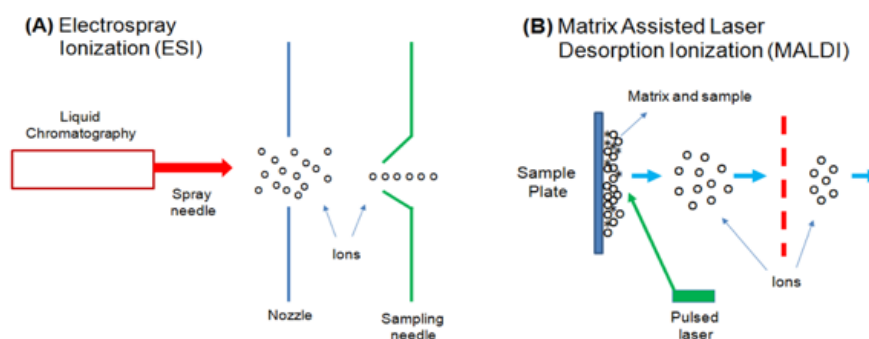


Figure 2.41. Mass spectrometers: (A) "Electrospray Ionization" (ESI) and (B) "Matrix-Assisted Laser Desorption/Ionization (MALDI). Adapted/ modified from the related literature (Aebersold and Mann, 2003).

Different mass analyzers with different design and performances - with advantages and limitations - are used today which includes "ion trap", "quadrupole", "Fourier transform ion cyclotron" (FT-MS), "Time-of-Flight" (TOF). Ion traps are quite sensitive analyzers and also relatively inexpensive, and therefore are widely used. However, their main limitation is the relatively low mass

accuracy which should be taken in consideration carefully (Hager, 2002). There are new generation - the so-called "3D-ion traps" - which are more sensitive with high resolution and mass accuracy. The FT-MS systems are similar to ion traps but work under high vacuum and magnetic field. They are highly sensitive systems with much higher mass accuracy and resolution however they are expensive and complex/difficult to use (Marshall, Hendrickson and Jackson, 1988; Martin et al., 2000).

ESI systems usually used with ion traps and 3D-quadrupole mass analyzers, needs also pre-separation systems and works on fragments. The outcome is a "fragment ion spectrum". However, MALDI systems are usually used with TOF mass analyzers in which whole (contact) molecular (e.g., peptides) masses are measured. The MALDI-TOF systems are simple, have excellent mass accuracy with high resolution/sensitivity. High throughput and speed can be achieved with the highly developed automated MALDI-TOF systems therefore it is considered as one of the top techniques for analysis of biomolecules (Marvin, Roberts and Faya, 2000).

Some examples of different instrumental configurations of TOF units are shown in Figure 2.42 (adapted from the related literature) (Aebersold and Mann, 2003). As depicted in Figure 2.42A schematically, in the "Reflector TOF" instruments, first the ions desorbed from the sample plate are accelerated to high kinetic energy. The ions having different $m/z$ values are separated during their voyage in the flight tube. The reflector compensates the kinetic energy differences and forwards to the detector. Then, the detector amplifies/counts the ions reaching. The second configuration is composed of two TOFs (the so-called, "TOF-TOF" instrument) in which there is a collision cell between two the TOFs. It should be noted that ions having the same mass-to-charge (**m/z**) ratios are separated in the first TOF section, fragmentation occurs in between two TOF sections (the collision cell section), and the masses of the fragments are separated in the second TOF section (Figure 2.42B). In the last example is the "the quadrupole TOF instrument" in which ions of a particular **m/z** are first selected ($Q_1$), separated in the collision cell ($q_1$), and then ions are detected in the last section (Figure 2.42C).
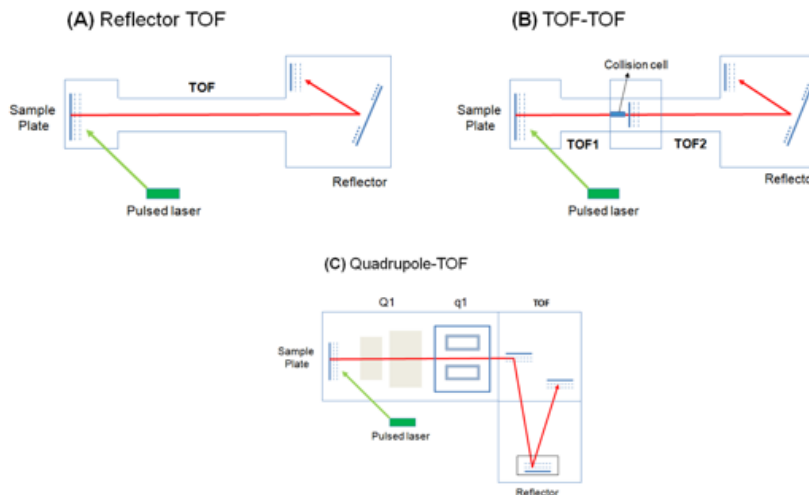
Figure 2.42. Different TOF instrumentation in MALDI-TOF: (A) "Reflector" TOF; (B) "TOF-TOF"; and (C) quadrupole integrated TOF. Adapted/ modified from the related literature (Aebersold and Mann, 2003).

In the MALDI-TOF analysis, firstly the sample is mixed/coated with solution of the "matrix" which is an organic substance with high energy absorption capability, and is placed onto a metallic target tray - a multiwell tray usually with 16-384 wells (Figure 2.43). The matrix (the mixture with the target) is crystalized/co-crystalized on the tray by simple drying. When the matrix crystallizes on drying, the target molecules entrapped within the matrix may also be co-crystallized. Several matrix materials are used as exemplified below. The tray is placed in the system which is transported to the measuring chamber; and vacuum is re-established; then the mixture (solid phase) is ionized from the surface by applying short laser pulses. The matrix absorbs energy from the laser and ionized/dissociated and allows ionization of the sample molecules as singly protonated ions (transferred from the matrix molecules) and desorbing in the gas phase. The protonated ions desorbed from the surface are accelerated/separated by their *m/z* values at a fixed potential. They pass through the focusing lens and enter to the drift path tube in vacuum. The time of flight for each individual ion is measured at the top of the vacuum flight tube by the detector. From these TOF information, a characteristic spectrum which is also so-called sample **"fingerprints"** of the sample is obtained, and characterized by using the reference databank in the software of the system.
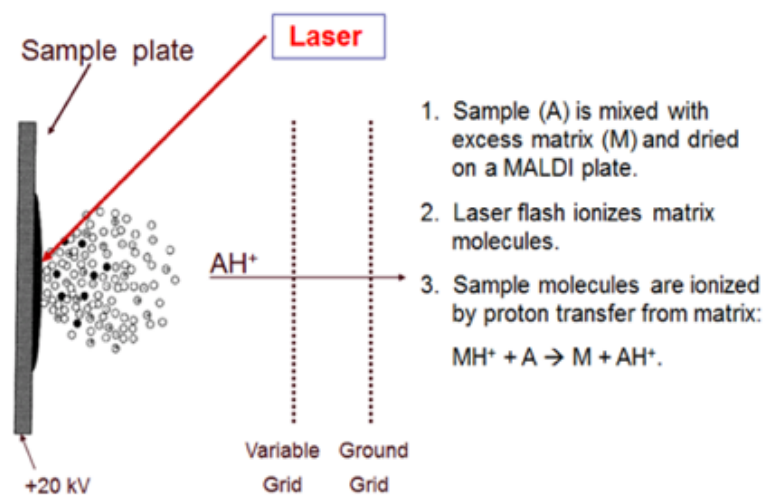
Figure 2.43. Ionization and detection in MALDI-TOF. Adapted/modified from the related literature (Slide Player, 2016).

There are several organic substances used as MALDI-TOF MS matrices such as cinnamic acid or benzoic acid derivatives. α-Cyano-4-hydroxycinnamic acid (CHCA), 2,5-dihydroxy benzoic acid (DHB), and 3,5-dimethoxy-4-hydroxycinnamic acid (sinapinic acid) have been proposed as the most successful ones for bacterial detections. The matrices are dissolved in several solvents - mixtures of water and organic solvents (e.g., ethanol/methanol or acetonitrile) and a strong acid (e.g., trifluoro acetic acid, TFA). In the case of bacterial detection - which is the matrix used also **in this PhD thesis** - the solvents help also extraction of the cellular proteins from the bacterial cells - which are detected. Solvents are evaporated during drying, target proteins are entrapped within the matrices crystals and even "co-crystallized" as mentioned also above.

Figure 2.44 describes schematically the relation between the flight time and *m/z* of the ions desorbed from the surfaces in simple, single acceleration stage, linear, TOF-mass spectrometer. As seen here there are two regions, an "ion acceleration region" and an "ion drift region" (the so-called "ion-free flight region"). The first part is an optical assembly consist of the following two elements: (i) A "repeller" lens and (ii) ground "aperture". Some potential (V) is applied to accelerate the ions to the repeller and the aperture is grounded. A positive voltage is applied for cations and negative for anions - note that only a single polarity of ions (cations or anions) are analyzed at any given time.
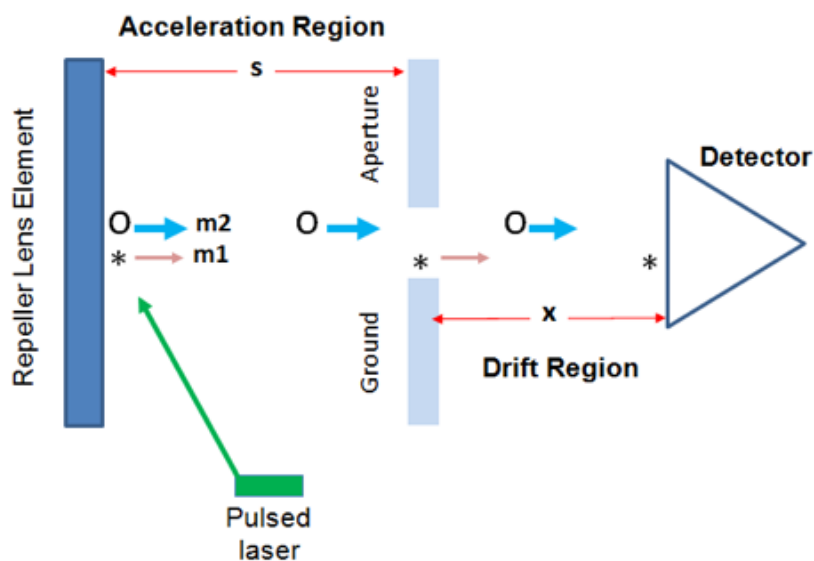
Figure 2.44. Schematic description of a simple linear MALDI-TOF MS. Two ions with the same charge but different masses, ($m_1 < m_2$) are accelerated at a constant electrical voltage. Adapted/modified from the related literature (Merchant and Weinberger, 2000).

The ions are accelerated and then are separated due to their "**m/z**" ratios (note that $m_1 < m_2$) are accelerated. In the "ion-free flight" region with a length of "**x**", the ions are separated (drifted out) clearly and reach to detector at different times depending on their "**m/z**" ratio which is usually described by the following expression.

$$m/z = k. \, t^2 \hspace{4cm} 2.2$$

Here the "k" constant includes also the distances **s** and **x** which are held constant via instrument design. Note that k is determined by calibration.

Both ESI and MALDI MS have used for identification of proteins from complex biological systems e.g., body fluid (blood, plasma, lymph, interstitial fluid, urine, etc.) and at cellular level (whole cells, cell lysates, microorganisms, etc.) which do contain hundreds of biological molecules (including mainly proteins) and also organic and inorganic salts which creates complexity in MS analysis (Merchant and Weinberger, 2000). Thus, significant sample preparation and purification steps are needed which includes liquid chromatography, electrophoresis, dialysis, centrifugation, etc. All these needs, which are often labor-intensive and increases the analyzing time and therefore operating cost.

There are a continuous affords to develop new strategies to overcome these limitations. One of the most important approaches is the Surface-Enhanced Laser Desorption/Ionization (SELDI) to study of peptides and proteins, but also to oligonucleotides, bacteria and small molecules as extensively reviewed recently (Hutchens and Yip, 1993; Merchant and Weinberger, 2000).

# 3. MATERIALS AND METHODS

## 3.1. Bacteria and Bacteriophages: Propagation and Characterization

As mentioned in the previous sections, the main bacterial target in this PhD thesis is *Escherichia coli (E.coli).* For comparison two more important pathogenic bacteria *Staphylococcus aureus* (*S.aureus*) and *Salmonella infantis* (*S.infantis*) were also included in some of the studies described in the later parts. Note that personal and environmental safety non-pathogenic strains of those three bacteria were selected/used in the studies here.

### 3.1.1. Propagation of Bacteria

The following bacterial culture the media and buffers were prepared freshly and used. All the respective reagents were purchased from Sigma-Aldrich (Germany). 25 g of the Luria Bertani (LB) powder was dissolved 1L of distilled water to obtain the LB medium which was prepared by adding 6 g of agar was added into in 400ml of LB media to prepare the LB-agar medium. The SM buffer was prepared by dissolving 5.8 g of NaCl, 2 g of $MgSO_4 \cdot 7H_2O$, 50 mL of 1M Tris–hydrochloride (pH 7.5) and 1mL of 10% (w/v) gelatin in 1L of distilled water. Tryptic soy broth (TSB) was made by dissolving 15 g of tryptone, 5 g of soytone and 5 g of NaCl in 1L of distilled water. The LB medium and buffers were autoclaved prior to use.

The bacterial strains mentioned above were propagated by a similar protocol that was widely used including our previous studies (Sambrook and Russell, 1989; Moghtader, Eğri and Piskin, 2017; Moghtader et al. 2017) which is as follows: The bacteria were first cultured in the sterile Luria Bertani (LB) medium (25 g LB powder in 1L of distilled water) at 37°C in a rotary shaker (200 rpm) until to reach the exponential growth phase (about OD 600nm) - which was followed spectrophotometrically. These bacterial cultures were centrifuged (at 6000 rpm for 5min) and the pellets precipitated were washed few times and re-suspended in the sterile PBS buffer with a pH of 7.2 (composed of 140 mM NaCl, 2.7mM KCl, 0.1mM $Na_2HPO_4$ and 1.8mM $KH_2PO_4$). This suspension was diluted to reach the desired/different concentrations and then plated in the LB agar (prepared by adding 6 g of granulated agar to 400 mL of LB media) and the total bacterial (viable) counts (color forming units, CFU) were estimated.

### 3.1.2. Propagation of Bacteriophages

Specific bacteriophages of the bacterial strains mentioned above were amplified using the bacterial suspension prepared in the previous step accordingly to the related literature (Sambrook and Russell, 1989; Boratynski et al., 2004; Moghtader, Eğri and Piskin, 2017; Moghtader et al. 2017). In a typical protocol bacteria and its specific bacteriophage from the stoke suspensions/nanoemulsions - 100 μL of each with concentrations of $10^8$ CFU/mL and $10^8$ PFU/mL, respectively. They were mixed in a test tube by using a vortex, incubated at room temperature for 15min and added to a 20ml tube containing the LB medium which was then incubated for 6h at 37°C in a shaking incubator (200 rpm). In the final step, chloroform was added - 10% (v/v) - which was kept at 4°C for about 20min. For purification, the medium was first ultra-filtered through a sterile 0.22μm filter to remove any remaining bacteria and then centrifuged at 4°C (12000g). The precipitated/purified phages were then re-suspended in the sterile PBS buffer. In order to obtain the bacteriophage concentration - as plaque forming unit per ml (PFU/mL) - the following protocol was applied. The bacteriophage nanoemulsion prepared in the previous step was diluted to obtain a series of phage suspensions with different phage contents. 100μL from each of those bacteriophage nanoemulsions and 400μL of the target bacterial suspension were mixed, added to the semi-liquid LB-agar (agar 7.5 g/L) and incubated at 37°C for 24h. The titration was performed by direct counting of lysis plagues. The phage stock produced were kept in the SM buffer.

The activity and specificity of T4 phages were demonstrated in typical bacterial culture tests. Plates containing the target bacteria bacteria on agar broth were prepared. The bacteriophages were put on the plates which were then incubated at 37°C overnight. Note that the bacterial lawn plates were originally turbid, but transparent zones were formed around the phage inserted areas which shows the activity of the bacteriophages. It should be noted that there were no transparent zones on the plates where cross-phages (not specific) added which demonstrated the specificity of the bacteriophages against their host bacteria only.

Note that fresh bacterial cultures were prepared from the stoke solutions for each new bacterial detection test group - in each day by incubating overnight at 37ºC.

After incubation, broth of each culture was transferred to 15 mL sterile centrifuge tubes, and centrifuged at room temperature at 5,000 rpm for 10min (Wisespin, Wise*d*. Laboratory Instruments, PRC). Bacterial pellets were washed by suspending in 10 mL of sterile deionized water and centrifuging for 3 times. Bacteriophages were taken from stokes which were purified previously and stored at 4ºC. The target bacteria and its specific bacteriophage with concentrations of $10^8$ PFU/mL and $10^8$ CFU/mL, respectively were used in the detection studies demonstrated here.

### 3.1.3. Characterization

The SEM micrographs of target bacteria were obtained using a Philips Ultra Plus High Resolution FESEM equipped with an in-lens secondary-electron detector (Philips, The Netherlands) at operating range 2-20 keV depending on sample charging. The suspensions were dropped onto the silica slides, dried at room temperature and then images were obtained.

A Nanosurf FlexAFM system (USA) operating in tapping mode at room temperature in air was for AFM imaging which were conducted at a various scaning speed. Oxide-sharpened silicon nitride tips with integrated cantilever with a nominal spring constant of 48 N/m were used. For AFM micrographs, 5 μL of the bacteria or bacteriophages nanoemulsions was dropped/fixed on Si (111) previously cleaned using Piranha solution, and AFM images were obtained.

### 3.2. Plasmonic Nanoparticles: Synthesis and Characterization

### 3.2.1. Synthesis

The following nanoparticles were synthesized and used: (i) AgNPs; (ii) AuNPs; and (iii) AuNRs. Brief descriptions of the preparation protocols are given below. Chemicals - i.e., hexadecyltrimethylammonium bromide (CTAB), tetrachloroauric (III) acid ($HAuCl_4$) and silver nitrate ($AgNO_3$), sodium borohydride ($NaBH_4$), L-ascorbic acid, tri-sodium citrate, and others were bought from Sigma-Aldrich (Germany) with high purity (≥ 99%) and used as-received. DI water (18.2 MΩ/cm) obtained from a reverse osmosis system was used.

The AgNPs were prepared by reducing silver nitrate with sodium citrate by a very classical protocol. Briefly, 18 mg $AgNO_3$ was dissolved in 100 mL distilled water. This solution was heated until boiling. Then, a 10 mL aliquot of 1% sodium citrate

was added dropwise into the the boiling which was continued for 1h. These AgNPs nanoemulsions were yellowish in color. It was possible to synthesis silver nanospheres from few nanometers up to 100 nm (by further aggregation) by simply changing the reducing agent type - using also extra reducing agents like NaBH$_4$ - and their concentrations. These AgNPs carrying citrate on their surfaces were negatively charged. They were stored at 4°C until use. Note that citrate groups on the nanoparticle surfaces were reduced by repeated centrifugation and ultrasonication just before use.

For synthesis of the AuNPs with positive surfaces charges (carrying CTAB on their surfaces) the following classical method was applied. An aqueous solution of CTAB (7.5 mL - 100 mM) was sonicated for 20 min at 40°C in a water bath. The HAuCl$_4$.3H$_2$O - aqueous solution (250 µL - 10 mM) was added to the CTAB solution with continuous stirring under nitrogen atmosphere. Then, an ice-cold aqueous solution of NaBH$_4$ (600 µL - 10 mM) was added under vigorous stirring in 1min to form the AuNPs. Note that these nanoparticles carrying CTAB on their surfaces were used as seed in the preparation of gold nanorods as described below, and/or they were simply aged about 20-30 days in dark at room temperature in closed caped vials for maturation and to reach the desired size. They were stored at room temperature until use.

The gold nanorods (AuNRs) were produced by a rather classical two-step process as also described in the related literature including ours, which is briefly as follows (Nikoobakht and El-Sayed, 2003; Gole and Murphy, 2004; Smith and Korgel, 2008; Huang et al., 2009; Congur et al. 2015; Tomak and Zareie, 2015; Moghtader, Eğri and Piskin, 2017; Moghtader et al. 2017; Moghtader et al., 2018). In the first step, in order to synthesize gold spherical nanoparticles, a 7.5 mL-100 mM aqueous solution of CTAB was sonicated for 20min at 40°C in a water bath. A 250 µL-10 mM HAuCl$_4$. 3H$_2$O aqueous solution was added with continuous stirring under nitrogen atmosphere to the CTAB solution. Then, 600 µL-10 mM ice-cold aqueous solution of NaBH$_4$ was added under vigorous stirring in 1min. The CTAB-capped nanospheres formed were used as seeds within 2-5h for preparation of the AuNRs in the next step. A 40mL of a growth solution consists of CTAB (100 mM) and HAuCl$_4$.3H$_2$O (10 mM) was prepared which was dark-yellow. A 250 µL - 10 mM AgNO$_3$, aqueous solution and then a 270 µL-100 mM ascorbic acid - a mild

reducing agent - (Sigma-Aldrich, USA) were added to the growth solution flask which resulted a colorless solution. Then, 210 µL of the CTAB-capped seed solution that was produced in the previous step was added to that flask, and the mixture was gently mixed. After 3h at 24°C, the color of the mixture turned into a dark-blue solution with a brownish opalescence which was an indication of formation of AuNRs. In order to remove most of the surfactants (CTAB) used in the preparation of the AuNRs, the nanoemulsions were centrifuged at 13500g (Wisespin, Wised Laboratory Instruments, PRC) and re-suspended in DI water (18.2 MΩ/cm) and sonicated for about 1h (Wiseclean, Wised Laboratory Instruments, PRC). This cleaning protocol was repeated at least three times.

### 3.2.2. Characterization

Transmission Electron Microscopy (TEM) images were obtained by using a TEM system (Tecnai G2 F30, FEI Company, USA). The Scanning Electron Microscopy (SEM) images of the AuNRs were also taken using a Philips Ultra Plus High Resolution FESEM equipped with an in-lens secondary-electron detector at operating range 2-20 keV (Philips, The Netherlands). A Zeta Sizer (Nanosizer, Malvern, UK) was used to determine the average size and size distributions and charges of the nanoparticles. Absorption peaks of the nanoemulsions were obtained by using an Ocean Optics USB2000+VIS/NIR spectrometer (350-1100 nm) (Nanodev Ltd., Turkey). All absorbance spectra were collected using quartz cuvettes.

### 3.3. Detection with SERS

### 3.3.1. SERS System Used

A photo of the Raman spectrometer (XploRA, Horiba, France) used in this PhD thesis is given in Figure 3.1, which is equipped with an Olympus BX41 Transmission and Reflection Illumination Microscope (Olympus, France) for imaging before taking the SERS spectra. A 532 nm laser was used for silver nanoparticles (AgNPs) while the 785 laser was applied for gold nanoparticles (AuNPs and AuNRs). Raman signals were collected in a spectral range of 450-3000 cm$^{-1}$, at 50mW power, using different objectives of 10x, 40x and 100x magnifications for focusing and collection of Raman-scattered light. For each sample, the Raman spectra were taken minimum 5 different locations repeated

more than 15 times and averaged to demonstrate the spectra. Each spectrum was normalized using the Labspec software. All the data collected were stored by describing the samples and the experimental conditions.
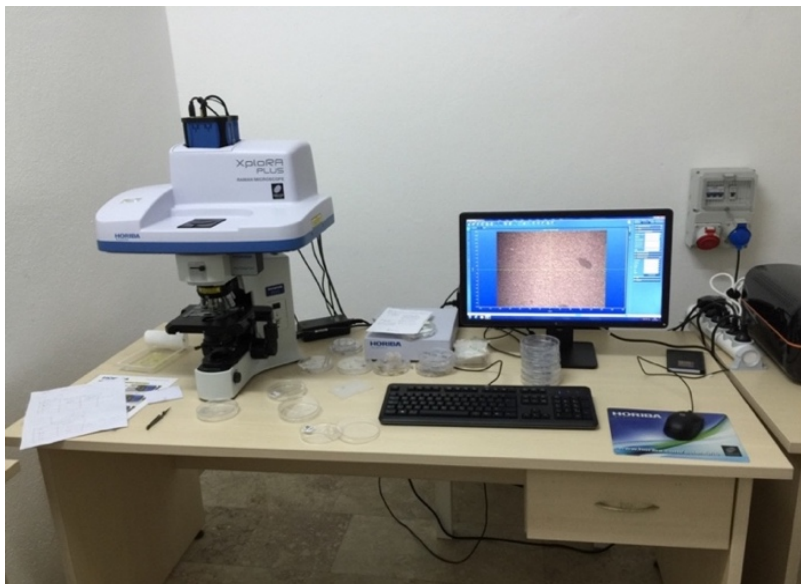


Figure 3.1.    The Raman spectrometer XploRA equipped with an Olympus BX41 Transmission and Reflection Illumination Microscope.

### 3.3.2. Preparation of the SERS/LSPR Platforms

In the "Surface Based" detection experiments - both for SERS and/or LSPR - two basic substrate/platforms were used in this PhD thesis which are: (A) The glass microscope slides from ISOLAB Laborgerate GmbH (Germany); and (B) the single side polished silicon wafers ("silica") (Silicon Inc., Idoha, USA) (Figure 3.2). The ISOLAB slides were modified by coating with polydopamine (PDA) in order to create positive charge on their surfaces. Both modified and non-modified glass slides were used in the tests. Only one set of experiments were done in which a commercial SERS substrate was used to take a series of representative SERS spectra of both three bacteria and their specific bacteriophages.

For polydopamine (PDA) coating, by an oxidation protocol oxidation method described in the related literature (Liu, Ai and Lu, 2014) which was briefly as follows: TRIS buffer (pH: 8.5) was used as an alkaline buffer for spontaneously self-polymerization of dopamine (Dopamine hydrochloride, Sigma-Aldrich,

Germany) with oxygen. 200 mg of dopamine was added in 100 mL of TRIS-HCl buffer solution (10 mM, pH: 8.5). The cleaned/dried slides were then put in this solution and incubated 1 min while shaking slowly. Surfaces were cleaned by washing few times and dried at room temperature for the further tests.
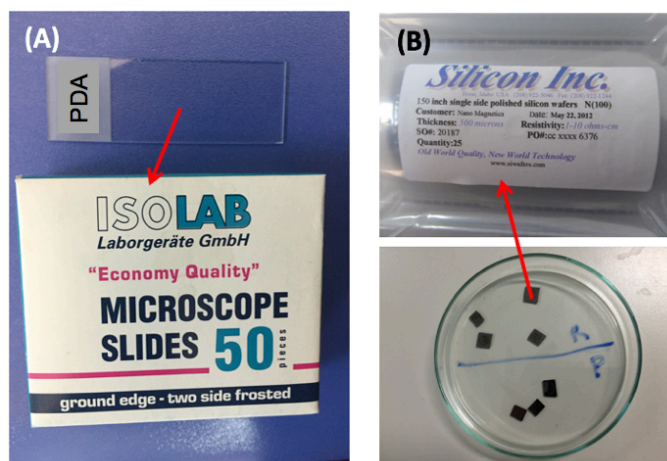


Figure 3.2.  Two substrates used as the basic platform in the SERS/LSPR studies: (A) surface modified commercial glass microscope slides (called as "glass slides") that were also further modified by PDA coating; and (B) a commercial - single side polished - silicon wafers (called as "silica slides").

For enhancement of the Raman signal in the SERS experiments and also to create localized plasmon effect for the LSPR studies, three different nanoparticles with plasmonic properties, namely AgNPs, AuNPs and/or AuNRs were deposited on these platforms. Production and characterization of these plasmonic nanoparticles are presented in the previous parts of this thesis.

It should be noted that the nanoparticles were firstly cleaned in order to remove most of the surfactants and possible ionic contaminations, then were used in each experimental day freshly. For cleaning the samples taken from the stoke nanoemulsions were pretreated as follows: They were centrifuged at 13500g (Wisespin, Wise*d*. Laboratory Instruments, PRC) and re-suspended in DI water (18.2 MΩ/cm) and sonicated for about 1h (Wiseclean, Wise*d*. Laboratory Instruments, PRC). This cleaning protocol was repeated three times (optimized in the preliminary studies).

For nanoparticle deposition, 15 µL of the nanoparticle nanoemulsions were dropped on the substrate surfaces, dried under nitrogen atmosphere at room temperature. This deposition step was repeated up to five times (optimized in the preliminary studies) in order to have high enough nanoparticles on the substrate surfaces that resulted clear and strong peaks in the SERS/LSPR spectra.

### 3.3.3. Detection with SERS

In the content of this PhD thesis two groups of SERS detection protocols were studied/applied - which are: (i) "Surface -based" and (ii) "suspension-based", which are described below.

### 3.3.3.1. Surface-Based SERS Studies

***SERS data for the platforms*** Two SERS platforms, the glass and silica slides - carrying also three different nanoparticles, i.e., AgNPs, AuNPs and AuNRs described above were used in the initial studies given below to find out the best platform to be used. It should be noted that in each test, surfaces were imaged (and representative pictures were taken) and then SERS spectra were collected from different surfaces.

**SERS analysis for bacteria and phages on surfaces:** 15 µL of three different bacteria (*E. coli*, *S.aureus* and *S.infantis*) and their specific/respective phages - from their stoke suspensions/emulsions were placed onto the AuNPs deposited silica substrates, dried in the safety cabinet in about 30 min at room temperature then SERS data were conducted. In order to observe the effects of phages on the target bacteria we have designed the following tests. Here after taking the images and SERS spectra of the target bacteria on the AuNPs deposited silica surfaces, 15 µL nanoemulsion of phages was dropped onto the substrate surface, and then SERS data were collected from the same spot at selected time intervals, 10, 20, 30 and 40 mins. Note that we have used specific phage only for the target ("its complementary") bacteria. Two representative microscopy images were taken just before dropping the phage emulsion onto bacteria on the surfaces and in the end (after 40 mins).

### 3.3.3.2. Suspension-Based SERS Studies

In this group of studies, an important alternative approach was applied. Here only gold nanorods were used in order to "the proof of concept" in this part of the study. The AuNRs were added to the target bacterial suspensions, incubated at room temperature about 30mins, then they were dropped onto the plane silica slides, dried and microscopy images were taken and SERS data were collected. It is very important to note that in this group of tests we were focusing the incident light on individual (single) bacteria, therefore the detection limit was almost a single bacterial cell level which is a very impressive result. Then the specific phages were added and the changes in the SERS spectra were observed. Note that for the demonstration of "the proof of concept" we have studied only with *E. coli* and its specific phage - T4 in this part of PhD thesis.

Before collecting the SERS data, we have first observed the surfaces with the Olympus BX41 transmission and reflection illumination microscope attached to the Raman spectrometer that we have used in this study. In order to demonstrate the power of the microscope, several images were taken at different steps of the SERS analysis.

One of the main objectives of this study is to obtain SERS data of the target bacteria using gold nanorods without using any SERS substrate. In the SERS analysis we have applied here the AuNRs were added to the target bacteria suspensions, incubated at room temperature about 30 mins, then they were dropped onto the silicone wafers; dried and the surfaces were first observed with the microscope (attached to the Raman Spectrometer) and images were taken. Then we have focused on the selected target bacteria and collected the SERS data. Note that it was possible to focus onto individual bacteria and take the SERS image, indicating that our data is demonstrating almost single bacterial detection.

In the following step, T4 phages were placed on the substrates having AuNRs accumulated bacteria, and SERS data were collected at selected time intervals (at 0, 10, 20 and 40 mins) Several data were collected at many different points on the sample, and these experiments were repeated many times.

## 3.4. Detection with LSPR

### 3.4.1. LSPR Experimental Setup

The schematic illustration of the LSPR Spectroscopy setup and an optical photograph used in this study - which was manufactured by Nanodev Ltd. (Cyberpark, Ankara, Turkey) are given in Figure 3.3 A and B, respectively. The LSPR data were collected using an optic fiber (HR2000, Ocean Optics Inc., USA) optically coupled to a light microscope in which an un-polarized white light by a tungsten-halogen lamp was used. The beam was passed through the sample with a 40X (NA=0.65) or 100X microscope objective (NA=1.25) that collects the light, whereas the transmitted light was focused into a 400μm core diameter optical fiber cable and directed into the spectrometer ranged from 450 nm to 1100 nm. The probe-light spot diameter was approximately 4 mm. The LSPR spectra were monitored using a data processing software (SpectraSuite, Ocean Optics Inc., USA). The LSPR spectra were collected from 10 different points of the sample in the ambient conditions with 1000 ms integration time. All data presented here were smoothed.
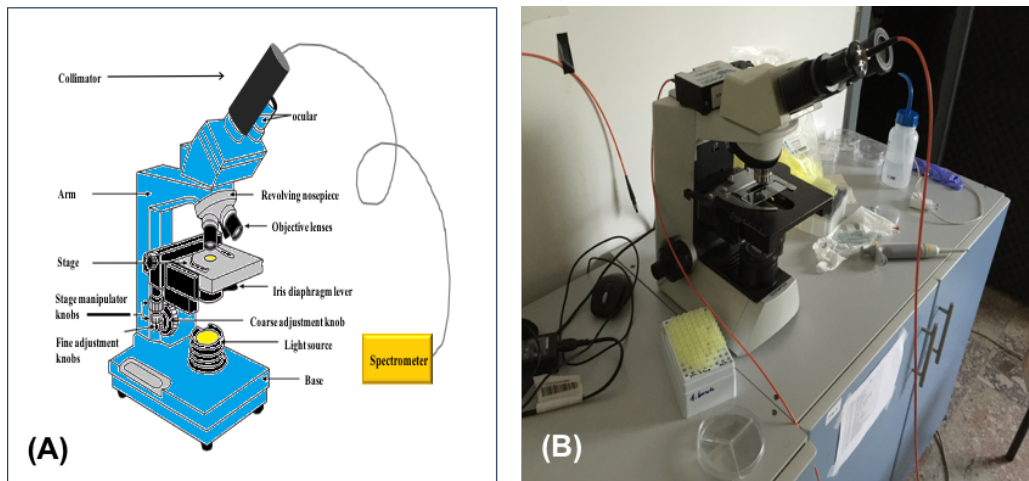


Figure 3.3.   LSPR Spectroscopy system used in this study: (A) Schematic illustration and (B) an optical photograph.

### 3.4.2. Detection with LSPR

In the LSPR tests, firstly the spectra of the substrates surfaces and NPs on these substrates were taken. Then, 5 μL bacterial (here *E. coli*) suspension was dropped onto the LSPR platform, dried in a safety cabinet for about 30 min at room

temperature then LSPR spectra were taken. These tests were repeated on three different surfaces, carrying AgNPs, AuNPs and AuNRs.

In the second step, 5 µL of phage emulsion was dropped onto the bacteria adsorbed surfaces and the LSPR spectra were collected after one hour which was enough time for bacterial infection by the phages and total destruction of their cell structure. Note that in the end of the selected time the surface was gently washed with water and the LSPR data was taken. As mentioned before the T4-phage was tested on *E. coli*. A cross phage (the phage specific to *S. aureus*) was also tested on *E. coli* as a specificity test.

### 3.5. MALDI-TOF MS for Detection of Bacteria Using Bacteriophages

The MALDI-TOF MS system used was a Bruker Autoflex III Smartbeam MALDI-TOF/TOF instrument (Germany) which is shown in Figure 3.4. A target plate (sample platform) - MTB 384 made of polished steel with transponder technology (Bruker Daltonik GmbH, Germany) was used which is shown on the upper left on the figure.



Figure 3.4.    The MALDI-TOF MS system used in this study by Bruker (Germany). The target plate with 384 spots used is on the top left.

The bacterial and/or bacteriophage suspensions (1 µL) were directly spotted onto the target plate (three samples from each target) and allowed to air dry. Matrix was prepared by following method: 2 mg 2,5-dihydroxybenzoic acid (DHB) was weighed and dissolved in 100 µL; 20% acetonitrile and 80% water with 0.1% TFA

final concentration. Then, 1 mg of alpha-cyano-4-hydroxycinnamic acid (CHCA) was weighed and dissolved in 200 µL - 20% methanol solution in acetone. These DHB and CHCA matrix solutions were mixed at a ratio of 2:1, spotted 1 µL on air-dried bacterial/bacteriophage spots which were on the stainless steel MALDI target and allowed to air dry. Mass spectra were obtained in the MALDI-TOF MS system used (Bruker, Germany) shown in Figure 2.4 using the Bruker MALDI-TOF/TOF instrument in a linear positive ion mode.

## 3.6. Bacteriophages in Gelatin Hydrogel Beads

In order to increase the stability and prevent activity lost of bacteriophages in storage and also in use we have encapsulated/loaded phages within two different hydrogel beads (microspheres), namely alginate and gelatin beads. Encapsulation of T4 bacteriophages and their stability and release in the simulated gastric and intestinal fluids at gastrointestinal tract conditions have been studied in detail in our previous study (Moghtader, Eğri and Piskin, 2017). Here, as an alternative approach T4 phages were loaded within the gelatin beads with a very simple methodology and released of phages from these matrices were investigated.

### 3.6.1. Preparation/Characterization of Gelatin Beads

Recently, gelatin hydrogel microspheres/beads were prepared by F. Moghtader by applying the original recipe developed by Tabata and his group in his laboratories at Kyoto University, Japan (Tabata, Nagano and Ikada, 1999; Takahashi, Yamamoto and Tabata, 2005; Tajima and Tabata, 2013; Tajima and Tabata, 2017) - which is briefly as follows: Firstly, an aqueous solution of gelatin - which was obtained from Nitta Gelatin Inc. (Osaka, Japan) with a weight average molecular weight of 100,000 and isoelectric point of 9.0 (prepared through an acidic process - the concentration was 10% in weight. 20 ml of this solution was heated up to 40°C and then dropped into about 600 ml of a special olive oil dispersion phase (Wako Ltd, Osaka, Japan). The gelatin solution dispersed in oil phase was achieved by stirring at 200-400 rpm for 10 min. This emulsion was then cooled down to 4°C for natural gelation to obtain the non-cross-linked gelatin beads. In order to remove all of the residual olive oil, the beads were washed three times with cold acetone by also centrifugation (at 5000 rpm at 4°C for 5 min). The beads were separated three different size fractions using three sieves with apertures of 20, 32, and 53 µm (Seisakusyo Ltd, Osaka, Japan) and then were air

dried at 4°C. The final step was cross-linking which determines the swellability in water of the gelatin hydrogel beads. The freeze-dried gelatin beads were kept at 140°C in vacuum (0.1 Torr) in a vacuum incubator for dehydrothermal crosslinking of gelatin structure for three different periods of time, 24, 48 and 72 h according to the method described by Tabata's group (Ozeki and Tabata, 2005).

These hydrogel beads were swollen in distilled water at 37°C for 24 h to reach the swelling equilibrium. Water uptake was calculated by using the weights of the swollen and dried gelatin beads and presented as percentage. Photographs of gelatin hydrogel microspheres in the water swollen state were taken with a microscope (CKX41, Olympus, Tokyo, Japan). In order to calculate the average diameter of the swollen beads, diameters of about 100 hydrogel microspheres (beads) within the sample were measured and the average values with standard deviations were calculated using the Image J (NIH, Bethesda, USA) computer program in the software of the microscope.

Facilitated degradation of the gelatin beads within HCL were investigated by following the protocol described/applied by Tabata's group in their earlier studies (Tabata, Nagano and Ikada,1999; Ozeki and Tabata, 2005; Takahashi, Yamamoto and Tabata, 2005; Patel et al., 2008; Narita et al., 2009;  Tajima and Tabata, 2013; Tajima and Tabata, 2017). Briefly, 5 mg of freeze-dried cross-linked gelatin beads were put into a 2 ml tube containing 750 µL double-distilled water and allowed to fully swell in about 1 h at 37ºC.  Then, 750 µL 2M HCl was added and incubated at 37ºC for different time periods to follow the degradation with time. At selected intervals, the tube was centrifugated at 5000 rpm for 5 min at 37ºC, 200 µL of the supernatant was taken, and 200 µL 2M HCl was added into the tube to continue the degradation test. Absorbance of 200 µl supernatant taken from the tube was measured at 260nm using a UV spectrometer (Ultrospec 2000, Pharmacia Biotech, Cambridge, UK). By using the absorbance values, the total mass remaining was obtained and plotted against time to demonstrate the degradation profile.

### 3.6.2. Bacteriophage Loading and Release within/from Gelatin Beads

*Loading.* For loading of bacteriophages within the gelatin beads, a very simple protocol was used as schematically demonstrated in Figure 3.6 which was adapted from the Tabata's group studies that have been attempted to load the

"Human recombinant BMP2" within very similar gelatin beads for another purpose in their recent study (Patel et al., 2008; Narita et al., 2009; Tajima and Tabata, 2017). We have used bacteriophage nanoemulsions ($10^8$ PFU/ml). 20 µL was added onto a tube containing 2 mg of cross-linked/freeze dried gelatin beads and incubated for 1 h at 37°C. Note that all the aqueous media was completely uptaken by the dried beads - because the amount of the aqueous phase much lower that the amount of water in the wholly swollen beads -  means that loading efficiency was almost 100%.

*Release.* For release of bacteriophages from the gelatin beads, a similar release study described above for alginate beads were applied. Briefly, about 200 mg of fresh gelatin beads carrying bacteriophages were incubated in 50mL PBS buffer at pH 6.8 - by gently shaking for up to 24 h. About 100 µL samples were withdrawn from the medium at selected time intervals (replaced with fresh medium), and the amount of active phages release were determined as described above. The cumulative amount of phages released during incubation period was plotted against time to demonstrate the phage release kinetics. The released of phage was followed by plague assay reported by (Kunisaki and Tanji, 2015).
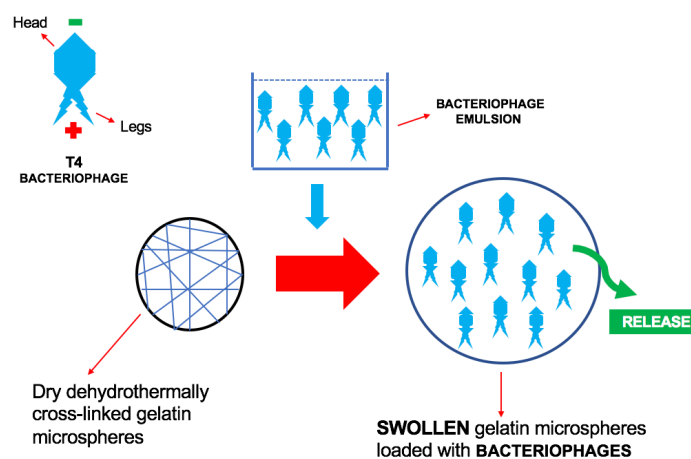


Figure 3.6.   Schematically description of bacteriophages loading protocol within gelatin hydrogel beads.

# 4. RESULTS AND DISCUSSION

## 4.1. Bacteria and Bacteriophages

Three bacteria, namely *Escherichia coli (E.coli)* (as the main target), *Staphylococcus aureus* (*S.aureus*) and *Salmonella infantis* (*S.infantis*) (for comparison) were propagated as described in the previous sections. Almost each test group of studies, bacterial suspensions were freshly prepared as exemplified in Figure 4.1.
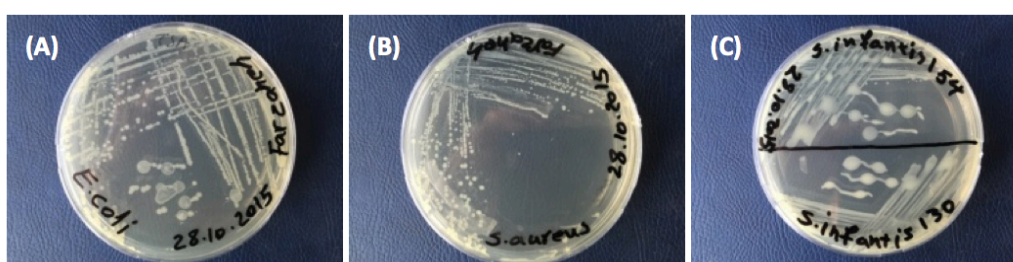


Figure 4.1. Representative optical micrographs of daily prepared fresh target bacterial cultures in petri dishes: (A) *E.coli*; and (B) *S.aureus*; and (C) *S.infantis*. This descriptive images are from the "Initial" group of studies explained below.

The AFM micrographs of both *E.coli* and its specific T4 phage were obtained as an additional demonstration. Some representative images of *E.coli* and T4-phage are given in Figure 4.2 A and B, respectively. Both micrographs nicely present the forms and dimensions of both *E.coli* and its specific phage that are very similar to the SEM images in the later part of this thesis.
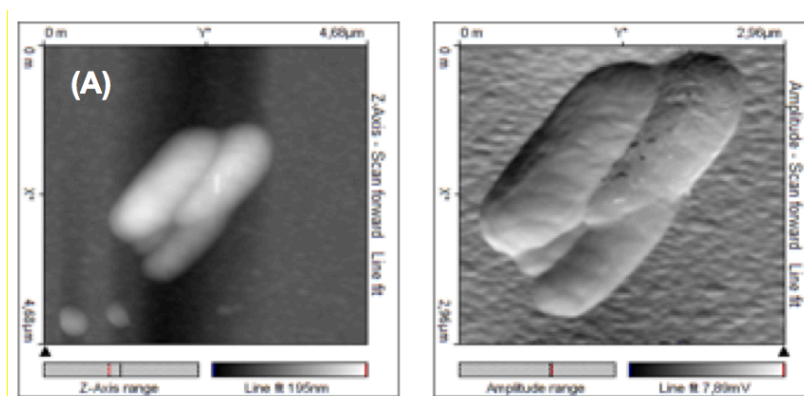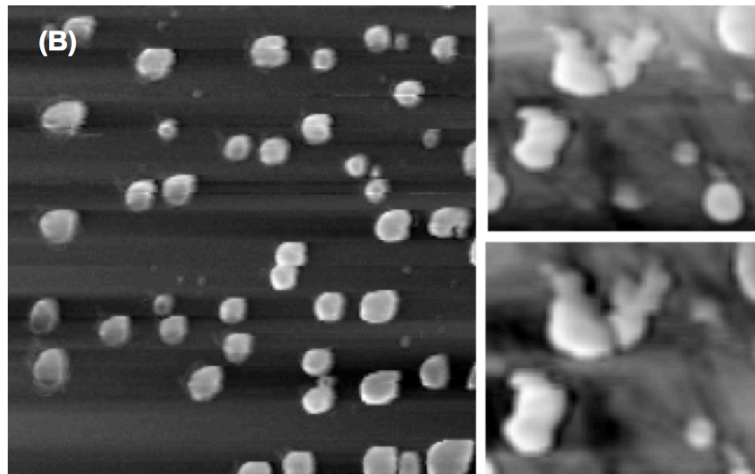
Figure 4.2. Representative AFM images of: (A) *E.coli*; and (B) its T4-phage.

T4-phage was amplified and purified using the bacterial suspension prepared in the previous step which are described in the previous sections in details using the bacterial stoke. The purified phages were stored at 4°C until use. The effectiveness - infection and destruction of the bacteria (*E.coli* here) by the T4 phages propagated in the previous steps was evaluated by a culture method ("agar overlay test"). An exemple is given in Fihure 4.3. Plates containing agar broth having the target bacteria *E.coli* were prepared. The phages with different concentrations were placed on the Agar in the plates which were incubated at 37°C overnight. Note that the developing *E. coli* lawn plates were originally turbid. However, *E.coli* was destroyed by the phages and transparent zones were formed due to lysis of the bacteria which exhibit the activity of the phages. As expected the diameter of the transparent zone increases with the phage amount.
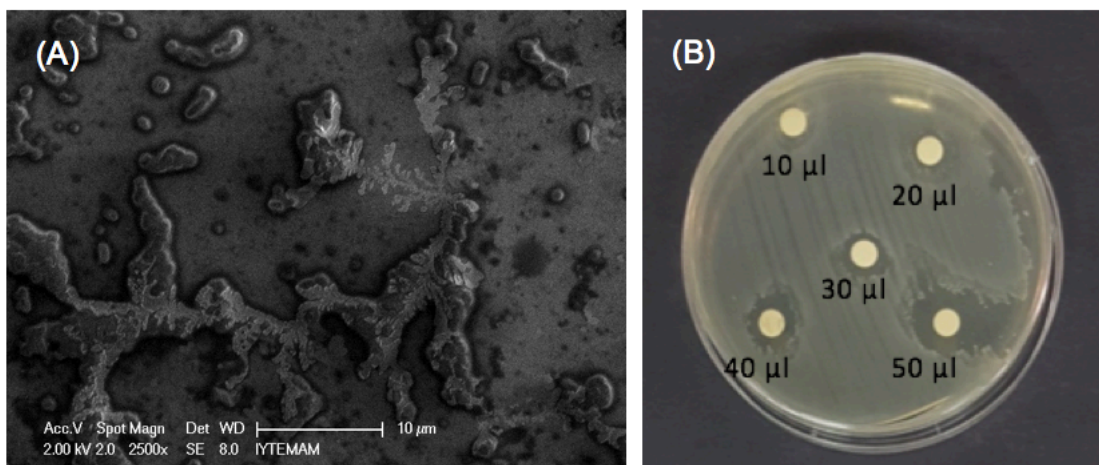
Figure 4.3.    (A) T4 phages attack *E.coli* and destruct the bacterial cells; and (B) Typical culture ("agar overlay") test. Different amounts of specific T4 Phages with different amount attack *E.coli* on the agar and kill them.


## 4.2. Plasmonic Nanoparticles

There different plasmonic nanoparticles, silver nanospheres (AgNPs), gold nanospheres (AuNPs) and gold nanorods (AuNRs) were synthesized/used. Transmission and Scanning Electron Microscopies (TEM and SEM) were used to obtain high resolution images of the nanoparticles. The average size/size distributions and charges of the nanoparticles were measured with a Zeta Sizer. Absorption spectra of nanoemulsions were obtained by using a UV-spectrometer.

Figure 4.4 A gives the representative TEM images of the AgNPs synthesized and used in this study. They are quite spherical and their diameters are in the range of 5-15 nm. Figure 4.4 B and C show the data obtained with the Zeta Sizer (Nanosizer, Malvern, UK). The apparent average Zeta potential is -9.43 mV with a Zeta deviation of 5.22 mV (the left plot). This demonstrate once again that AgNPs are negatively charged. There are three peaks in the size distribution plot (the right plot). About 62.5% (by volume) of the particles were having an average diameter of 6.058±1.582 nm. There were also bigger ones (about 14.2% by volume) having an average diameter of 24.87±14.80 nm and even agglomerates (5% by volume) with an average size and standard deviation of 241.3±146.0 nm. It should be noted that these original nanoemulsions were stored until use. However, - before use - they were first cleaned (for removing the excess citrate) by repeated (at least three times) centrifugation-precipitation-replacement of the supernatant and suspended by sonication - which allowed us to remove also larger size aggregates. Absorbance spectrum of the silver nanoemulsions were also obtained by LSPR (see also Section 4.4). The maximum absorbance peak ($\Delta\lambda_{max}$) value was 430 nm which is typical for AgNPs and represents roughly their size range.
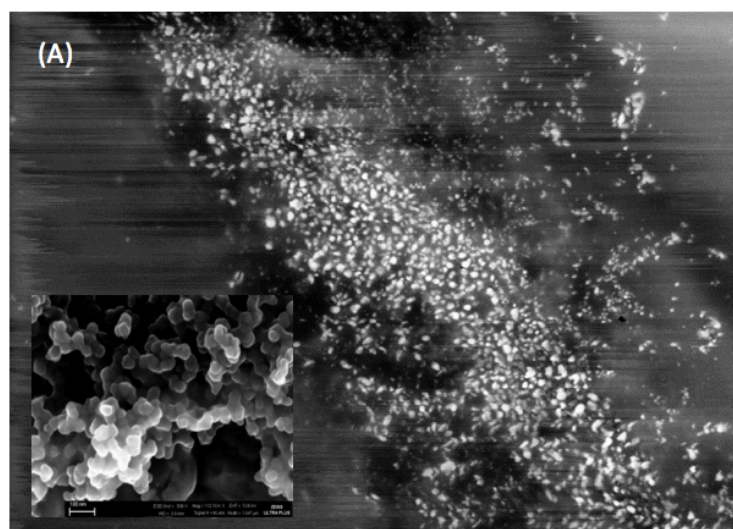
| | | Mean (mV) | Area (%) | St Dev (mV) |
|---|---|---|---|---|
| Zeta Potential (mV): -9,43 | Peak 1: | -9,43 | 100,0 | 5,22 |
| Zeta Deviation (mV): 5,22 | Peak 2: | 0,00 | 0,0 | 0,00 |
| Conductivity (mS/cm): 0,599 | Peak 3: | 0,00 | 0,0 | 0,00 |
| Result quality : Good | | | | |

| | | Size (d.nm): | % Volume: | St Dev (d.nm): |
|---|---|---|---|---|
| Z-Average (d.nm): 88,99 | Peak 1: | 6,058 | 62,5 | 1,582 |
| Pdl: 0,662 | Peak 2: | 24,87 | 14,2 | 14,80 |
| Intercept: 0,837 | Peak 3: | 241,3 | 5,0 | 146,0 |
| Result quality : Good | | | | |
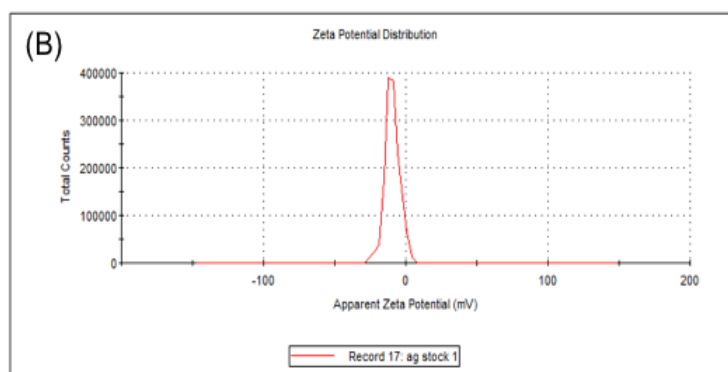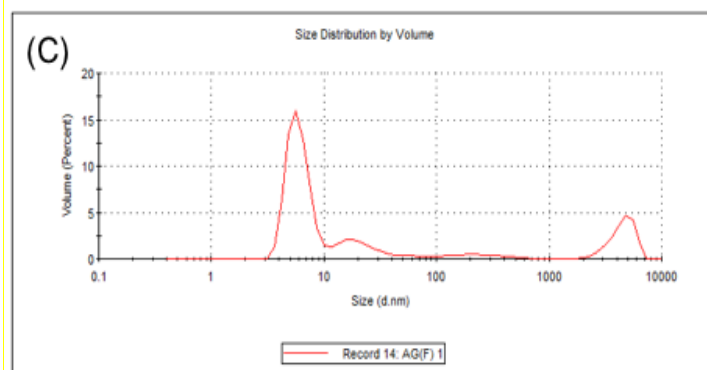
Figure 4.4. AgNPs synthesized in this study: (A) Representative TEM micro-graphs; (B) Zeta potentials; and (C) the particle size distributions.

A representative TEM image of the AuNPs synthesized in this study by using CTAB - as described in the previous section - is given in Figure 4.5 A.  The diameter of these spherical AuNPs was in the range of 30-50 nm. Figure 4.5 B and C show the data obtained with the Zeta Sizer (Nanosizer, Malvern, UK). The apparent average Zeta potential is 49.4 mV with a Zeta deviation of 12.6 mV (the left plot). There are two peaks in the size distribution plot (Figure 4.5 C). About 88.5% (by volume) of the particles were having an average diameter of 47.4±18.25 nm which is quite closed that were observed on the TEM pictures. There were also aggregates (about 11.5% by volume) around 5500 nm which were eliminated just before use at the cleaning process for removal of the excess surfactant (CTAB here). Absorbance spectrum of the gold nanoemulsions were also obtained by LSPR (see also Section 4.4). The $\Delta\lambda_{max}$ value is 523 nm which is typical for AuNPs in that size range.

AuNRs were synthesized by a two step process as described in the previous section. The SEM micrograph given in Figure 4.6A shows that the gold nanorods produced here are quite homogeneous in size and shape - there are only few nanospheres (seed particles) left from the first step - which demonstrates the success of the synthesis protocol applied here.  The average sizes of AuNRs that we have used in the later parts of this study were 10±2 nm (diameter) and 30±5 nm (length) and according to SEM analysis - estimated with a classical software (Adobe Photoshop CS6). A representative UV-vis absorption spectrum of the AuNRs synthesized/used in this study is given in Figure 4.6B. As seen here two peaks at 510 nm and 670 nm are due to the radius and length, respectively. It should be noted that both the position and intensity of the peaks are representative properties of those AuNRs produced.
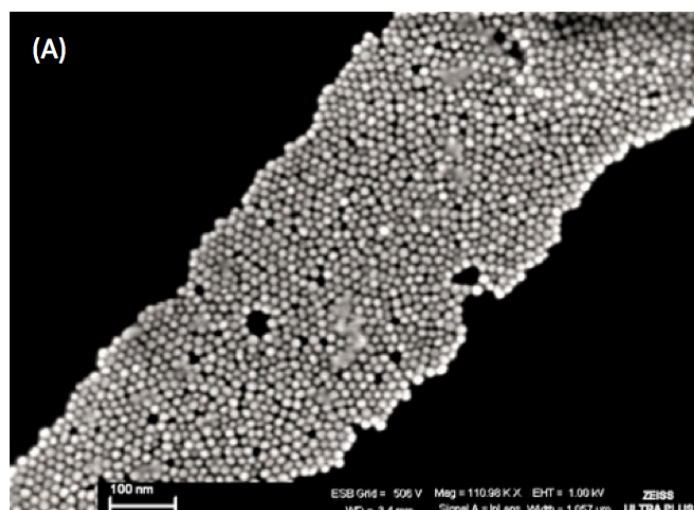
| | | Mean (mV) | Area (%) | St Dev (mV) |
|---|---|---|---|---|
| Zeta Potential (mV): 49,4 | Peak 1: | 45,4 | 85,5 | 7,60 |
| Zeta Deviation (mV): 12,6 | Peak 2: | 74,8 | 14,5 | 5,05 |
| Conductivity (mS/cm): 0,337 | Peak 3: | 0,00 | 0,0 | 0,00 |
| Result quality : See result quality report | | | | |



| | | Size (d.nm): | % Volume: | St Dev (d.nm): |
|---|---|---|---|---|
| Z-Average (d.nm): 57,94 | Peak 1: | 47,74 | 88,5 | 18,25 |
| Pdl: 0,303 | Peak 2: | 5438 | 11,5 | 641,9 |
| Intercept: 0,914 | Peak 3: | 0,000 | 0,0 | 0,000 |
| Result quality : Good | | | | |
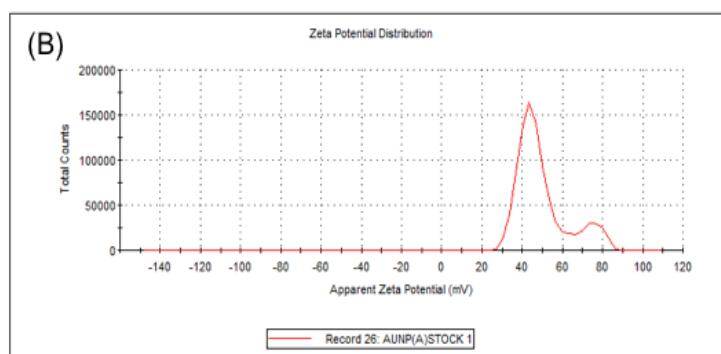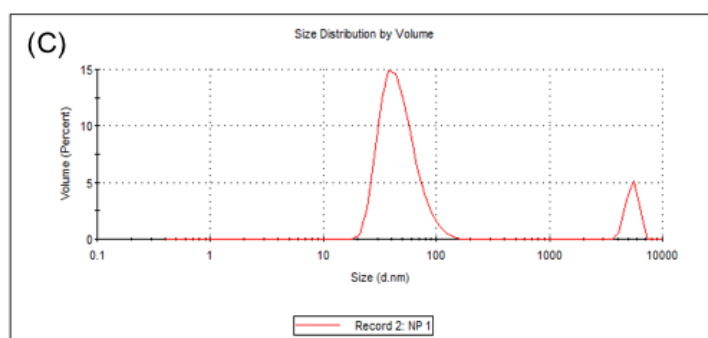


Figure 4.5.  AuNPs synthesized in this study using CTAB - positively charged (A) Representative TEM micrographs; (B) Zeta potentials; and (C) the particle size distributions.
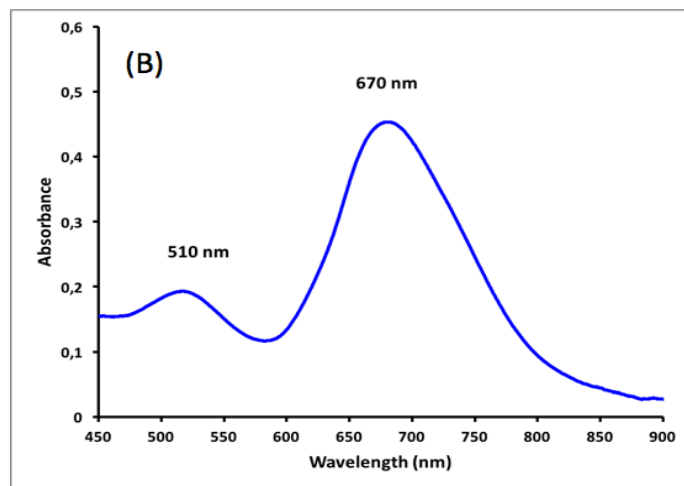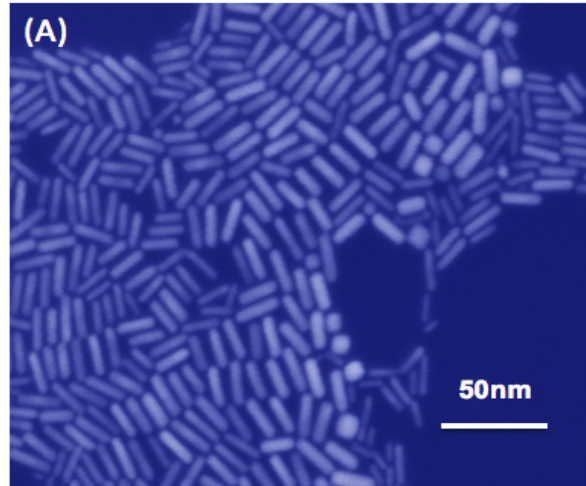
Figure 4.6.    AuNRs synthesized/used in this study: (A) A representative SEM micrographs; and (B) a representative absorbance curve.

## 4.3. Detection with SERS

In the content of this PhD thesis, three group of SERS studies were performed:

(i) **Initial studies**: Here two different basic substrates (see also Section 2), namely glass slides and silica slides were tested. Three plasmonic nanoparticles were used, i.e., spherical silver nanoparticles (AgNPs), spherical gold nanparticles (AuNPs), and rod-shaped gold nanoparticles (AuNRs) - see the Section 3 for synthesis and characterization of these nanoparticles. Three different bacteria, namely *Escherichia coli* (*E.coli*), *Staphylococcus aureus* (*S.aureus*) and *Salmonella infantis* (*S.infantis*) and their respective/specific bacteriophages were propagated as described in the Section 3.

(ii) **"Surface-based" SERS studies**: Here, the plain "silica slides" were the basic substrate; spherical gold nanparticles (AuNPs) were used as the plasmonic nanoparticles which were deposited on the silica slides and then used in the SERS experiments. In this group of tests only the main target pathogen *Escherichia coli* (*E.coli*) and its specific T4-phage were included. Firstly, AuNPs were deposited on the silica slides, then *E. coli* was placed on this surface it, and finally bacteriophages were added on these slides. SERS spectra were taken at each step and compared.

(iii) **"Suspension-based" SERS studies**: In this last group, the plain silica slides were used as the basic platform - it should be noted carefully that these are not SERS substrates - the gold nanorods (AuNRs) were interacted with the target bacteria, *E.coli* in suspensions. They were dropped onto the silica slides, and then its specific T4-phage was added on them and the SERS spectra were collected at selected intervals to follow the destruction of *E.coli* with its specific T4-phage, on the silica substrate with SERS which is actually the main detection strategy of the target developed in this thesis. All these studies are demonstrated/discussed below in separate sub-sections, and in the final part, the results were discussed using the literature studies.

### 4.3.1. Initial Studies

### 4.3.1.1. Nanoparticles on Substrate Surfaces

For enhancement of the Raman signal in the SERS measurements and also to create localized plasmon effect for the LSPR studies, three different nanoparticles with plasmonic properties, namely AgNPs, AuNPs and AuNRs were deposited on these platforms - both the glass and silica slides ("silicone wafers"). Figure 4.7 shows three different nanoparticles on the PDA coated glass slides. The micrographs were taken by the microscope attached to the Raman system - the Olympus BX41 Transmission and Reflection Illumination Microscope (Olympus, France). As seen here all surfaces covered with NPs - quite evenly distributed - not as single particles but rather as aggregates - which was the main objective in this part of studies to have high enough surface enhancement for the Raman spectroscopic analysis and to create the LSPR effect on the platform surfaces.
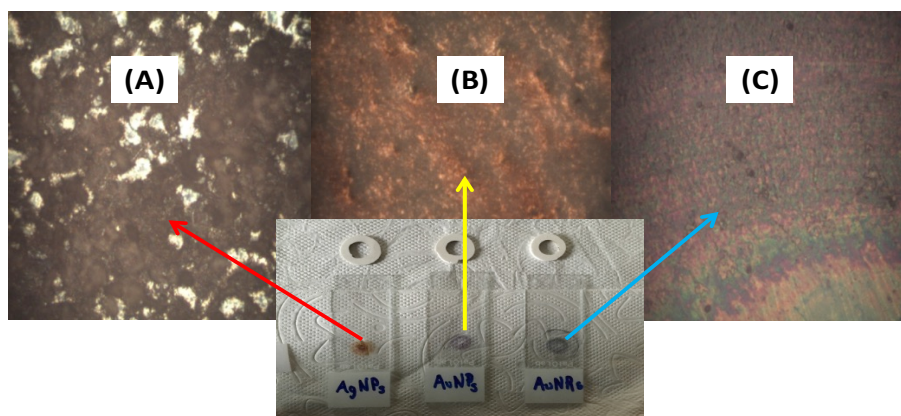
Figure 4.7.    Three different plasmonic nanoparticles deposited on the PDA coated glass substrate surfaces. These representative images of surface taken with the microscope attached to the Raman system: (A) AgNPs; (B) AuNPs; and (C) AuNRs.

Figure 4.8 A, B and C give representative Raman spectra of the "glass slides" carrying two different amounts of the nanoparticles - called as "low" (that was prepared only one step nanoparticle deposition - means low amount of nanoparticle aggregates) and "high" (means more nanoparticle aggregates on the substrate surfaces - prepared by repeating deposition protocol five times). Note that the strong (intensive) peaks on both spectra seen in Figure 4.8 A - for the AgNPs deposited glass platforms - are coming from the glass substrate. Deposition of more nanoparticles decreased those peak intensities, but it was still very significant. Note also that, the peaks were in the range that we receive also the characteristic peaks of the bacteria tested in this study as presented below. Therefore, we concluded that we should not use these glass substrates in further studies.

Figure 4.8 B gives representative SERS spectra of the AuNPs deposited glass substrate surfaces. The preparation protocol was the same as for the AgNPs, however the peaks for gold nanoparticles were different, even at low deposition. The peaks of CTAB coming from the preparation of those gold nanospheres (located at the outer surfaces of the nanoparticles) were trying to push out as - becoming more visible - we see in the figure.

As seen in Figure 4.9 the characteristic peaks of CTAB were matching the peaks on the AuNPs deposited surfaces - which was good however not still very

satisfactory - because there is swelling in the peaks around 1300-1500 cm$^{-1}$ due to the glass substrate. Therefore, we have still decided not to use these glass based substrate in further studies.

We have also tested gold nanorods on the PDA coated glass substrate surfaces. The AuNRs were deposited at two different surface densities and then SERS spectra were collected (Figure 4.9 C). The peaks of coming from the outer layers - the surfactant (CTAB) surrounding these gold nanorods - were not very intense but visible. However, the peaks coming from the glass background were overlapping and led swelling in the peaks for the gold. We have concluded once again that the glass slides were readily available and inexpensive/easy to modify, however due to those background peaks they should not be used for bacterial detection with SERS.

As an alternative to glass slides we have also used silica slides. Figure 4.10 A, B and C give representative SERS data for the silica slides carrying AgNPs, AuNPs and AuNRs, respectively, again at two different deposition densities. Even a single layer deposition exhibited very nice spectra, quite different than those observed on the glass based substrates. There was an intensive/sharp peak around 500 cm$^{-1}$ which is typical peak of silica substrate (Figure 4.10 A) - however this was out of the characteristic peaks region of the target bacteria that is discussed below which was a good result that we were willing to see. Increasing the amount of deposition suppresses the silica peak and the peaks at higher wavenumbers are look-like swollen (much wider - not sharp) which is not desirable. As conclusion AgNPs on silica with low deposition may be good to work in the later parts. However, considering possible antibacterial effects of silver nanoparticles on the target bacteria we have decided not to use these platforms in further studies.
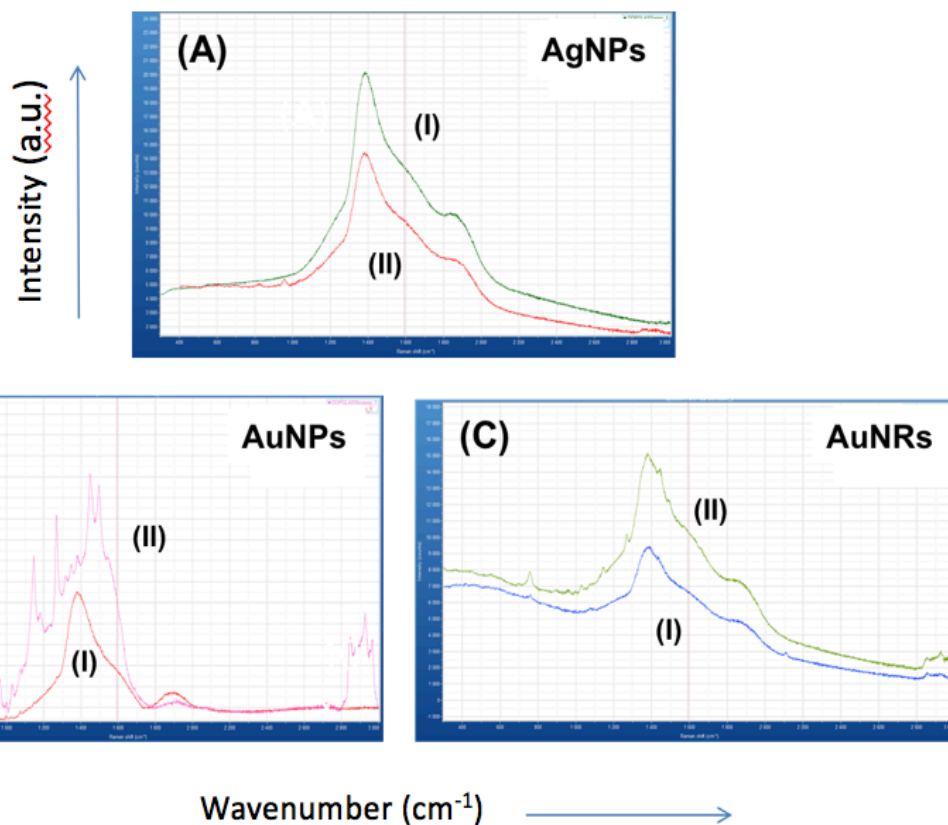
Figure 4.8.    Representative SERS spectra of the glass surfaces carrying nanoparticles with two different surface densities (I-low/one time) and (II-high 5 times): (A) AgNPs; (B) AuNPs; and (C) AuNRs.
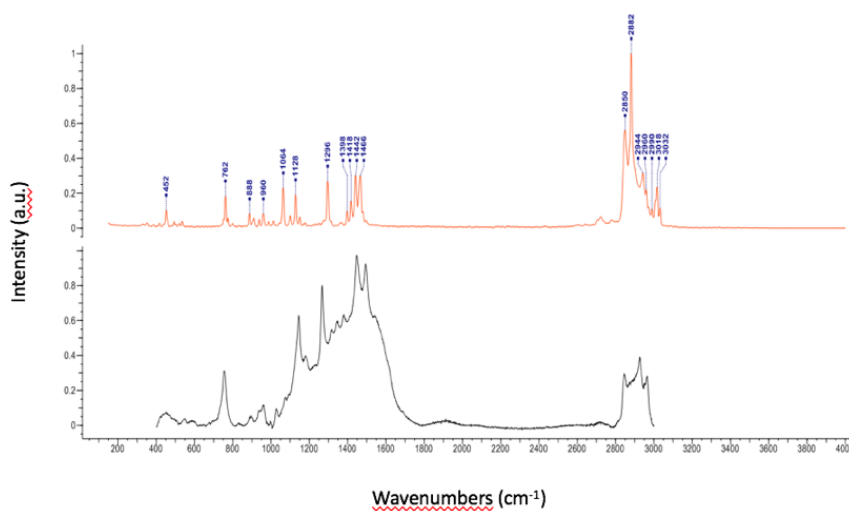


Figure 4.9.    Comparison of SERS spectra of CTAB (taken from the library) and the AuNPs deposited on the glass slides. Taken from the software of the SERS system used.

Figure 4.10 B gives representative SERS data of the spherical AuNPs on silica substrates, at two different deposition densities. Even a single layer deposition exhibited nice spectra. The spectra were quite good with sharp and descriptive peaks. Therefore, we concluded that the silica substrates carrying AuNPs could be used successfully for the bacterial detections with SERS as exemplifies below.

Very similar behaviour was observed the silica substrates carrying the gold nanorods (AuNRs) - similar to both AgNPs and AuNPs (Figure 4.10 C). They were also successful substrates with clear and sharp peaks. Characteristic peaks of silica were visible, it was possible to suppress by using more nanoparticles on the surface, but it was not critical because the peaks were not affecting bacterial peaks as discussed below.
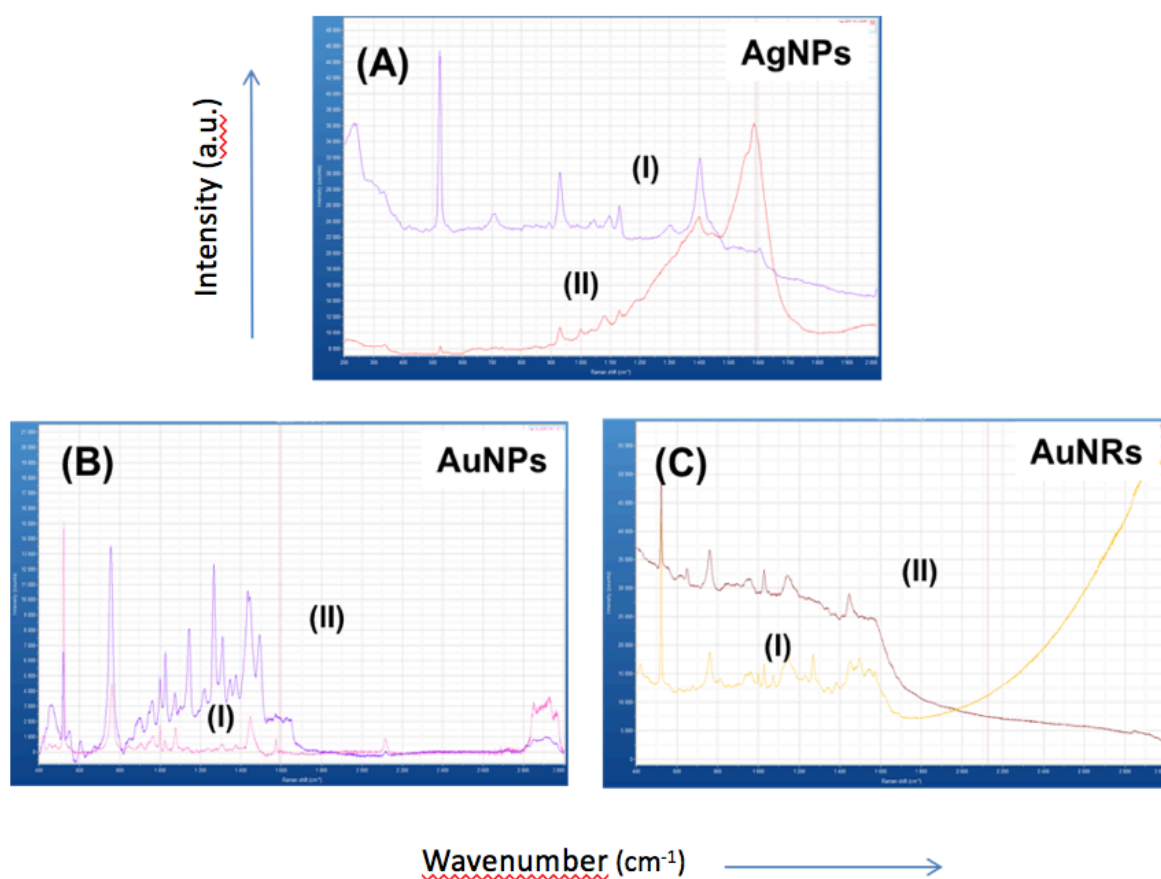


Figure 4.10. Representative SERS spectra of the silica surfaces carrying nanoparticles with two different surface densities (I-low/one time) and (II-5 times): (A) AgNPs; (B) AuNPs; and (C) AuNRs.

### 4.3.1.2. Bacteria and Bacteriophages on Substrate Surfaces

This group of studies were conducted also in the "initial" studies" part. Firstly, 15 µL of three different bacteria (*E.coli*, *S.aureus* and *S.infantis*) and their specific/ respective phages - from their stoke suspensions/emulsions were placed onto the AuNPs deposited silica substrates, dried in the safety cabinet in about 30 min at room temperature then SERS measurements were performed.

Representative SERS spectra of three bacteria and their respective/specific phages are given in Figure 4.11 A and B, respectively. Note that in the tests, firstly the surfaces were observed with the microscope attached to the Raman system. It was possible to see the target bacterial cells individually and their aggregates clearly. The agglomerations were at the side of droplets when it was dried out, however there were also many individual cells that were usually scanned and the signals were collected around them. When the spectra were compared it is easily seen the similarities and differences. The assignments of these peaks are discussed in the later part below. However even from this rather simple diagram, it can be said that it is possible to identify different bacteria by using SERS spectra taken in a very simply approach presented here as also mentioned in similar but quite limited number of studies reported in the related literature.

Representative SERS spectra the bacteriophages are presented in Figure 4.11 B. SERS spectra were collected from both individual phages and aggregates, and the averaged are presented on the graphs. There were very clear and different sharp peaks in each phage spectra which show that they can be easily identified by using SERS data. Note that there are quite a few studies about the assignment of those specific peaks which are discussed below.

In this last group of "initial" studies, in order to observe the effects of phages on the target bacteria we have designed the following tests. Here after taking the images and SERS spectra of the target bacteria on the gold nanosphere (AuNPs) deposited silica surfaces, 15 µL nanoemulsion of phages was dropped onto the substrate surface, and then SERS data were collected from the same spot at selected time intervals, 10, 20, 30 and 40 mins. Note that we have used specific phage only for the target ("its complementary") bacteria. Two representative

microscopy images were taken just before dropping the phage emulsion onto bacteria on the surfaces and in the end (after 40 mins).

As seen in the microscopy images, the target bacteria were quite healthy and in good shape (as individuals or aggregates) just after addition of the phages on the substrates. However, in the end there were almost no bacteria around - only some areas where phages were not able to reach the bacteria. Cloudy views/ appearances were observed most probably due to very high concentration of the phages (new born) in all three cases mentioned above.
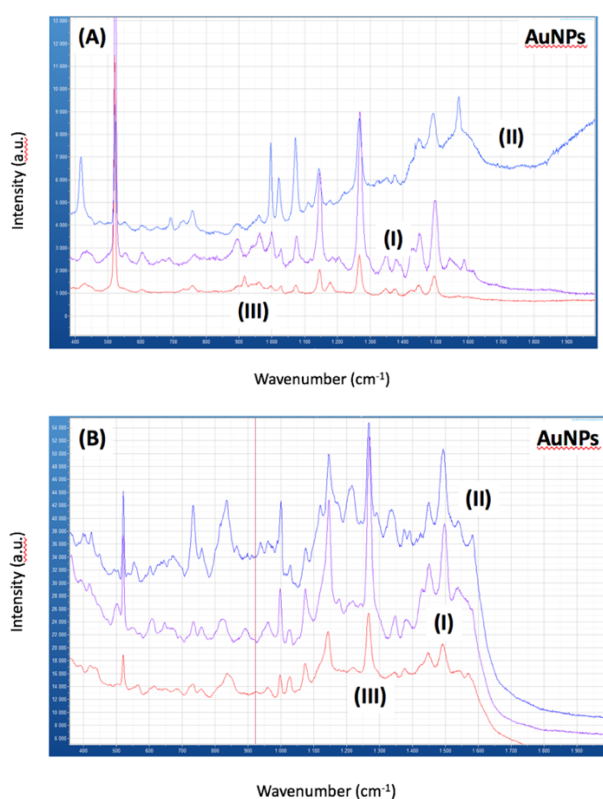


Figure 4.11. Representative SERS spectra of three different bacteria on the AuNPs deposited silica substrates: (A) Bacteria - (I) *E.coli*; (II) *S.aureus*; and (III) *S.infantis*; and (B) Bacteriophages - (I) *E.coli* phage; (II) *S.aureus* phage; and (III) *S.infantis* phage.

Representative SERS data are presented in Figure 4.12 A, B and C. Notice that we have demonstrated the change of the specific peaks of the phages with time. It was very interesting to observe the change of the peak height with time which nicely demonstrated the infection of bacteria with the phage which resulted

significant increases in the number of new (baby) phages which were followed by the increases in the peak heights. Note that the peaks coming from the bacteria were exist but with lower peak heights as expected. This is one of the most impressive results obtained in this thesis. It may be concluded that with a very simple protocol one could detect the bacteria very specifically on SERS substrates by adding bacteria first and then phage on the surfaces. Note that each phage works well for their target bacteria specifically. There were no increases in the peak heights when we used cross phages for different bacteria (for instance *E. coli* phage for *S.aureus* bacteria, so on). This is of course one another important observation showing the specificity of each phage.
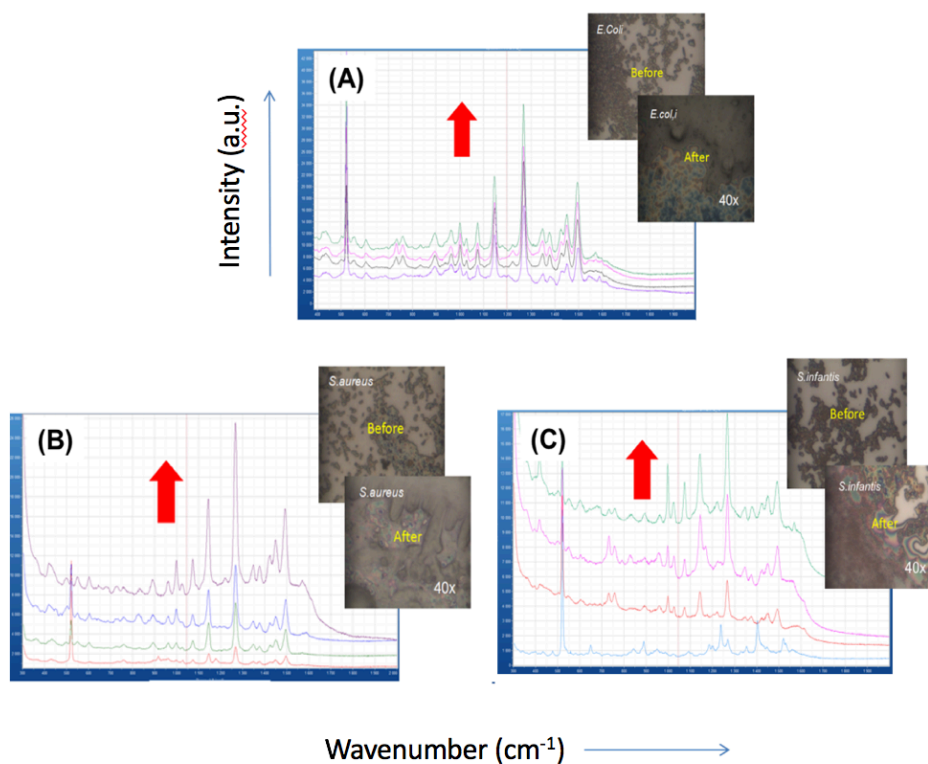


Figure 4.12. Representative SERS spectra and Raman microscopy images of three different bacteria and their bacteriophages: (A) *E. coli* and its phage; (B) *S. aureus* and its phage; and (C) *S. infantis* and its phage on the AuNPs deposited silica surfaces loaded also with the target bacteria. After adding the respective phages which infected the target bacteria. SERS data were collected at selected time intervals. Microscopy images were taken just before addition of phages onto bacteria and in the end (after) of incubation period (40 mins).

### 4.3.2. "Surface-Based" SERS Studies

In this rather new set of "Surface-based" studies, *E. coli* and its specific T4-phage were used. The gold nanospheres (AuNPs) were deposited on the silica slides as described above which were then used in this group of tests to demonstrate their use as a possible the SERS substrate. Figure 4.13 gives representative SEM micrographs of the gold nanospheres used in this part of study at different magnifications - the red arrows indicate the increase in the magnification. They are positively charged and quite homogeneous in size and spherical in shape seems that they are quite suitable to prepare the SERS platforms by simple deposition onto the silica slides.
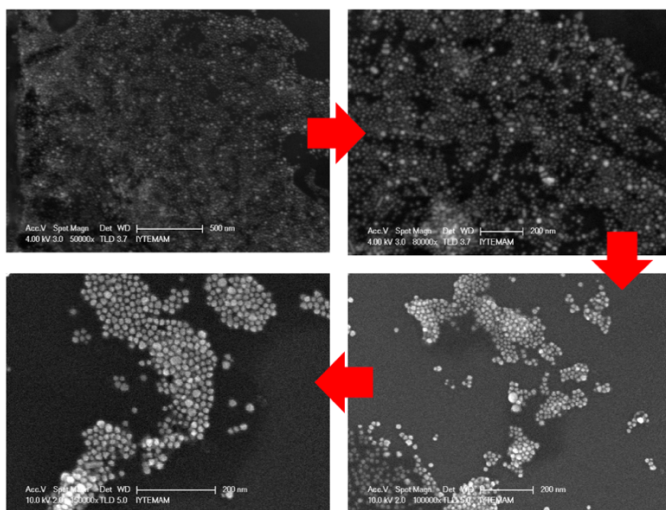


Figure 4.13. Representative SEM micrographs of the gold nanospheres used in this part of study at different magnifications - the red arrows indicate the increase in the magnification.

Representative SERS spectra of the AuNPS deposited on the silica substrates are given in Figure 4.14A and B which are taken from the same surfaces, in addition the wavenumbers of the peaks are indicated in "B". The strong and sharp peak at 520 cm$^{-1}$ is the main representative peak of silica, the other are mostly coming from the surfactant (CTAB) - the leftovers - used for the preparation of the AuNPs - which cannot be removed wholly. The wider peak at around 2900 cm$^{-1}$ is the hydrogen peaks of Au.
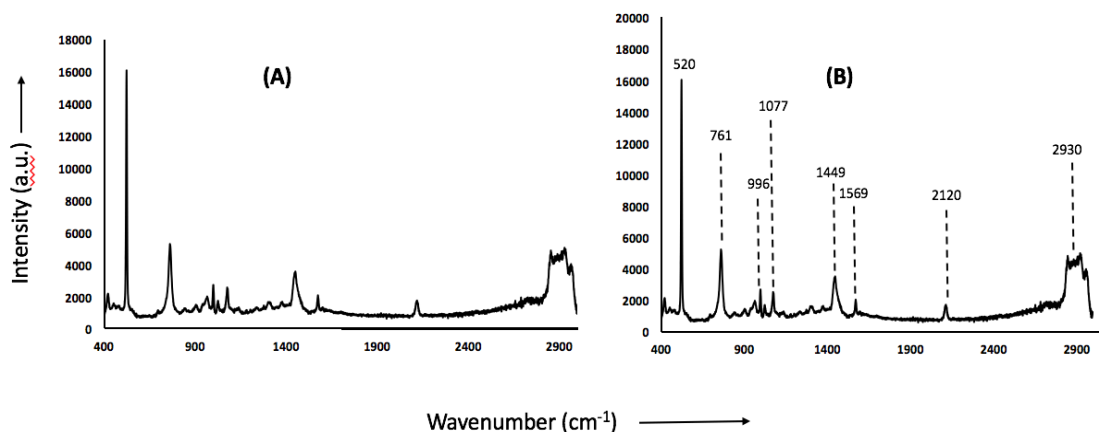
Figure 4.14. Representative SEM micrographs: (A) The AuNPs loaded silica surfaces; and (B) the same sample with the peaks assigned.

Following the previous step, the samples of the suspensions carrying *E.coli* were dropped onto the silica slides loaded with AuNPs and SERS spectra were collected. Representative spectra are given in Figure 4.15A and B. The silica peak was maintained in Figure 4.15A - however, only the peaks wavenumber region (650 - 1750 cm$^{-1}$) are given in Figure 4.15B with the numerical values of the peaks - which are mainly *E.coli* peaks. These are discussed in detail in the last part of this section.

Figure 4.16 gives representative SERS spectra taken after dropping of T4-phages on the AuNPs loaded surfaces which are carrying also the target bacteria *E. coli*. The peaks assigned are very similar to the previous graph in which there are only *E.coli* on the AuNPs loaded surfaces. It is almost impossible to distinguish if we added the phage or not. It is expected because the graph is taken in very early time after addition of bacteriophages - since there is no destruction yet which means that one could detect the target bacteria only by using these specific bacterial peaks - no effect of phage. This is even an important observation means demonstrating that the gold nanopheres that we have synthesized in this study can be deposited onto the silica surfaces in a very simple way and then can be used to collect SERS data of the target bacteria - which be further evaluated to match the assigned peaks with the correct library for the identification of the type of the target bacteria.
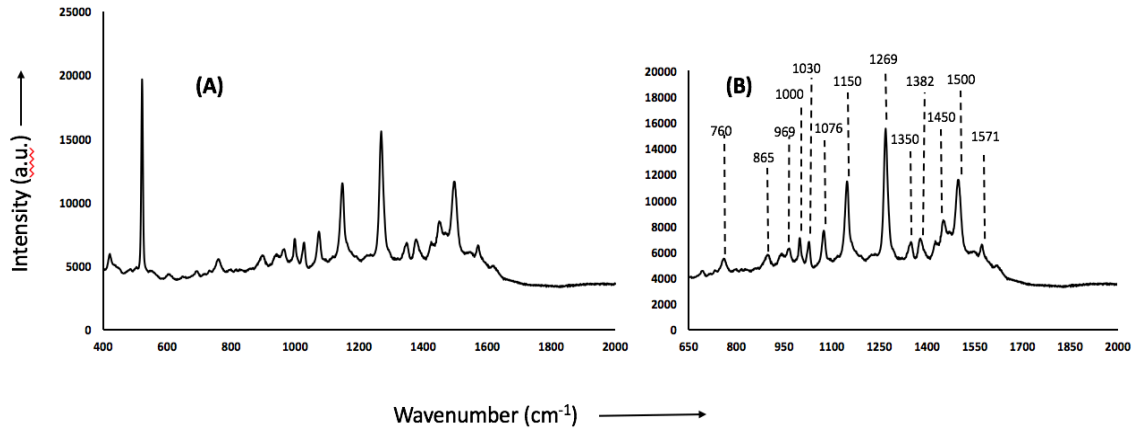
Figure 4.15. Representative SEM micrographs: (A) *E.coli* on the AuNPs loaded silica surfaces; and (B) the same sample with the peaks assigned.

Figure 4.17 is prepared by putting together three representative spectra, given in the previous figures - just to make the comparison between the spectra especially for the *E.coli* and *E.coli* + T4-phage. Again it can be concluded that the platforms prepared by deposition of AuNPs on silica slides are excellent SERS platforms - very easy to prepare - and quite successful to obtain very clear peaks descriptive for the bacteria but not differs the bacteriophages if there is no destruction.
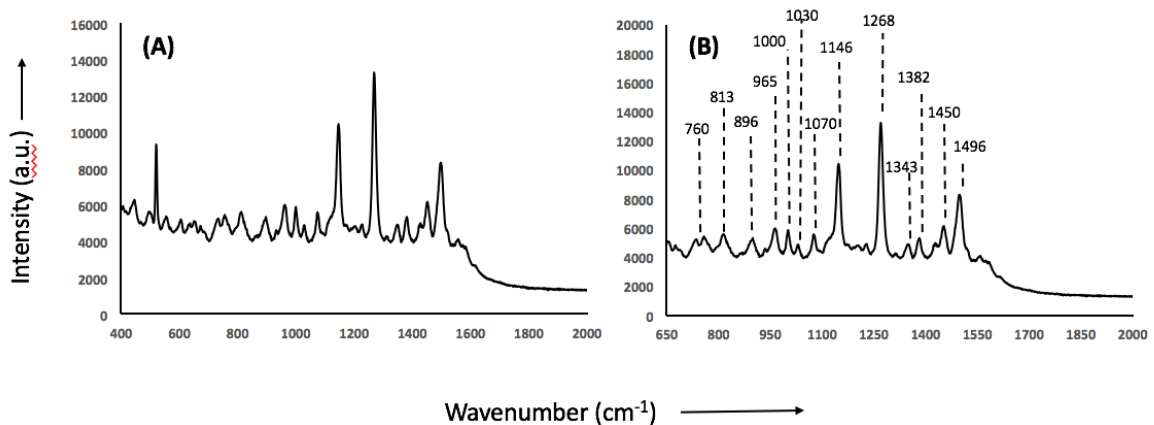


Figure 4.16. Representative SEM micrographs: (A) T4-Phage dropped on the AuNPs loaded silica surfaces carrying also *E.coli* (very early phase - not destruction of *E.coli* yet); and (B) the same sample with the peaks assigned.
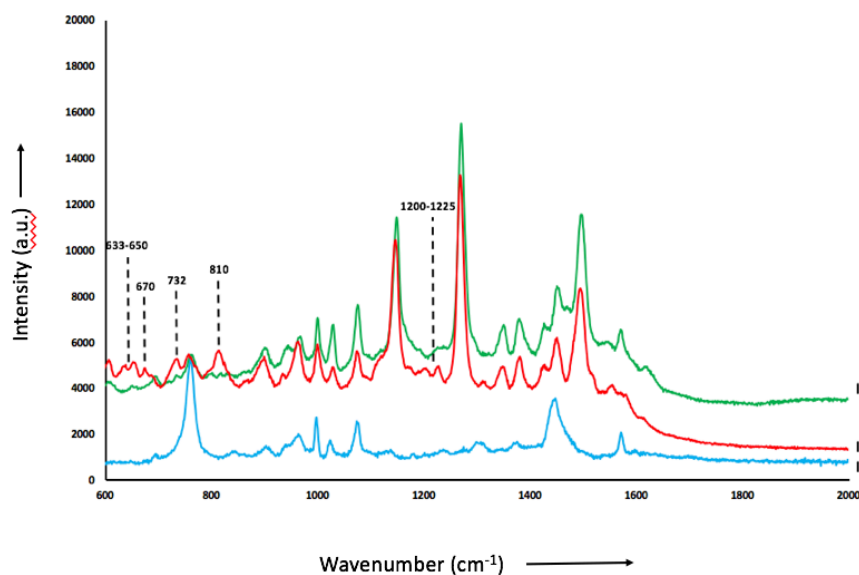
Figure 4.17. Comparing representative SEM micrographs of: (A) AuNPs on silica; (B) *E.coli* on the AuNPS deposited silica; and (C) T4-phage on the AuNPs loaded silica surfaces carrying also *E.coli*.


### 4.3.3. "Suspension-Based" SERS Studies

In this group of studies, an important alternative approach was applied. Here only gold nanorods were used in order to "the proof of concept" in this part of the study. The AuNRs added to the target bacterial suspensions, incubated at room temperature about 30 mins, then they were dropped onto the plane silica slides, dried and microscopy images were taken and SERS data were collected. It is very important to note that in this group of tests we were focusing the incident light on individual (single) bacteria, therefore the detection limit was almost a single bacterial cell level which is a very impressive result. Then the specific phages were added and the changes in the SERS spectra were observed. Note that for the demonstration of "the proof of concept" we have studied only with *E. coli* and its specific phage - T4 in this part of studies.

Representative SEM images of the components used here - which are taken on the basic substrate platform - "silicone slides" - are given in the figures presented below. Gold nanorods (AuNRs) are clearly observable which are with quite narrow size distribution and have excellent rod shape with very close dimensions (Figure 4.18A). The images of T4-phages and *E.coli* are typical, as also demonstrated in the related literature discussed in the later part of this section (Figure 4.18 B).

88
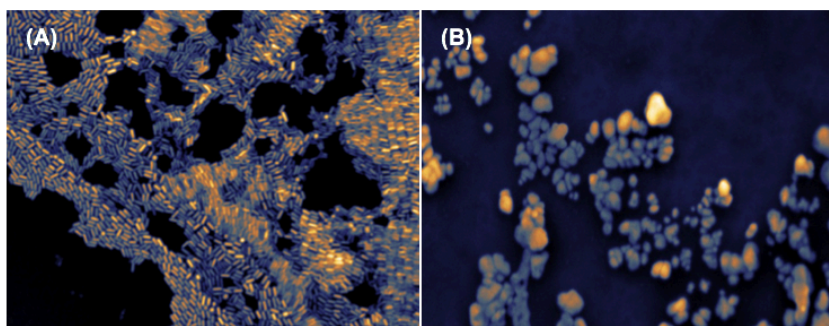
Figure 4.18.  Representative SEM images taken on the substrate -  silicon slides: (A) AuNRs; and (B) T4 phages.

Representative images of *E.coli* at different magnifications are shown in Figure 4.19A and B, in which some of the bacteria are already invaded (destructed) by T4- phages - as exemplified in the inset - as mention also in the previous sections.
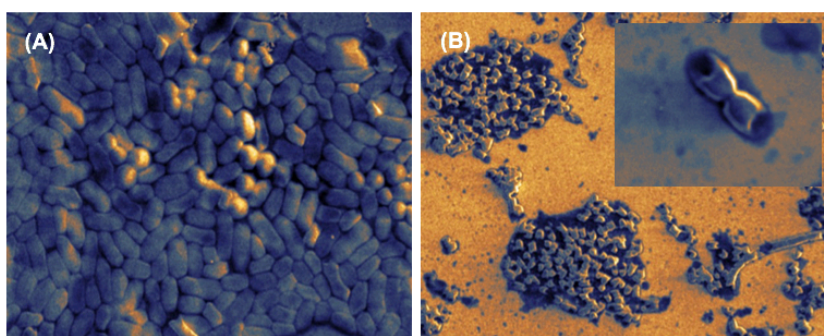


Figure 4.19.  Representative SEM images taken on the substrate - silicon slides: (A) *E. coli*; and (B) *E. coli* after interaction with its phage - very early time - bacterial destructions just started as seen in the inset.

Representative SEM images of the target bacteria, *E. coli* after interactions with the AuNRs in suspension (then dropped on the platform surfaces) are given in Figure 4.20A and B. As seen here positively charged gold nanorods were accumulated on the negatively charged bacterial surfaces quite heavily and evenly, which allowed clear detection of the target bacteria without using any SERS substrate - on the simple silica slides ("silicone wafers") surface as discussed below. The closer look given in Figure 4.20B demonstrates how gold nanorods are accumulated on one single bacterial cell -  that allows single bacterial detection by the localized plasmon effect of the AuNRs aggregates.
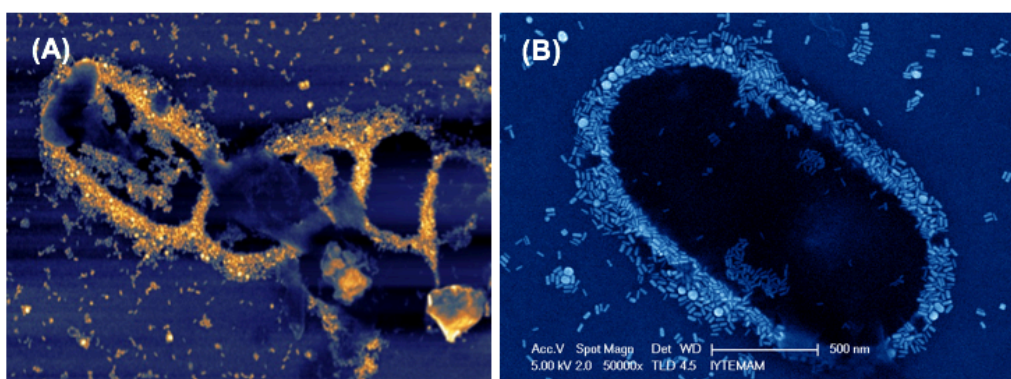
Figure 4.20.  Representative SEM images taken on the substrate - silicon slides: (A) AuNRs accumulated around the target bacteria, *E.coli*; and (B) this closer look demonstrates how gold nanorods are accumulated on one single bacterial cell -  that allows single bacterial detection by the localized plasmon effect of the AuNRs aggregates.

Three main elements of the system, i.e., *E.coli* + AuNRs attached to the bacteria + T4 phages are shown together in the same representative figures (Figure 4.21 A and B) which were taken at very early stage - no bacterial destruction yet - only AuNRs and T4 phages were accumulated on *E.coli* - the target bacteria). This is an excellent demonstration of how gold nanorods and bacteriophages could work on the same bacterial target cells.

Before collecting the SERS data, we have first observed the surfaces with the Olympus BX41 transmission and reflection illumination microscope attached to the Raman spectrometer that we have used in this study. In order to demonstrate the power of the microscope, several images were taken at different steps of the SERS analysis. Figure 4.22 gives representative images: (A) *E. coli* on the substrate surfaces; (B) after additions of the nanoemulsions of AuNRs onto those surface - notice that the AuNRs are accumulated on the bacteria and create a shining redlike color; and (C) about 30-40 mins after addition of the T4 phages onto the previous surface in which the bacteria have already totally destructed by the T4-phages and an oily-look images are observed which nicely demonstrates what happens on the surfaces and exhibits of the power of our Raman system.
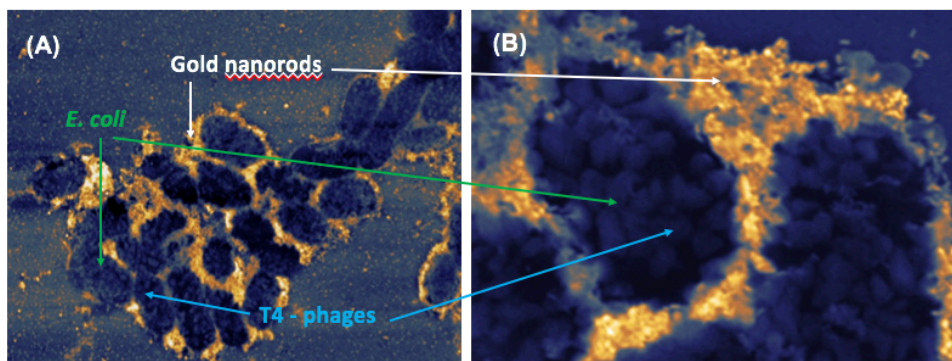
Figure 4.21. Representative SEM images taken on the substrate - silicon slides: (A) AuNRs and T4-bacterophages accumulated onto the target bacteria - *E.coli* – not the destruction started yet only bacterial adhesion on the bacterial cell wall; and (B) a closer look showing accumulation of both gold nanorods and phages on the bacterial cell wall.
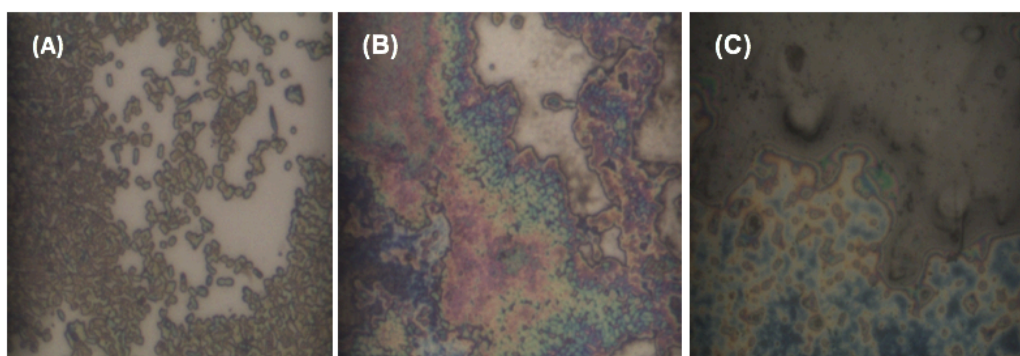


Figure 4.22. Representative images taken with the "Transmission and reflection illumination microscope" attached to the Raman spectrometer: (A) *E.coli* on substrate surfaces; (B) AuNRs on bacteria (shinning red-like color); and (C) after addition of phages which destructed almost all bacteria on the surfaces and an oily-look images were observed.

One of the main objectives of this study is to obtain SERS data of the target bacteria using gold nanorods without using any SERS substrate. In the SERS analysis we have applied the following protocol: AuNRs were added to the target bacterial suspensions, incubated at room temperature about 30 mins, then they were dropped onto the silicone wafers; dried and the surfaces were first observed

with the microscope (attached to the Raman Spectrometer) and images were taken. Then we have focused on the selected target bacteria and collected the SERS data. Note that it was possible to focus onto individual bacteria and take the SERS image, indicating that our data is demonstrating almost single bacterial detection.

In order to demonstrate SERS data of the components of the detection strategy SERS spectra of each component were collected in an order. The representative spectra of *E.coli* on the silica substrate are shown in Figure 4.23A and B. As seen here there are only two peaks, one is at 520 cm$^{-1}$ which is the typical peak representing silica substrate, and the other is at 950 cm$^{-1}$ which is coming from *E. coli* dropped on the silica slide. In Figure 4.23B - the ordinate is extended to make the peak more visible - it is quite weak and does not represent any *E. coli* bacteria on the surface.
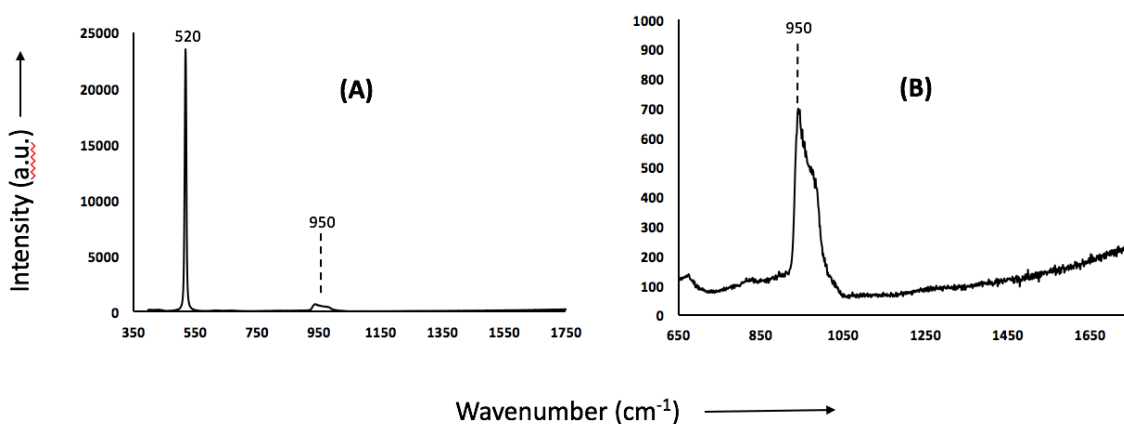


Figure 4.23. Representative SERS data for *E.coli* on the silica slide (A). The ordinate was enlarged to make the peak of *E.coli* more visible (B).

Figure 4.24 give the representative spectra of *E.coli* first interacted in suspension with the gold nanorods and dropped on the silica surface for collecting SERS data. It seems that even using only AuNRs quite clear and strong peaks can be obtained. Notice that silica is not a SERS platform and it is not possible to get the bacterial peaks as demonstrated in the previous paragraph. The plasmonic gold nanorod aggregates on the bacterial cell walls allowed us to get the spectral peaks of *E.coli*. This is a quite nice finding. The specific peaks of *E.coli* are also indicated in Figure 4.24 B, that will be further discussed in the end of this section.

In the following step, the samples of the nanoemulsions carrying T4-phages were dropped on the substrates already having the AuNRs accumulated bacteria, and SERS data were collected at selected time intervals. Several data were collected at many different points on the sample, and these experiments were repeated many times. Representative SERS spectra are given in Figure 4.25A-H. The peaks are quite sharp and intense, note that these were single bacterial cell level therefore "the limits of detection" which was cellular level - should be considered as very significant result of this study. This may be attributed to the localized surface plasmon effects of the gold nanorod aggregates on the bacterial cell wall as also demonstrated above.
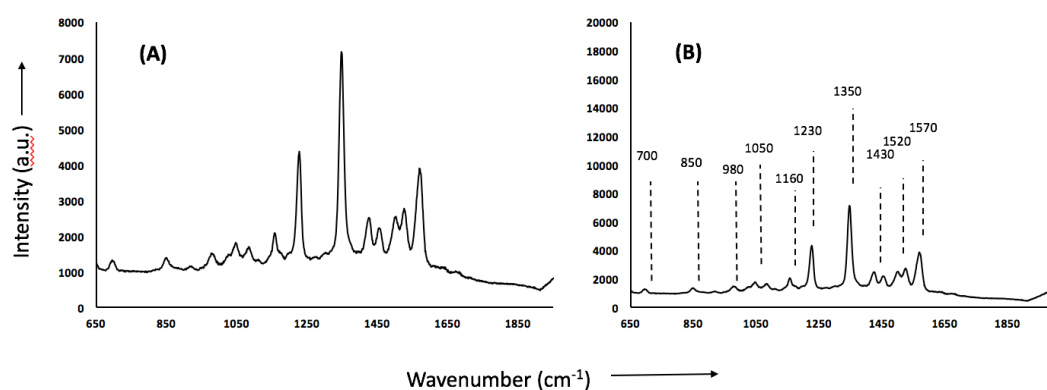


Figure 4.24. Representative SERS data for *E.coli* + AuNRs (interacted in the suspen-sions and dropped on the silica slides: (A) Typical extended spectrum obtained; and (B) the wavenumbers are placed on characteristic peaks.
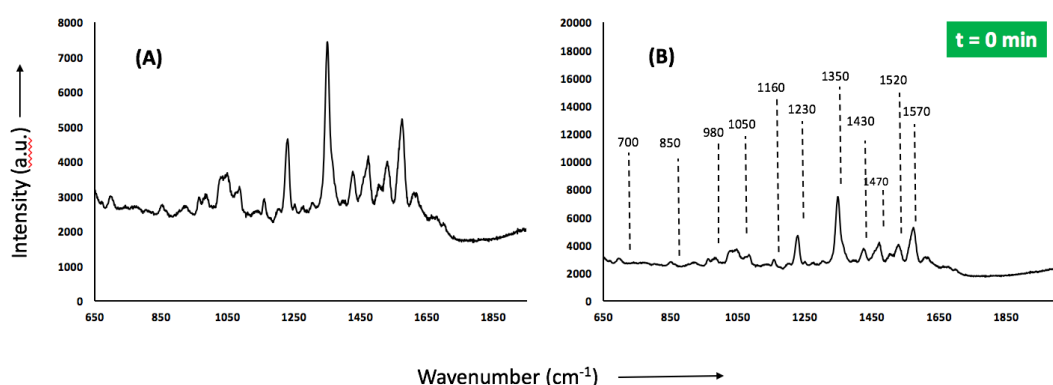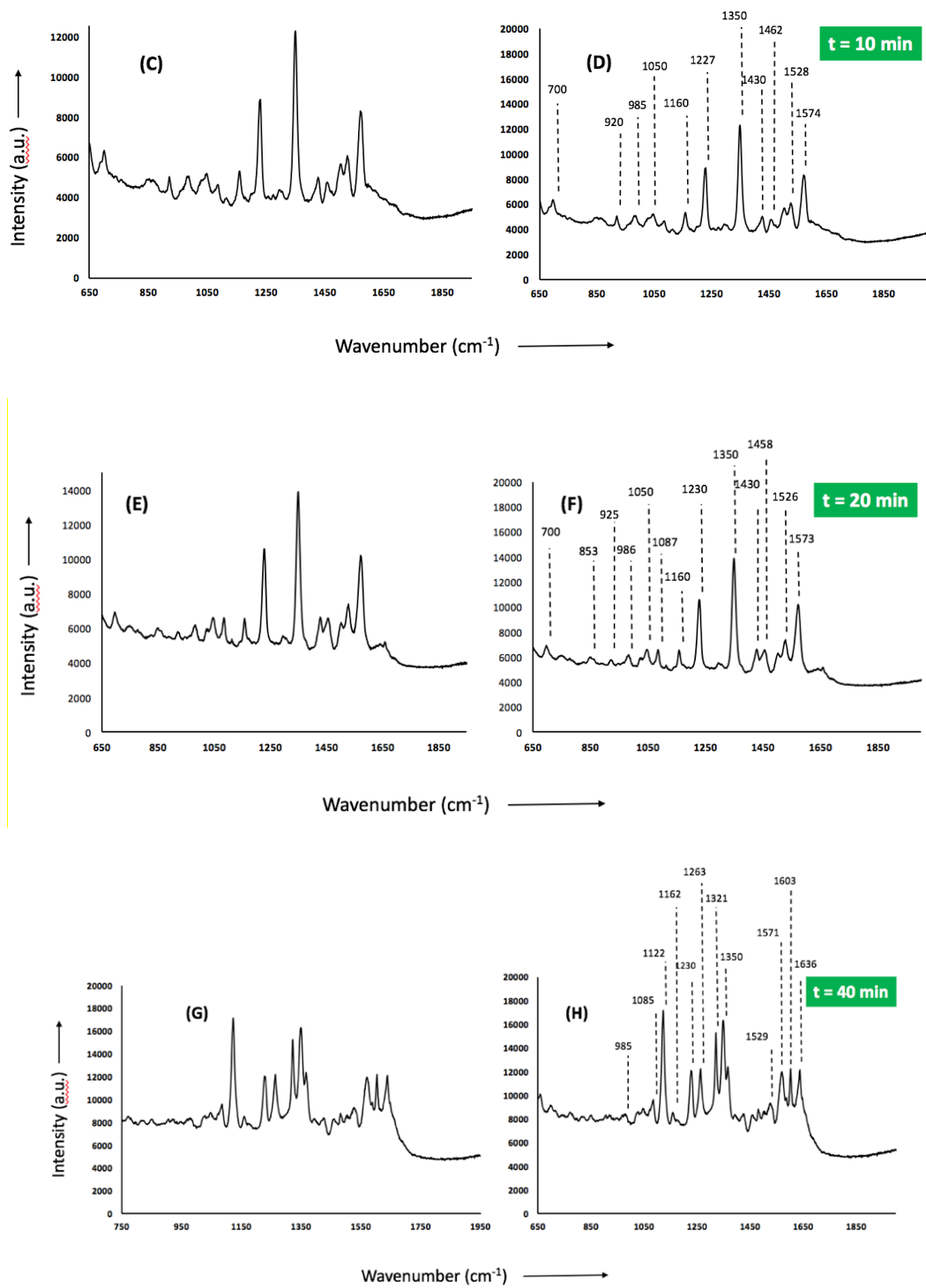
Figure 4.25. Representative SERS data for *E.coli* + AuNRs (interacted in the suspensions and dropped on the silica slides: (A, C and D) Typical SERS spectra obtained at different times (0, 10, 20 and 40 mins) after addition of the T4 phages; and (B, D and H) the wavenumbers are placed on characteristic peaks.

Figure 4.26 which summarizes the results of the whole steps in this suspension-based detection approach in one graph - brings together the whole SERS spectra given in Figure 4.25A-H. Once again it should be noted that the substrate platform was silicon wafer - which does not give any spectral response between 650-1800 cm$^{-1}$ therefore could not overlap the bacterial/phage peaks. The spectrum of the surfaces carrying only bacteria (no AuNRs no bacteriophages) is in the bottom of the figure (the Curve I) which is expected because the silica surface is not a SERS substrate, rather a platform with no plasmonic properties. The Curve II is a typical spectrum of *E. coli* carrying AuNRs on their surfaces, due to very strong plasmonic effects of the AuNRs aggregates on the bacterial wall allowed us to obtain the Raman spectra of the *E.coli* with sharp and clear representative peaks.

In the second step the T4-phage nanoemulsions were dropped onto the silicone wafers evaluated in the previous step - carrying *E.coli* + AuNRs and SERS data were collected at selected time intervals - 10, 20 and 40 mins. The representative spectra are illustrated as the Curves III, IV, V and VI respectively. Notice that the first three curves are almost identical - there are changes in the intensities of some peaks but not significant. However, the curve VI was very different than the others. It should be noted that phages did attack their target bacteria, infected and destructed almost all in about 30-40 mins. There were few new/very strong peaks at 1124, 1260, 1320, 1367, 1602 and 1639 cm$^{-1}$ which do not exist (or very weak) in the *E. coli* spectra (the curves II). It is important also to note that instead of T4 phage which is specific to *E.coli* we have repeated these experiments using the phage specific to *S.aureus* not to *E.coli*, and observed no changes in the Raman spectra of *E. coli* which exhibited the specificity of the T4 phage..

### 4.3.4. Discussions Using the Related Literature

Bacterial infections are among the most serious and costly public health concerns worldwide. Monitoring/early detection of pathogenic bacterial contaminations/ infections is one of the most important priority globally. Development of fast, accurate and sensitive detection and monitoring of pathogens, which should be miniaturized/portable automated therefore cost effective, is a very important challenge. The main aim of this study is to develop alternative bacterial detection strategies using mainly "bacteriophages" with plasmonic "gold nanorods" by Raman spectral analysis - in other terms by SERS.
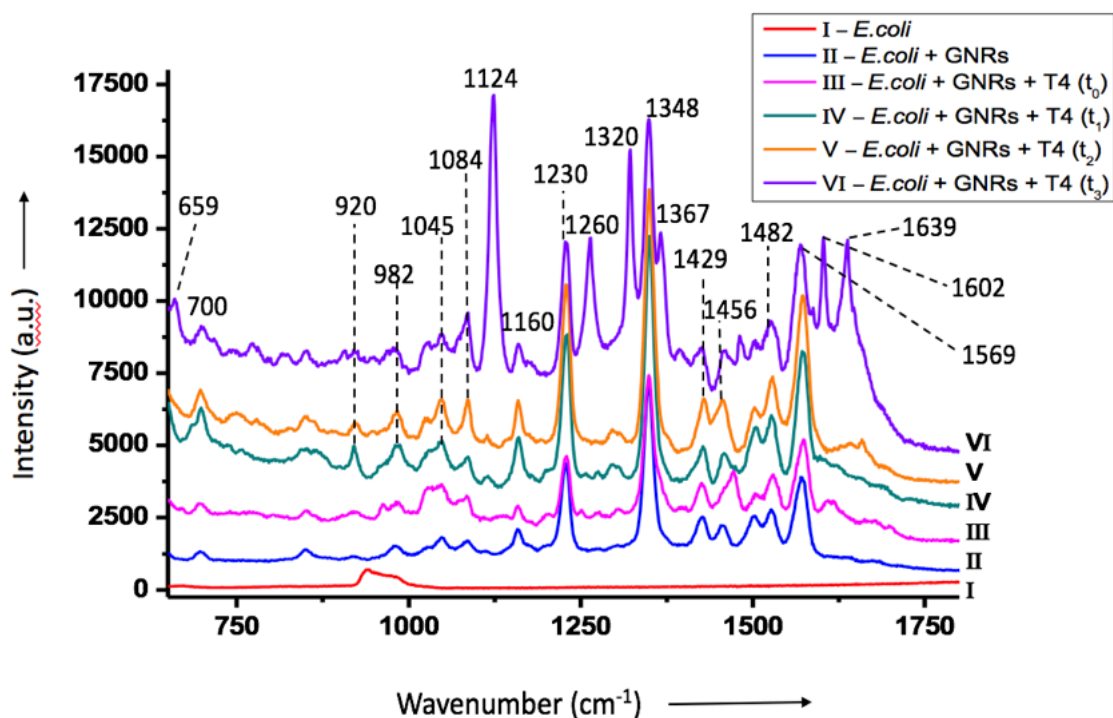
Figure 4.26. Representative SERS spectra: (I) *E.coli* on the substrate (silica) surfaces; (II) *E.coli* first interacted with the AuNRs in suspensions then dropped on the substrate surfaces; (III) T4 phages nano-emulsions were dropped on the substrates carrying *E.coli* and AuNRs - just after addition of phages (t=0, $t_0$); (IV) the same - after 10 mins (t=10 mins, $t_1$) (V) the same - after 20 mins (t=20 mins, $t_2$) and (VI) the same after 40 mins (t=40 mins, $t_3$)

It should be noted that Raman spectra for many rather small molecules/ biomolecules are very unique. Therefore, it is rather easy to identify these molecules - quite specifically and sensitively - by using those SERS spectra - commonly called "fingerprints". There are also several studies in the related literature for detection of bacteria including *E.coli* with SERS using silver and gold nanoparticles and nanostructured surfaces for enhancement. Almost all of them based on target identification of the peaks (fingerprints) on the spectra for detection of bacteria - which is the main point/difference of the present study in which we are not targeting identification of those peaks for detection but using specific phages as described above. The rational of this way of thinking is that there are differences and similarities in the peak positions and also intensities of

the SERS spectra obtained for different bacteria - but more importantly there are also significant differences in the *E. coli* spectra published by different groups for *E. coli*. It is quite understandable, bacteria are not a simple molecule/entity, it is a huge pool of different molecules from simple to highly complex 3D structures and molecular weights. Especially biopolymers, like DNA/RNA, proteins, poly-saccharides are formed of similar units but with different numbers. Having the same or even similar SERS spectra - even for the same target bacteria is almost impossible - assignments of the characteristic peaks is only an approximation. The differences could also be due to different methods of sample preparation and measurement and possible conformational changes of the cellular biopolymers (proteins, etc.) when they interacted with different platform nanostructured surfaces or nanoparticles. When using nanoparticles as SERS enhancers, it is generally agreed also that colloid reproducibility, particle size and aggregation, and their relative number to the target bacteria within the medium may also influence the magnitude of enhancement and therefore the intensities.

Some of the characteristic peaks can be summarized as follows: It is generally agreed there are some representative similar peaks mostly in the regions 500-800 cm$^{-1}$ and 1100-1700 cm$^{-1}$ but there are differences mostly in the region 800-1000 cm$^{-1}$ (Zeiri et al. 2004; Zeire and Efrima, 2005; Jarvis and Goodacre 2004; Jarvis, Brooker and Goodacre, 2004; Sengupta, Mary and Davis, 2005;  Sengupta, Mirna and Davis, 2006; Sil et al., 2017). The double peak at about 960 cm$^{-1}$ is due to the C-C stretch (or C-C-N stretch) which is abundant for various proteins in the cell (Spiro and Gaber, 1977; Sengupta, Mirna and Davis, 2006). Note also that the peaks in the regions 600-900 cm$^{-1}$ and 1200-1400 cm$^{-1}$ for *E.coli* are similar to those for flavin adenine dinucleotide (FAD). The flavin FAD and flavin adenine mononucleotide (FMN), which are located in the cell walls of bacteria, are coenzymes that participate in the respiratory processes in a living cell (Morris and Beinstock, 1986; Zeiri et al. 2004; Sengupta, Mirna and Davis, 2006). The bacterial amide fingerprint located are observed at 1620-1640 cm$^{-1}$ in the SERS spectra for *E. coli*, however it may be overlayed with the water peak at 1635 cm$^{-1}$ (Sengupta, Mirna and Davis, 2006).

Lan et al have reported the strict differences for *E.coli* and *S.typhimurium* in the peak position and relative strength (Lan et al., 2015). They have pointed out the

following peaks and and corresponding sources: 659 cm$^{-1}$ for guanine (C-S); 722 cm$^{-1}$ for adenine; 960 cm$^{-1}$ for C=C or thyrosine; 997 cm$^{-1}$ for phenylalanine or glucose; 1027 cm$^{-1}$ for a ring stretching, or (C-H) deformation; 1086 cm$^{-1}$ for phenylalanine; 1169 cm$^{-1}$ for 12-methyltetradecanoic acid or 15-methylpalmitic acid or acetoacetate; 1248 cm$^{-1}$ for C-H$_2$ stretching; 1335 cm$^{-1}$ for C-H$_2$ deformation or tryptophan; 1472 cm$^{-1}$ C-H$_2$ deformation of the protein molecules; 1535 cm$^{-1}$ for adenine, cytosine and guanine; 1601 cm$^{-1}$ for tyrosine, (C-N) stretching vibration; 1715 cm$^{-1}$ for C=O.

Naja et al. have reported that peaks at 600-800 cm$^{-1}$ and at 1500-1700 cm$^{-1}$ could be attributed to nucleic acids and reflected the presence of adenine, guanine, cytosine and thymine (or uracil for RNA) molecules (Naja et al., 2007). The peak at 990 cm$^{-1}$ indicates the presence of phenylalanine molecule as an important aromatic amino-acid residue. The peaks at 721 and 1029 cm$^{-1}$ correspond to the presence of carbohydrate compounds. The peaks at 1300-1400 cm$^{-1}$ are generally assigned to protein groups whereas peaks around 1462 cm$^{-1}$ are attributed to lipids.

The band attribution of the *E.coli* spectrum obtained in this work was based on similar spectra found in the related literature. In detail, the vibrational spectra of *E.coli* exhibited some bands near 2922 cm$^{-1}$ (not shown) due to the CH$_2$ asymmetric stretching vibration and the peaks at 1605-1690 cm$^{-1}$ are due to the deformation vibration of N-H or the stretching vibration in C-N of the amide I groups. The 1552 cm$^{-1}$ peak corresponds to different organic vibrations between C, N and H in amide or other groups. The peaks at 1485, 1462, 1355 and 1271 cm$^{-1}$ are attributed to the NH$_2$ stretching in adenine and guanine, to the CH$_2$ scissoring deformation in lipid groups, to the CH deformation vibrations and to amide III components. In addition, the peaks at 1056 and 1235 cm$^{-1}$ are attributed to the stretching vibration of C-C in alkanes and to the vibration of N-H, respectively. The band attribution in the region of 500-800 cm$^{-1}$ are more difficult since the peaks were weaker and less resolved. The observed peaks come from amino-acids, polysaccharides, lipids, and sugars. The 1008 cm$^{-1}$ band associated with the aromatic ring breathing mode. In brief, the Raman spectrum was reported to consist of several small peaks, occurring between 500 and 1700 cm$^{-1}$, and two dominant peaks, at 1355 and 1635 cm$^{-1}$, respectively.

The results of different bacteria like *E.coli* and *S.typhimurium* show the differences in structure and composition of proteins in both species. The peaks at 1530 and 1535 cm$^{-1}$ represent adenine, cytosine and guanine. Amide III band is observed at 1232 cm$^{-1}$ in the *S.typhimurium* spectrum The bands at 722 cm$^{-1}$ and 729 cm$^{-1}$ in are the deformational vibrations of adenine, and these bands are the typical spectral characteristics of DNA in *E.coli* and *S.typhimurium.* There are also different bands which are not interpreted in detail as they are not very conclusive, but they might be affected by cell lysates.

### 4.3.5. Conclusion of SERS Studies

In this "the proof of concept" study a very simple SERS strategy was applied in which target bacteria (i.e., *E.coli*) were interacted with AuNRs in suspensions, and then they were dropped onto plain silica substrate surfaces for detection.  As clearly demonstrated in the electron microscope images the positively loaded AuNRs were heavily accumulated around the negatively charged bacterial cell walls which allowed us to collect the SERS spectra (the "fingerprints" of the target bacteria) without using any SERS platform - only as a result of enhancing effects of the plasmonic AuNRs accumulated onto the bacteria - which was one of the important results of this study. In the second step, bacteriophages (as the specific bioprobes) were dropped onto those surfaces and SERS data were collected by focusing on even individual bacterial cells at different time intervals up to 40 mins. Bacteriophages are viruses which do infect only living bacteria quite specifically even at serotype level. When they infect their target bacteria, after an about 20-40mins propagation process their number increases about 300 times even larger - that means a very significant increase in the detection signal. In this study the SERS data collected with time in the tests after addition phages onto the AuRs-bacteria complexes on the silica platforms exhibited that a number of new quite intense/sharp were appeared in about 30-40mins. It should be noted that there was no change in the SERS spectra of the nontarget bacteria (i.e., *S.aureus* here) with time after addition of T4-phage which was specific only for the target bacteria (i.e., *E.coli* here). This was the main result of this study - demonstrated that one could detect the target bacteria very specifically and sensitively (even at one bacterial cell level) using bacteriophages as bioprobes and plasmonic nanoparticles (i.e., AuNRs here).

## 4.4. Detection with LSPR

In the LSPR experiments, firstly the spectra of the substrates surfaces and NPs on these substrates were taken. Then, 15 µL bacterial (here *E.coli*) suspension was dropped onto the LSPR platform, dried in a safety cabinet for about 30 min at room temperature then LSPR spectra were taken. These tests were repeated on three different surfaces, carrying AgNPs, AuNPs and AuNRs.

In the second step, 15 µL of phage emulsion was dropped onto the bacteria adsorbed surfaces and the LSPR spectra were collected after one hour which was enough time for bacterial infection by the phages and total destruction of their cell structure. Note that in the end of the selected time the surface was gently washed with water and the LSPR data was taken. As mentioned before the T4 phage was tested on *E.coli*. A cross phage (the phage specific to *S. aureus*) was also tested on *E.coli* as a specificity test.

### 4.4.1. LSPR Spectra of Substrates

In order to select the types of the substrate we have conducted LSPR on two different surfaces which were loaded with AgNPs. Figure 4.27 gives representative spectra of these two surfaces for comparison. Typical LSPR peaks obtained were quite close to each other. Slightly stronger peaks were observed for the PDOM coated glass slides. Considering also possible positive effects of dopamine coating in the bacterial cell adhesion (see below) we decided to use the PDOM coated glass slides in the follow-up tests presented below.
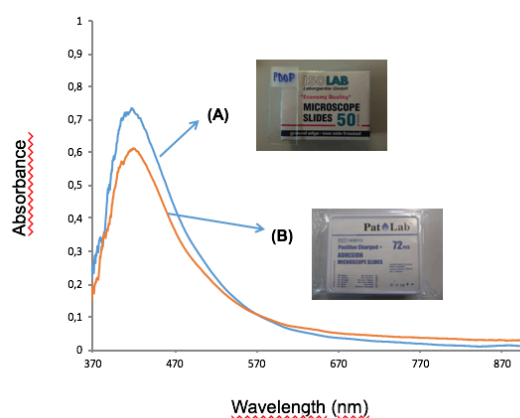


Figure 4.27. LSPR data for two different substrates loaded with AgNPs: (A) The polydopamine (PDA) coated glass slides; and (B) the positively charged adhesion microscope slides

## 4.4.2. LSPR Data for the NPs Deposited Surfaces

One of the main aims of this group of studies is to investigate LSPR agglomerations of three different NPs - therefore their LSPR performances. Possible agglomeration behaviour studied here is schematically described in Figure 4.28. As expected spherical NPs can densely pack and the gaps (pores) in the agglomerates are bigger when the NPs are larger. However, packing is looser in the case of nanorods. Note that the best results - the strongest peaks were obtained with AgNPs. This can be explained as follows: AgNPs are spherical and their average size is 5-10 nm which is the smallest NPs used here, and therefore get closely packed on the surfaces when they are agglomerated and therefore exhibited stronger LSPR effect. The spherical AuNPs were also used with an average size of 45 nm, which were much larger than AgNPs. The distances between the particles - the pores in their aggregates were larger as expected, means less change to exhibit high local plasmon. The AuNRs are "rod shape" with the aspect ratio of 2.5 that were used in this group of experiments - the largest nanoparticles with rod-like shape. It is known that they could result strong LSPR peaks. However, as expected in their agglomerated forms it is not easy to bring them into the oriented forms and bring all of them close enough to allow plasmon enhancements, rather loosely packed structures may be resulted in some parts however most probably the parts getting closer resulted stronger plasmon effects - better than those for spherical AuNPs.
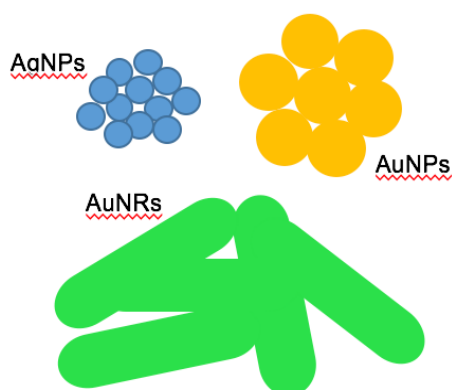


Figure 4.28.  Schematically drawing describing agglomeration scenario for NPs with different size and shape, AgNPs and AuNPs - "nanospheres" and AuNRs - "nanorods".

Figure 4.29 gives representative LSPR spectra of the NPs deposited (agglomerated) onto the PDA coated glass slides. The typical LSPR - $\Delta\lambda_{max}$ values for the AgNPs, AuNPs and AuNRs deposited surfaces were 430 nm, 523 nm and 674 nm, respectively. In order to these results here one may propose to use AgNPs due to their more intense peaks. However, the target that we were attempting to detect in this specific case is bacteria. It is well known that silver nanoparticles are strong antibacterial agents, may result bacterial dead like the phages that we used here. Therefore, we decided not to use AgNPs in further studies presented below. We eliminated also the rod shaped AuNRs even if they resulted better performance than spherical gold nanoparticles (AuNPs). The main reason to do this may be explained from the scenario demonstrated in Figure 4.29. Dropping these rod-like structures also forms aggregated but not controllable manner. One may get each time different agglomerated structures, means that the LSPR effect will not be reproducible. Therefore, we conducted the bacterial tests given below by using only AuNPs.
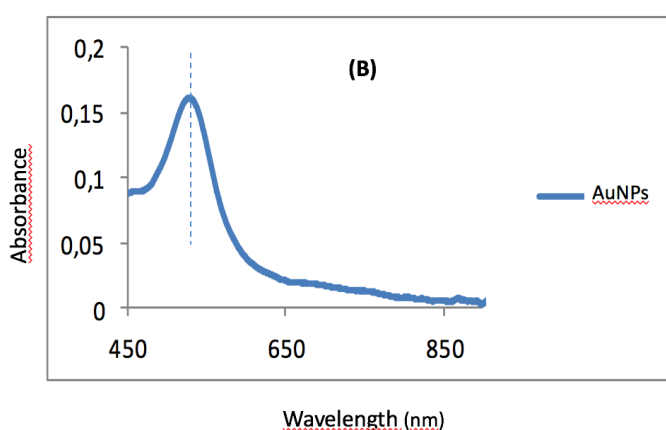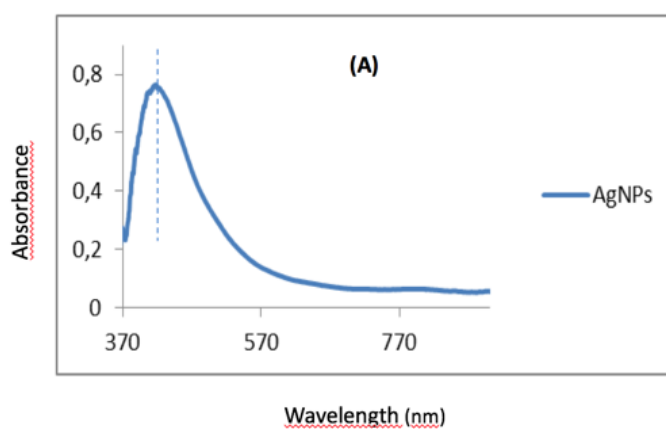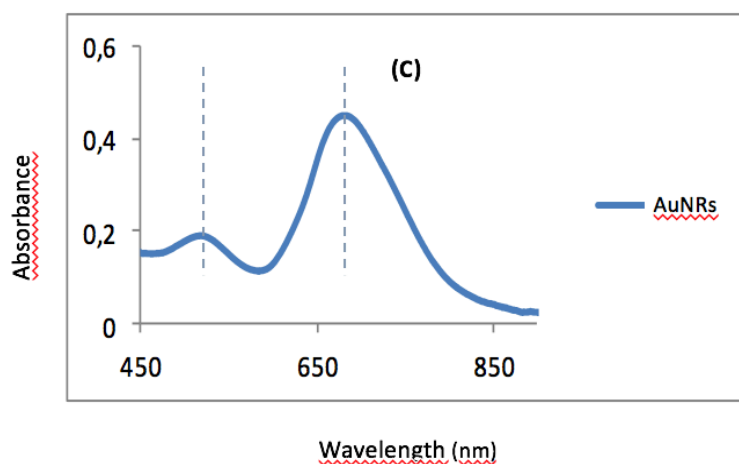
Figure 4.29. Representative LSPR spectra of three different NPs on the PDA coated glass slides: (A) AgNPs; (B) AuNPs; and (C) AuNRs.

## 4.4.3. Following LSPR Spectra for Bacteria-Bacteriophage Interactions

Figure 4.30 gives the LSPR spectra of *E. coli* on substrate surfaces carrying the agglomerates of AgNPs, AuNPs and AuNRs. For comparison, the LSPR spectra of bacteria on substrates (no NPs agglomerates), the spectra of surfaces carrying only NPs agglomerates (no bacteria) and both with and without bacterial adhesion are placed on the same plot. When only bacteria were dropped onto the plain substrate surfaces (no NPs agglomerates) there was no any respond. However, when the bacterial suspensions were dropped onto the LSPR platforms carrying the NPs, it was possible to detect an LSPR peak for the bacteria which was much less intense and with loose the peak form. Note that very similar curves were obtained for all three different bacteria (not presented here). These results are saying that it is not possible to detect different bacteria by this LSPR data by using this nonspecific surface interaction.

We have also applied an interesting set of tests in which we were able to describe target bacteria detection with very simple protocol which is as follows:  After receiving the LSPR signal of the target bacteria on different substrate surfaces carrying the nanoparticle agglomerates (only the spherical AuNPs were used in this group of tests), 5 µL of the phage emulsion was dropped onto the bacteria adsorbed surfaces and change of the LSPR measurement was repeated after washing the surface with water in the end of the test (after about 1h).
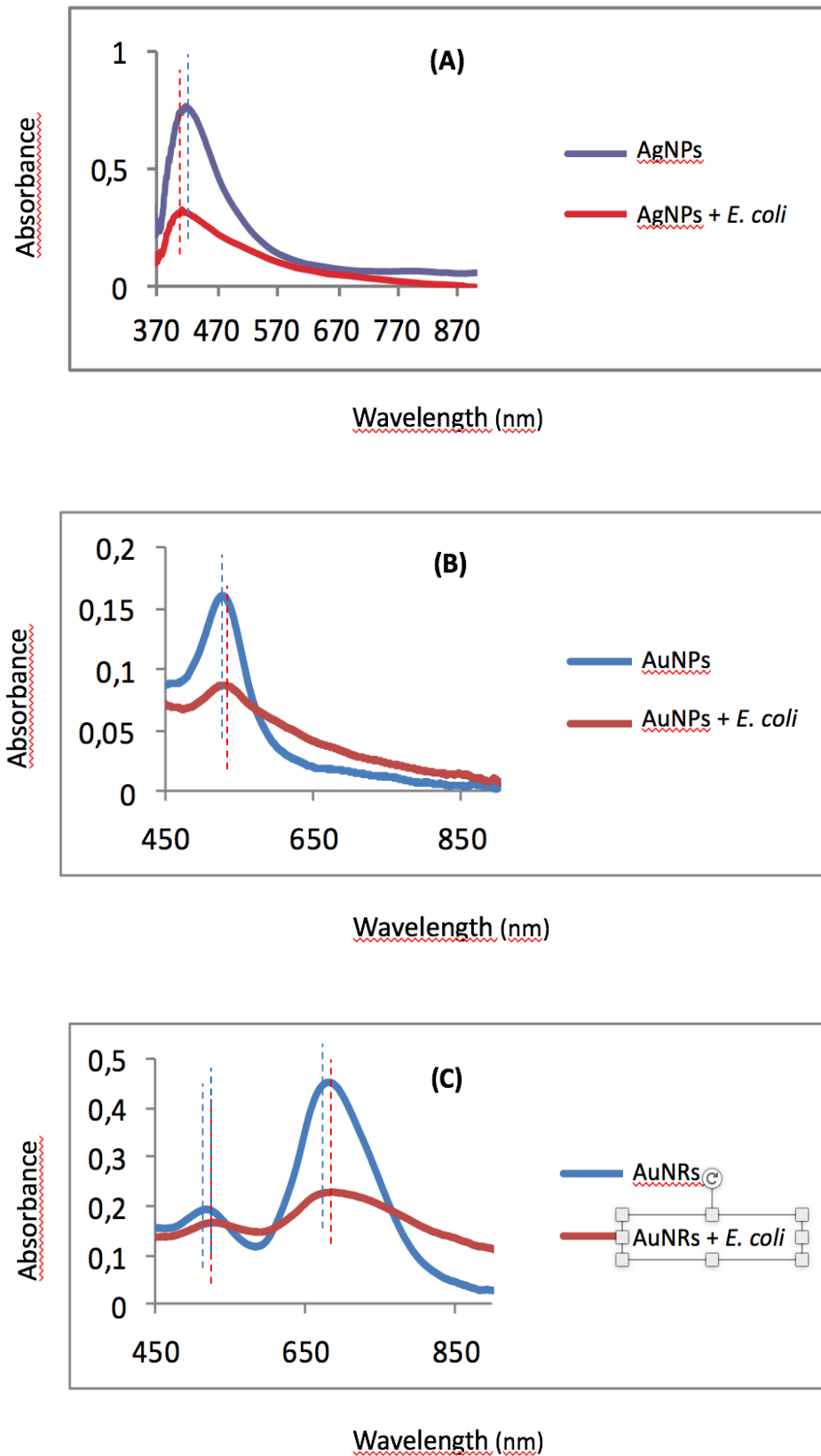
Figure 4.30. Representative LSPR spectra of the target bacteria, *E.coli* on the PDA coated glass slides loaded with three different NPs: (A) AgNPs; (B) AuNPs; and (C) AuNRs.

Typical LSPR plots of *E. coli* treated with its specific phages T4 are given in Figure 4.31. Note that the peak of bacteria was disturbed significantly in about one hour showing the infection of bacteria with its specific phage on the substrate surfaces. Note that a cross phage (here *S. aureus* phage) was also used to demonstrate specificity. There was no any change on the surface in 1h. This was concluded as a positive respond, showing the destruction of bacteria with their specific phages could be observed by LSPR data.

### 4.4.4. Conclusion of LSPR Studies

We have concluded in this part of the PhD thesis as follows: The agglomeration of nanoparticles allows getting strong peaks which depends strongly on the type and size of the nanoparticles. Measuring the changes in the peak height may be used to follow the bacterial adhesion on the surface, and further - after adding specific phages - which cause changes the peak height and shape as a result of infection of bacteria with phages. Studies in micro channels to apply LSPR in flow condition in which target bacteria are bring together with the NPs first and then injected in the channels are under investigation.



105
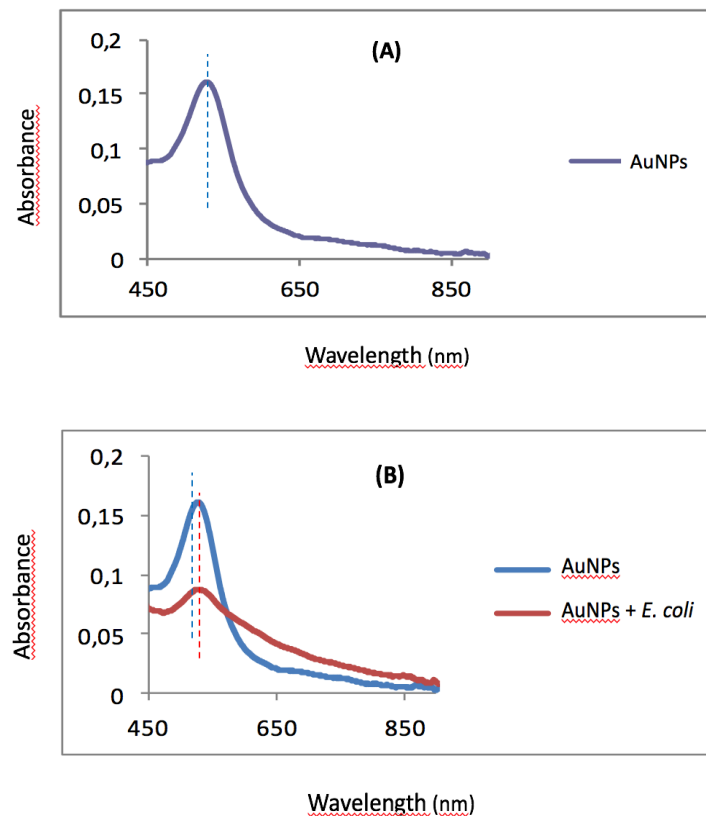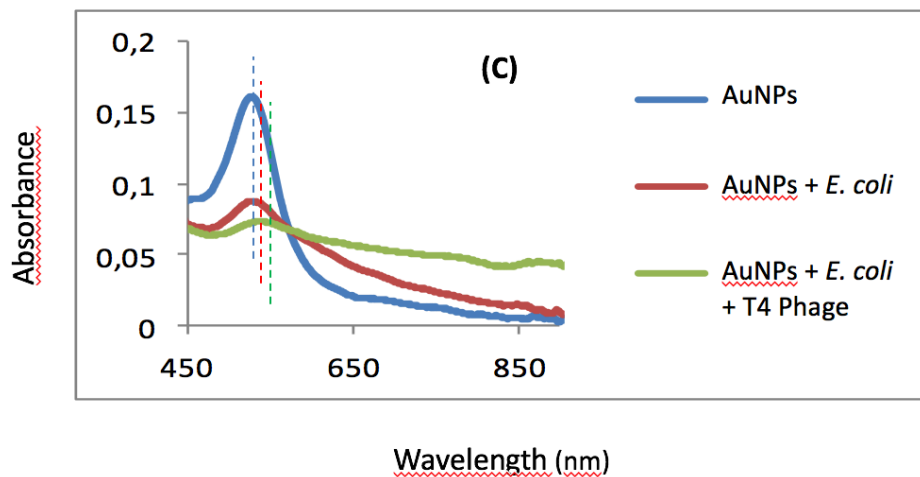
Figure 4.31. Representative LSPR spectra of on the PDA coated glass slides: (A) loaded only with AuNPs; (B) after dropping the target bacteria, *E. coli;* and (C) after adding specific bacteriophage, T4.

## 4.5. Detection with MALDI-TOF MS

Recently MALDI-TOF MS have been used with an increasing interest to identify microbial (bacteria, yeast, etc.) infections at clinical samples by several groups and the correlation between mass spectroscopy with other accurate standard biochemical techniques were found over 90% (Marshall, Hendrickson and Jackson, 1988; Eigner et al., 2009; Seng et al., 2009). In recent years the reference databases have been improved significantly for several bacteria including *Cam-pylobacter, Clostridia, Enterobacteria-ceae, Helicobacter, Myco-bacteria, Neisseria, Salmonella, Staphylococci, Streptococci,* etc. have been identified by MALDI-TOF MS with very high identification rates almost close to 100% (Pignone et al., 2006; Friedrichs et al., 2007; Barbuddhe et al., 2008; Dieckmann et al., 2008; Grosse-Herrenthey et al., 2008; Ilina et al., 2009; Ilina et al., 2010; Dieckmann and Malorny, 2011; Holler et al., 2011; Martin et al., 2011; Panda et al., 2013; Panda et al., 2014). Recent studies have also demonstrated that many bacteria *Salmonellae, Francisella tularensis, Bacteroides fragilis, Streptococcus agalactiae, Yersinia enterocolitica*, etc., could be identified on a subspecies level successfully by MALDI-TOF MS (Arnold and Reilley, 1998; Lartigue et al., 2009; Dieckmann and Malorny, 2011; Espinal et al., 2011; Nagy et al., 2011; Blattel et al., 2013).

Figure 4.32 gives examples of the MALDI-TOF MS spectra (typical "fingerprints") of three bacteria - *Escherichia coli*; *Staphylococcus aureus*; and *Salmonella* sp., which are also studied in this PhD thesis. In this study, Panda et al., have used freshly grown bacterial isolates obtained from clinical samples (Panda et al., 2013; Panda et al., 2014). They have used α-cyano-4 hydroxy-cinnamic acid as the matrix and demonstrated that the accuracy - which was at the species level - were around 98.78% for all these three and also for the others (total 14 bacteria in 82 clinical samples - not all included here). They have concluded that MADLI-TOF MS is sensitive/fast technique for clinical microbiology testing (Panda et al., 2014).

Figure 4.33 gives representative MALDI-TOF MS spectra - finger prints - of the three bacteria, i.e., *E.coli, S.aureus and S.infantis* and their respective phages that we have studied in this PhD thesis. Note that the intensities and sharpness of the peaks for these three different bacteria were different (between each other and the spectra for the similar bacteria reported in the related literature (see Figure 4.33 for comparison). These differences are expected because the species (also strains) of the bacteria, their concentrations and the matrix material that were used were different. It should be note that these spectra are presented only to demonstrate the differences - very significant in the case of bacteria. In order to identify unknown bacteria in a sample (especially in clinical samples), a very strong data base is needed which was neither exist in the system that we have used nor it was not attempted here in this thesis.

Figure 4.34 gives the finger prints of the phages that we have used in this thesis which were more simple - as expected - comparing to the bacteria and were also similar. Two double peaks were observed one at around 2000-2300 *m/z* and the other is around 2500-2800 *m/z*. Interestingly the second double peak (on the right) was stronger than the other (on the left) in the case of *S. aureus* which needs database evaluation to make for further comment.
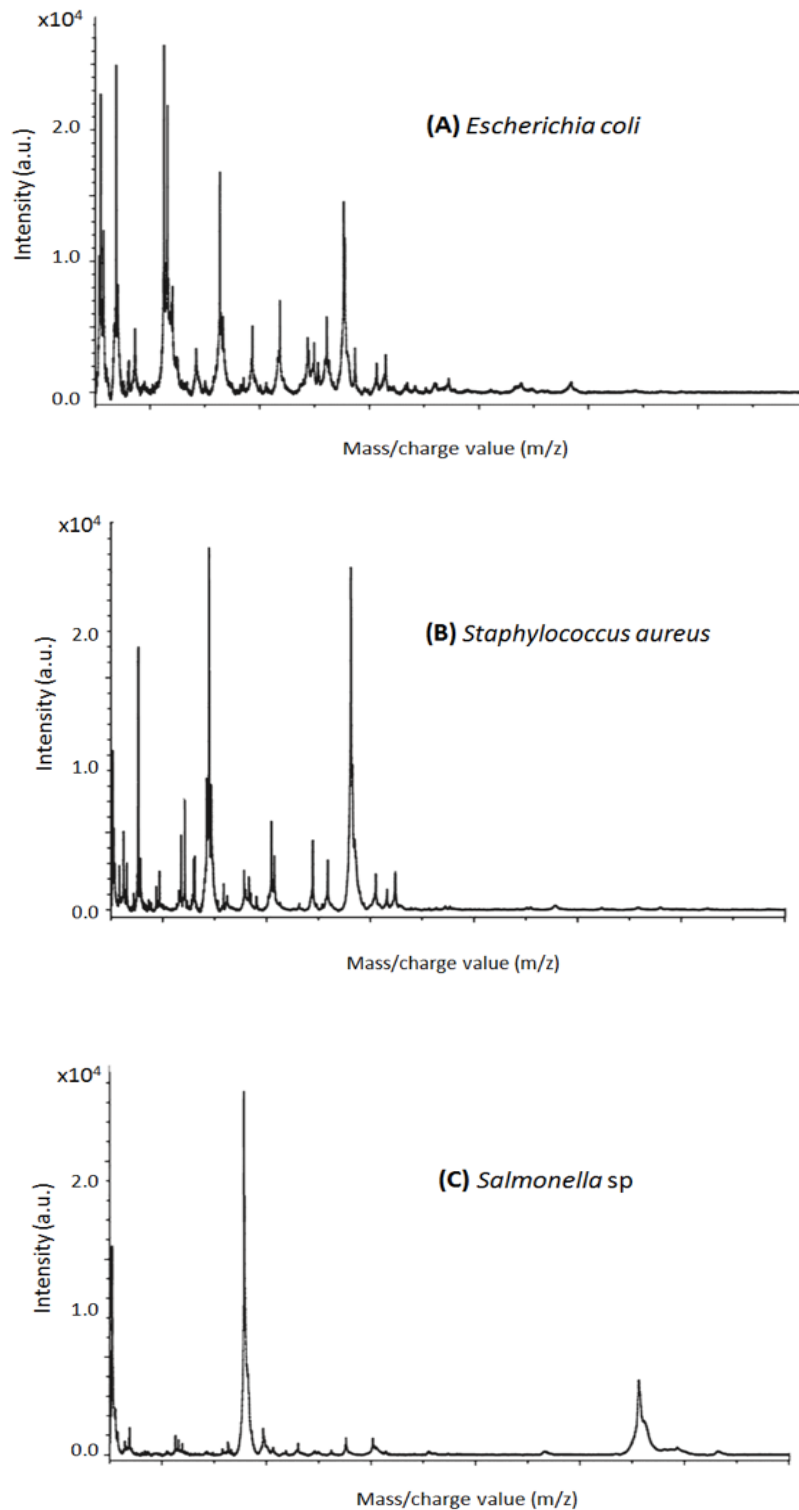
Figure 4.32. Representative MALDI-TOF MA spectra - "fingerprints" - the following three bacteria: (A) *Escherichia coli* (B) *Staphylococcus aureus* and (C) *Salmonella* sp. Adapted/modified from the related literature (Panda et al., 2014).
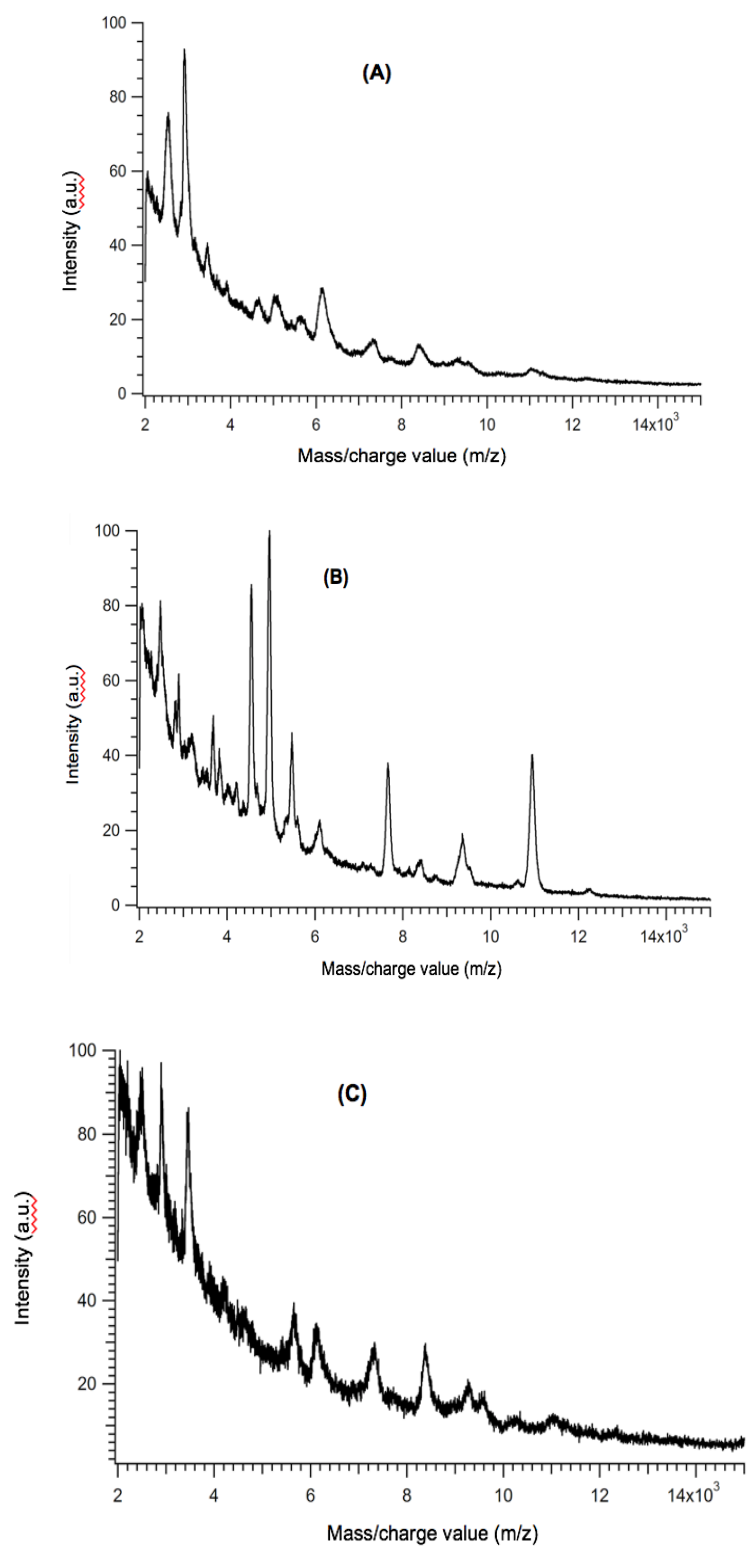
Figure 4.33. Representative MALDI-TOF MA spectra - "fingerprints" - the following three bacteria obtained in this PhD thesis: (A) *E.coli*; (B) *S.aureus*; and (C) *S.infantis*.
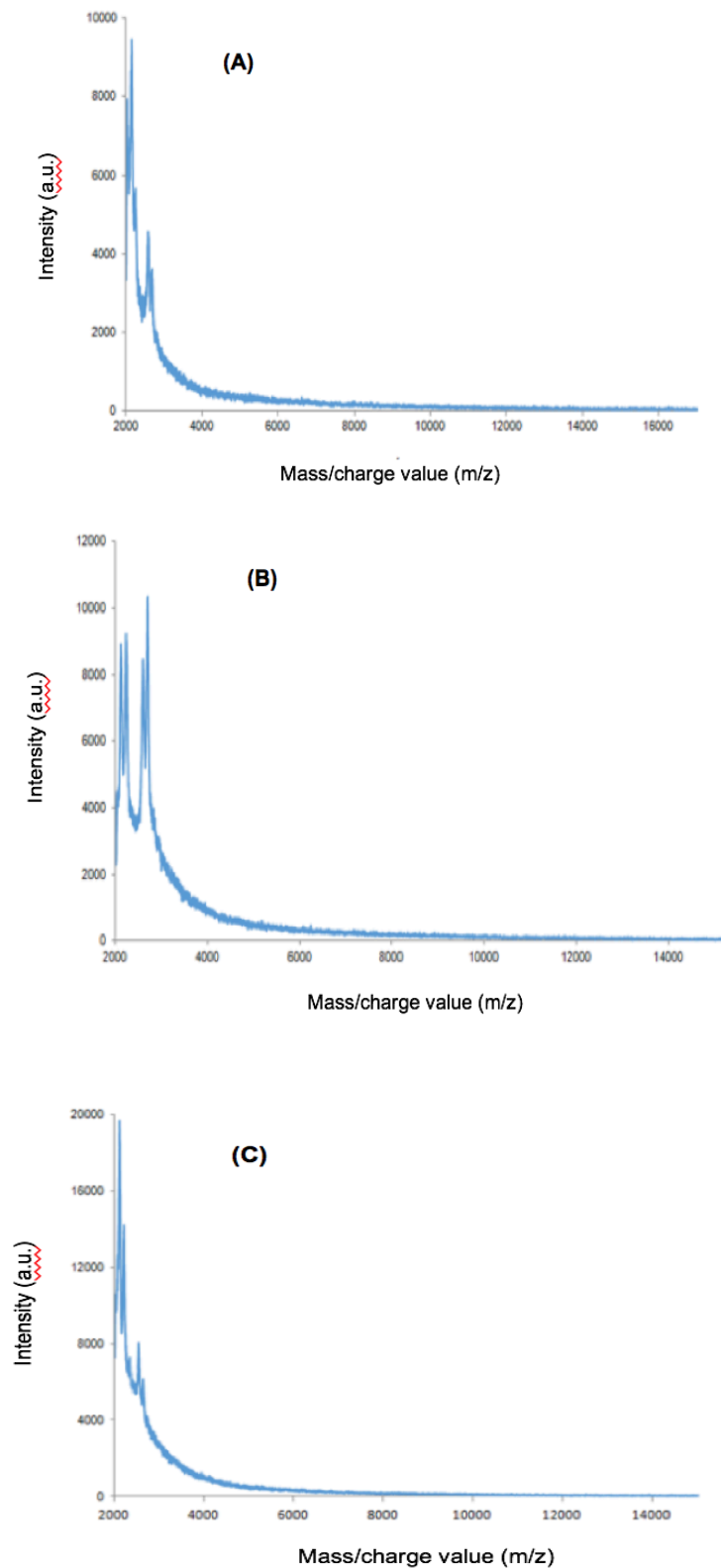
Figure 4.34. Representative MALDI-TOF MA spectra - "fingerprints" - the following three bacteriophages obtained in this PhD thesis: (A) *E.coli* phage; (B) *S.aureus* phage; and (C) *S.infantis* phage;

In this PhD thesis - in this section, our main objective was to follow interaction of phages with their specific bacteria on the target plates of MALDI-TOF MS in time and look for the possibility using this rather novel alternative strategy for pathogen detection. In the related test, the phage nanoemulsions were spotted onto the target bacteria and incubated for different periods of time and the spectra were taken. Figure 4.35 summarizes the results. For simplicity the spectra obtained at three different time were presented here. Note that "0" min means when we dropped the phage nanoemulsion onto the bacteria on the target plate. It took about 10-15 mins to take the real reading. Therefore, we obtained strong phage peaks, it was about 3000, 11000 and 37000 (a.u) (the peak on the left) for *E.coli, S.aureus* and *S.infantis*, respectively. The peak heights (intensities) increased very significantly when the incubation time increased in all cases and about 130000, 95000, and 97000 (a.u) (the peak on the left) for *E.coli, S.aureus* and *S.infantis*, respectively. These were very impressive findings which proofed the concept which are due to infection of the target bacteria phage number (as a result of propagation of the phages) increased very significantly as demonstrated by the characteristic peak heights. This was the conclusion of this part of the thesis and triggered us to plan/do more molecular identification studies using existing data base and improving new ones.
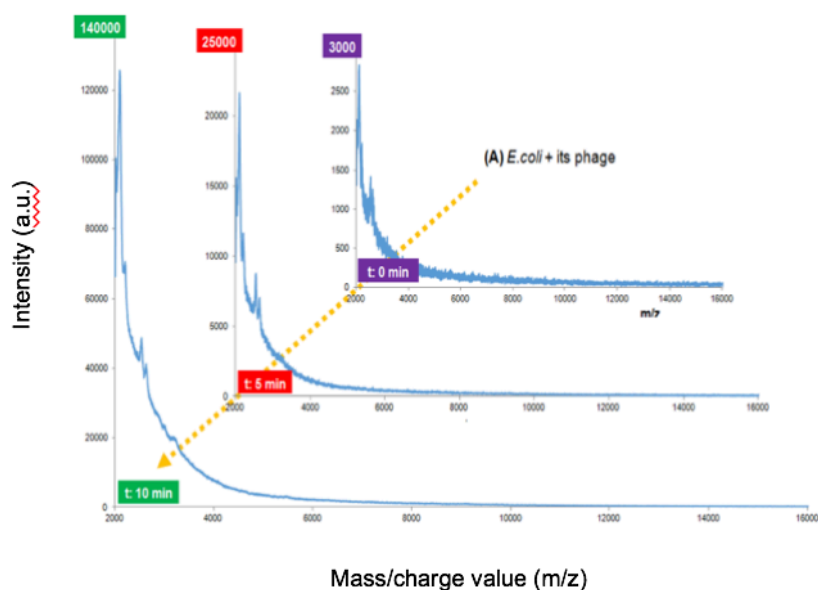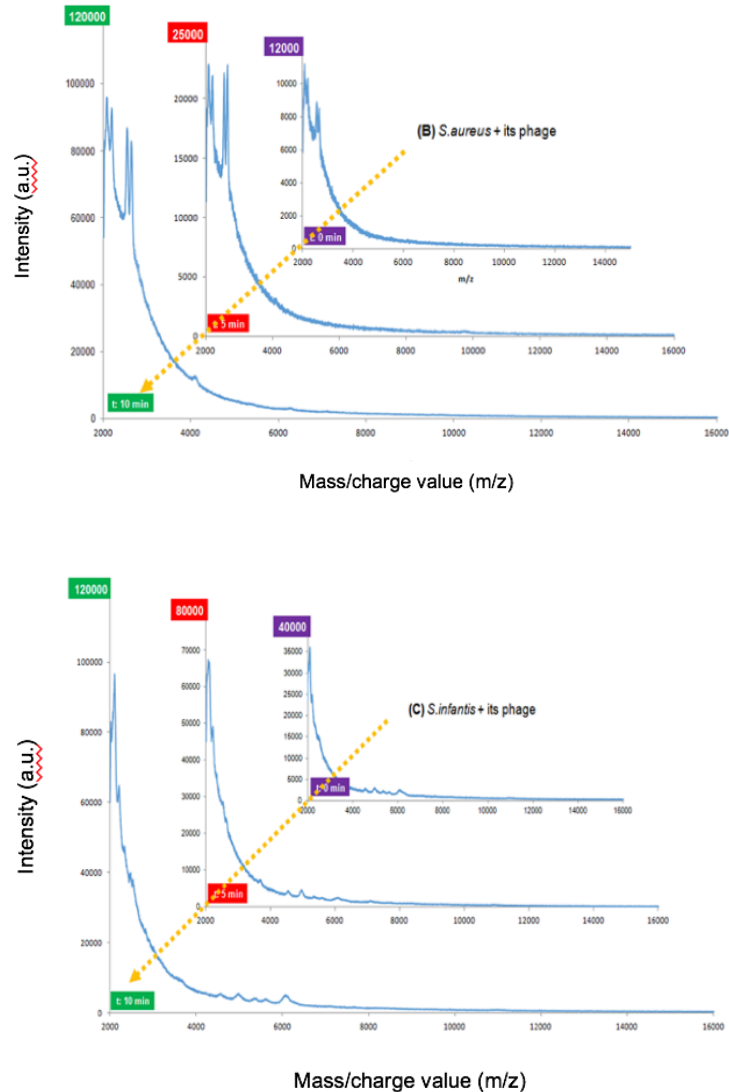
Figure 4.35. Representative MALDI-TOF MS spectra of the three bacteria after interaction with their phages for different times: (A) *E.coli* and its phage (B) *S.aureus* and its phage and (C) *S.infantis* and its phage

## 4.6. Bacteriophage Loading and Release

*Escherichia coli* (*E.coli*) and its specific bacteriophages (T4) were selected as the model system to be used in this group of studies. Both *E.coli K12* and T4-phages produced by us (first at Eliava Institute (Tbilisi, Georgia), later at Hacettepe University) and/or purchased from ATCC were used. Propagation and characterization of both bacteria and respective phages are given in Section 2 in detail. Stokes suspensions/emulsions $10^8$ CFU/mL of *E.coli* and $10^8$ PFU/mL of T4 phage were stored at 4°C until use.

### 4.6.1. Previous Studies

In our previous studies phages were encapsulated within alginate beads as described in detail elsewhere in which nanoemulsions of phages mixed with sodium alginate and added into calcium chloride solutions by drop wised, and further coated (stabilized) with chitosan or poly ethyleneimine (PEI) (Moghtader, Egri and Piskin, 2017). The phage stability and release have been studied in three simulating aqueous media, namely, "Simulated Gastric Fluid" (SGF), "bile salts" and in "Simulated Intestinal Fluid" (SIF) - in order to simulate behaviour of both free and encapsulated phages in gastrointestinal track (US Pharmacopeia Convention, 2004).

These alginate beads were around 1 mm and the size distributions were quite narrow as exemplified in Figure 4.36. The phage loading efficiencies were almost 90% which was quite high comparing similar immobilization techniques.
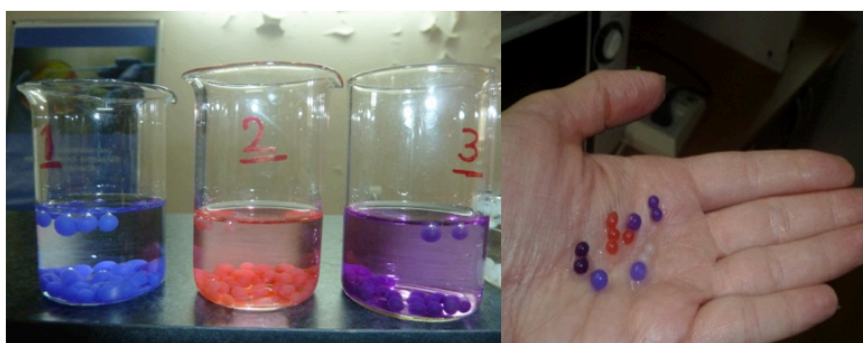


Figure 4.36. Representative pictures of phages encapsulated within alginate beads and further coated with chitosan or PEI. Different colors indicate different coatings.

Higher stabilities - prevention of activity at quite low pH in stomach conditions - were observed in the case of chitosan and PEI coatings similar to the related literature (Gåserød, Smidsrød and Skjåk-Bræk, 1988; Tang, Dettmar and Batchelor, 2005). The viability of phages in alginate beads coated with chitosan or PEI were better in bile salts similar to the related literature reports (Koo, DePaola and Marshall, 2000; Murata et al., 1999; Lui et al., 2002; Krasaekoopt, Bhandari and Deeth, 2004; Xue et al., 2004; Ma et al., 2008; Ma et al., 2012).

Due to quite specific properties, the hydrogels made of alginate do swell in and further disintegrated with in the intestinal pH conditions. We have observed that phage release from $Ca^{+2}$-alginate is rather fast due to disintegration/erosion - about 80-90% of the phages were released in about 6h, and release was completed in about 12h. However, the release was significantly slowdown in the case of polycation treated alginate beads similar to the related literature studies due to changes in the network structure of the coatings (Andersen et al., 1977; Kikuchi et al., 1999; Ma et al., 2012).

Figure 4.37 demonstrates that T4 phages in the alginate beads were still quite active as indicated in the plaque tests. These beads carrying T4 phages were in the refrigerator at +4ºC for about three years. Different colors indicate the type of the coating mentioned above. This was actually one of the main rational of encapsulation of phages within hydrogel capsules which is to extent their shelf-life in storage.
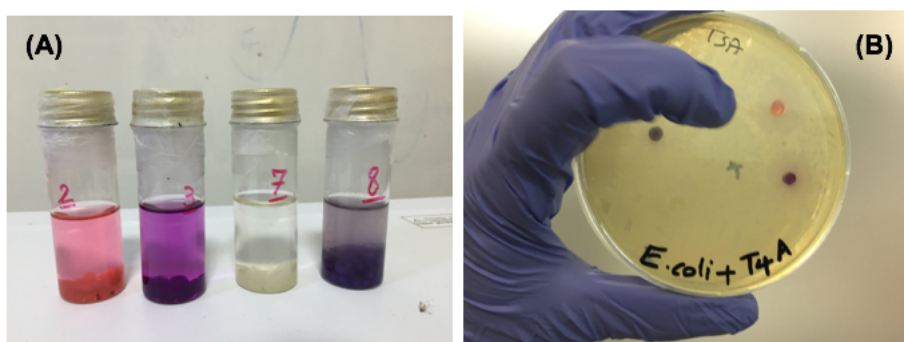


Figure 4.37. (A) The alginate beads carrying T4 phages after three year-storage in refrigerator at +4ºC - different colors indicate different type of coatings mentioned above. (B) A typical plaque test showing that T4-phages are still quite active to destroy their target bacteria, *E.coli*.

These previous studies have been concluded as follows: Phages can be encapsulated with in alginate beads quite effectively with high loading efficiencies. They are pH sensitive which is good for sustained release in GIT. Both chitosan and PEI coatings should be applied in order to increase their stability (even at very low pH).

Considering other applications other than pH sensitive sustained release at the GIT conditions, recently we have investigated loading and release of phages within/from gelatin beads. The preliminary results of these ongoing studies are briefly discussed below.

### 4.6.2. Bacteriophage Loaded Gelatin Beads

### 4.6.2.1. Gelatin Hydrogel Beads: Preparation

As explained in detail in Section 3.6.2 gelatin beads were prepared by two step process. In the first step non-cross-linked gelatin beads were formed by gelation in dispersion-in-oil phase. The average size of these non-cross-linked beads does change with several parameters both in the recipe and preparation conditions – may be the most important parameter is the agitation rate. We have not attempted to optimize neither the recipe nor the processing parameters. We have preferred to follow the experience in the Tabata's group there and used the recipe and condition proposed us. As mentioned before we have used a set of sieves with three different apertures - means that we have fractionated (sieved) the gel beads taken from the gelation reactor into three size ranges. Most of the beads (more than 80%) were between the sieves 32 μm and 53 μm - this was actually the size range we have targeted - which was also the reason that we have decided to use the recipe and processing conditions defined in the previous sections. In the second step, the non-cross-linked gelatin beads were freeze-dried and dehydrothermally cross-linked at 140°C in vacuum for three different periods of time, i.e., 24, 48 and 72 h.

There are several methods for cross-linking of gelatin - four of them have studied comparatively by Ozeki and Tabata (2005), i.e., cross-linking with a cross-linker (glutaraldehyde (GA) - which is one of the most popular coss-linking agent), dehydrothermal cross-linking that we have used also in our studies presented here, and two radiation based cross-linking UV- and electron beam-irradiations. They have discussed that dehydrothermal cross-linking occurs between the amino and carboxylic acid side chain groups on the collagen polypetide chains (Weadock et al., 1999; Ueda et al., 2003; Ozeki and Tabata, 2005). However they have to come close each other to have this reaction which is not that easy. In contrast, GA

molecules get in the collagen chains more easly and cross-links the functional goups (such as amino groups) more evenly in the structure. There are several

drawbacks using GA - especially in medical applications due to possible toxicity of GA. Therefore we have decided to use dehydrothermal approach option for cross-linking the gelatin beads that we have produced in the previous step - that was also proposed by Tabata's group that we work together in this group of studies - which are on-going. This is also very easy method, the freze dried gelatin beads are just incubated in a vacuum oven at 140°C for the desired period of time.

Representative microscopic pictures of these gelatin beads with different sizes are shown in Figure 4.38. They were spherical in shape and had smooth surfaces. There was a size distribution of the beads coming from gelation reactor. We have used the fraction - the one between the sieves 32 µm and 53 µm. After dehydrothermal cross-linking the beads were swollen in distilled water to reach the equilibrium, and the sizes were measure microscopically - the average diameters were obtained which were 42.5 ± 8.4 µm, 40.2 ± 5.6 µm and 41.7 ± 7.4 µm for the beads treated in vacuum for 24, 48, and 72 h, respectively. As seen here the changes were observable but not that significant. We have also found percent water uptake (water content) of the beads (% by weight) which were 96.5 ± 2.7, 94.8 ± 1.2, and 92.6 ± 2.6 for the gelatin beads cross-linked for 24, 48, and 72 h, respectively. In cross-linking reactions, one expects that increasing the cross-linking density (amount of cross-linker) in the hydrogel beads the extent of swelling decreases and therefore water uptake decreases - which may be quite significant depending on the extent of cross-linking. GA cross-linking is an example of this - if more GA is used swelling decreases significantly (Özeki and Tabata). It was similar in our case in which higher cross-linking densities (less swelling) were observed when we increase the treatment time in our hydrothermal cross-linking process. However, it was noticed that the changes of the swelling extent (water uptake) was not that significant. This may thay be due to two opposite effects. Cross-linking increases with the treatment time, but opposite to this, longer treatment times at high temperatures - that is in our case - could cause more degradation in the polymer chains.
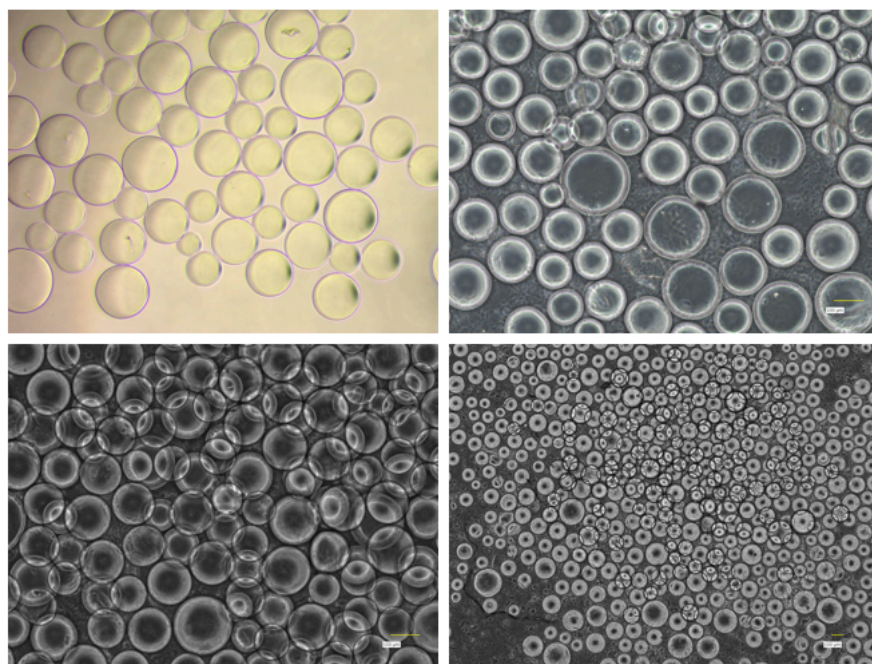
Figure 4.38. Representative microscopic pictures of the gelatin hydrogel beads with different sizes.

### 4.6.2.2. Gelatin Hydrogel Beads: Degradation and Phage Release

***Degradation.*** *In vitro* degradation behaviour of gelatin beads have been studied in a protocol where the medium is quite acidic (HCl) as decribed in the Section 3. Tabata's group was applying this approach in their releted studies in many years. This is a kind of facilitated degradation - it was used actually to test the relative cross-linking in the dehydrothermally cross-linked gelatin beads with different extens of cross-linking. As proposed by this group we have obtained the degradation kinetics of the gelatin beads that we have produced at three different treatment times, 24, 48 and 72 h. Figure 4.39 shows the representative results. As seen here all three hydrogel matrices (beads) are degraded in about 12 h totally. There were observable differences - when the treatment time increases the degradation rate decreases due to possible cross-linking density increase in the network. However, these data are not enough to have a straight-forward correlation between the cross-linking density and degradation rate - note that most probably the cross-linking network in this dehydrothermal cross-linking protocol is not homogeneous.
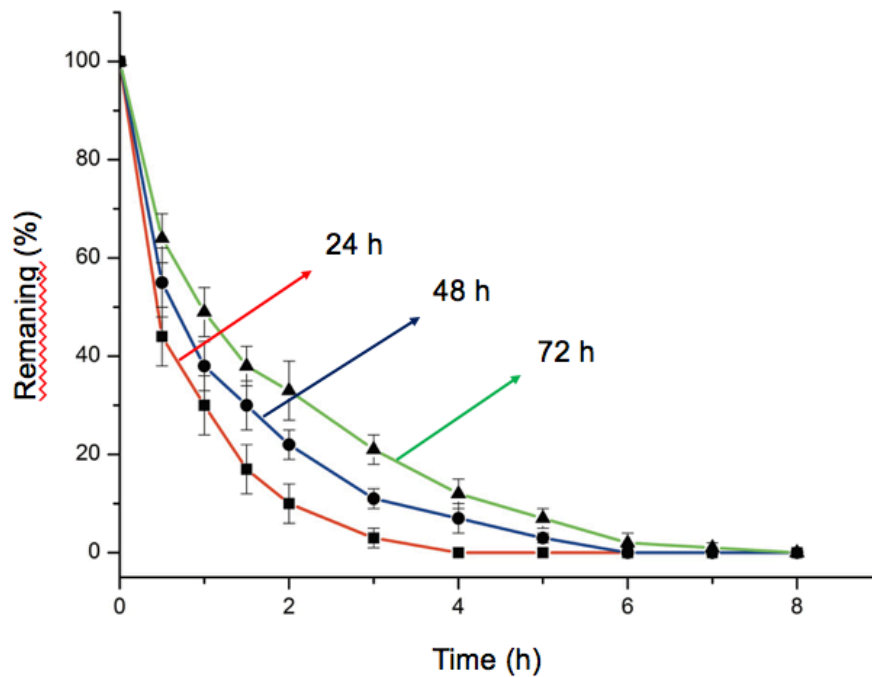
Figure 4.39.  Representative degradation curves of the gelatin beads cross-linked with dehydrothermal treatments at three different periods, 24, 48 and 72 h. The treatment periods are indicated on the curves.

*Release.* Release of behaviour bacteriophages from the gelatin beads with three different cross-linking were also investigated. Figure 4.40 shows the reperesentative results. As expected, about 60-70 % of the phages loaded are release in 12 h, and almost completed in 24 h. Higher release were observed for the less cross-linked beads (treated for 24 h). There were differences but not very significant. The phage loading was quite rapid in which phage emulsions were just put on the dried gelatin beads - the loading was simply by sucking the driy gels the water phase which was very quick, but during storgae most probably the phage molecules diffused trhough the core of the beads, therefore the release was not that fast comparing the loading. Initial high release values (could be called as burst) may be result of higher concetration of the phages near the surface of the beads.

We concluded that the release rates are good enough to use these phage releaseing formulations effectively. The storage will be effective to keep the stability/activity of the phages within these matrices. One could control the long term stable/active storage of phages by controlled freeze-drying the gelatin gels -

118

they do swell very effectively in aqueous media and release the phages quite rapidly in use. The concentration of the phages in the initial loading medium can be changed therefore any amount of phage could be loaded within these gel beads very easly and therefore the desired amounts and release rates could be easly arranged/controlled. These phage releasing gelatin beads/microspheres carrying also stem cell aggregates are underinvestigation for a combined therapy of infected wound as tissue engineering bioactive hybrid materials.
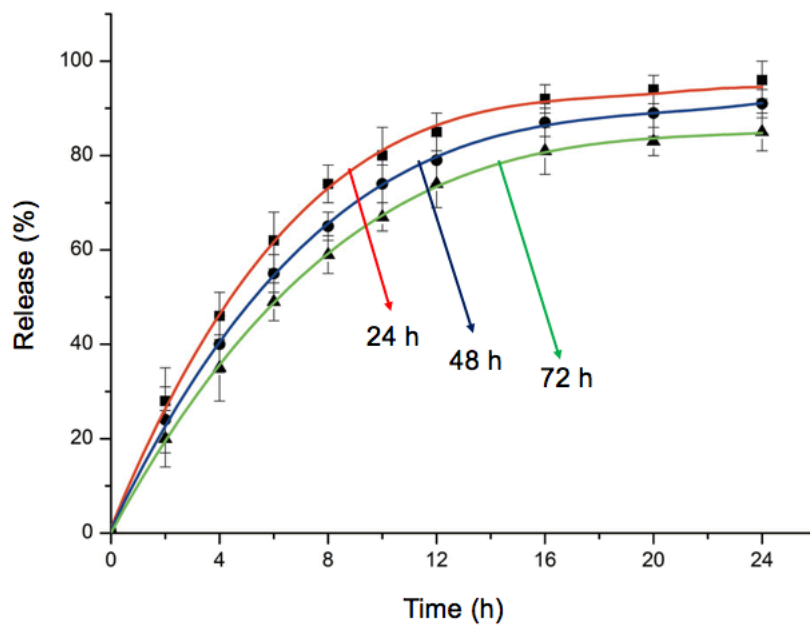


Figure 4.40.   Representative phage release curves from the gelatin beads cross-
            linked with dehydrothermal treatments at three different periods, 24,
            48 and 72 h. The treatment periods are indicated on the curves.

# 5. CONCLUSIONS

Bacterial infections are among the most serious and costly public health concerns worldwide. Monitoring/early detection of pathogenic bacterial contaminations/ infections is one of the most important priority globally. Development of fast, accurate and sensitive detection and monitoring of pathogens, which should be miniaturized/portable automated therefore cost effective, is a very important challenge. The main aim of this study is to develop alternative bacterial detection strategies using **"bacteriophages"** with **"plasmonic nanoparticles"** mainly by "Surface Enhanced Raman Spectroscopy" (**"SERS"**). Two alternative optical techniques, namely LSPR and MALDI-TOF MS were also applied. In parallel in order to increase the stability of bacteriophages in storage and use, phages were immobilized within alginate and gelatin microsphere hydrogels.

## (1) Bacteria and Bacteriophages

The main target bacteria was *Escherichia coli* (*E.coli*), in addition two more pathogenic bacteria, namely *Staphylococcus aureus* (*S.aureus*) and *Salmonella infantis,* (*S.infantis*) were also included in some part of studies for comparison. They and their specific bacteriophages were mainly supplied from American Tissue Culture Collection (ATCC) and other sources (by donation, e.g., Eliava Institute, Tbilisi, Georgia). Both bacteria and phages were propagated/purified in large enough quantities by rather traditional techniques. Bacterial cultures were prepared freshly in each work day from the stokes. Phage antibacterial activities were quite high which were tested in the plaque assays using the target bacterial cultures in petri dishes. The initial (stoke) concentrations of the target bacteria and their specific phages were around $10^8$ CFU/ml and $10^8$ PFU/ml, respectively. These specific bacteriophages were used as bioprobes successfully in the following group of studies.

## (2) Nanoparticles

Three different nanoparticles, silver nanospheres (AgNPs) and gold nanospheres (AuNPs) and gold nanorods (AuNRs) were synthesized in different size ranges therefore optical properties by using mainly citrate and CTAB as the reducing agent and stabilizer. It was possible to produce nanoparticles with desired size range and shape with quite low size distribution and also charge (negative or

positive). The selected ones were used in the following sections for enhancement of the target bacteria detection together with the respective bacteriophages, as bioprobes. These metallic nanoparticles (both spheres and rods) were used as "surface enhancers" (due to their strong plasmonic properties) in the SERS and LSPR studies.

## (3) SERS Studies

In this group of studies three different bacteria, *E.coli, S.aureus* and *S.infantis* and their specific phages were used together with AgNPs, AuNPs and AuNRs synthesized in this thesis. Two alternative detection strategies were applied. In the first one nanoparticles were deposited onto glass/silica surfaces to create SERS platforms then the target bacteria or phages - separately were dropped onto these surfaces - observed by the microscope attached to the Raman system used, and spectra from the targeted area were obtained. In the second approach, target bacteria (i.e., *E.coli*) were interacted with gold nanorods in suspensions, and then they were dropped onto plain silica surfaces for detection. Especially second strategy gave excellent results - it was possible to obtain quite sharp (intense) peaks (even at one bacterial cell level) - fingerprints of the target bacteria without using any bacteriophages. After taking SERS spectrum of the surfaces loaded with bacteria, specific phages were dropped onto those surfaces and changes of the spectrum were monitored (taken) with time. These results were impressive and demonstrated that how one can apply phages for the detection of the target pathogenic bacteria very effectively in a quite simple tests. Identification at molecular level by using also the data base will be studied in the flow-up projects.

## (4) LSPR

LSPR spectroscopy was also applied for the detection of bacteria (*E.coli*) by using bacteriophage (T4). AgNPs, AuNPs and AuNRs were used in this part of the thesis. The agglomeration of nanoparticles allows getting intense peaks which depends strongly on the type and size of the NPs. AuNPs were found most suitable ones. We concluded that measuring the changes in the LSPR peak height could be used to follow the bacterial adhesion on the surface, and further adding specific phages changes the peak height and shape as a result of infection of bacteria with phages - which is simple and challenging approach for detection of pathogenic bacteria.

121

**(5) MALDI-TOF MS**

MALDI-TOF MS studies were performed with three different bacteria, *E.coli, S.aureus* and *S.infantis* and their respective phages. Similar peaks were observed both in the spectra bacteria and phages, however distinct characteristic peaks that needs more studies especially using the related data bases. Interaction of bacteria and their specific phages on the target plates of the system demonstrated very promising - impressive results showing that MALDI-TOF MS could be a very important detection system for identification of target bacteria using bacteriophages as very specific bioprobes. Further studies - more molecular identifications - are underinvesgitation.

**(6) Bacteriophage Loading and Release**

In order to increase stability and allow controlled release bacteriophage were encapsulated and loaded within alginate (in our previous studies) and gelatin (in the the recent studies) beads, respectively. Both methods were very simple and in expensive. Very high loading percentages (yields) were achieved. It was concluded that they could be stored safely/actively (keeping phage activities) up to three years. Loading amount therefore release could be increased to the desired kinetics by just adjusting the initial concentration of the phages in their nanoemulsions.

# REFERENCES

Abu Al-Soud, W. and Rådström, P., Applied Environmental Microbiology, 64 (**1998**) 3748.

Abu Al-Soud, W. and Rådström, P., Journal of Clinical Microbiology, 39 (**2001**) 485.

Aebersold, R. and Mann, M., Nature, 422 (**2003**) 198.

Anany, H., Chen, W., Pelton, R. and Griffiths, M.W., Applied Environmental Microbiology, 77 (**2011**) 6379.

Andresen, I.L., Skipnes, O., Smidsrod, O., Ostgaard, K. and Hemmer, P.C., Cellulose Chemistry and Technology, 48 (**1977**) 361.

Arnold, R.J. and Reilly, J.P., *Rapid Communications in Mass Spectrometry,* 12 (**1998**) 630.

Arya, S.K., Singh, A., Naidoo, R., Wu, P., McDermott, M.T. and Evoy, S., Analyst, 136 (**2011**) 486.

ASM Org - www.asm.org - **2016**.

Atlas, R.M. and Bej, A.K., in: Methods for General and Molecular Biology, Gerhard, P. (Ed), American Society for Microbiology, Washington, D.C., **1994.**

Balasubramanian, S., Sorokulova, I.B., Vodyanoy, V.J., and Simonian, A.L., Biosensors and Bioelectronics, 22 (**2007**) 948.

Barbuddhe, S.B., Maier, T., Schwarz, G., Kostrzewa, M., Hof, H., Domann, E., Chakraborty, T. and Hain, T., Applied and Environmental Microbiology, 74 (**2008**) 5402.

Bassetti, M., Poulakou, G., Ruppe, E., Bouza, E., Van Hal, S.J. and Brink, A., Intensive Care Medicine, 43 (**2017**) 1464.

Batz, M.B., Doyle, M.P., Morris, J.G., Painter, J., Singh, R., Tauxe, R.V., Taylor, M.R., Won, D.M., Emergency Infectious Diseases, 11 (**2005**) 993.

Belgrader, P., Benett, W., Hadley. D., Richards, J., Stratton, P., Mariella, R. and Milanovich, F., Science, 284 (**1999**) 449.

Benette, A.R., Davids, F.G., Vlahodimou, S., Banks, J.G. and Betts, R.P., Journal of Applied Microbiology, 83 (**1997**) 259.

Benoit, P.W. and Domahue, D.W., Journal of Food Proessing and Preservation, 66 (**2003**) 1935.

Bisconte De Saint Julien, J-C., US Patent 6143577, **2000**.

Blair, J.M., Webber, M.A., Baylay, A.J., Ogbolu, D.O. and Piddock, L.J., Nature Reviews Microbiology, 13 (**2015**) 42.

Blattel, V., Petri, A., Rabenstein, A., Kuever, J. and Konig, H., Applied Microbiology and Biotechnology, 97 (**2013**) 4597.

Bocklitz, T., Putsche, M., Stüber, C., Käs, J., Niendorf, A., Rösch, P. and Popp, J., Journal of Raman Spectroscopy, 40 (**2009**) 1759.

Bocklitz, T., Walter, A., Hartmann, K., Rösch, P., Popp, J., Analytica Chimica Acta, 704 (**2011**) 47.

Bohren, C.F. and Huffman, D.R., Absorption and Scattering by Small Particles, Wiley-Interscience, New York, **1983**.

Boisselier, E. and Astruc, D., Chemical Society Reviews, 38 (**2009**) 1759.

Boken, J., Khurana, P., Thatai, S., Kumar, D. and Prasad, S., Applied Spectroscopy Reviews, 52 (**2017**) 774.

Boratynski, J., Syper, D., Weber-Dabrowska, B., Lusiak-Szelachowska, M., Pozniak, G. and Gorski, A., Cellular Molecular Biology Lettres, 9 (**2004**) 253.

Brenner, D.J., Krieg, N.R. and Staley, J.T., in: Bergey's Manual of Systematic Bacteriology, 2nd ed., Spring-Verlag, New York, 2005.

Britannica - www. britannica. com - **2016**.

Brown, A.E. and Smith, H.R, Benson's Microbiological Applications: Laboratory Manual in General Microbiology, McGraw-Hill Education, 14th ed, New York, **2016**.

Buchholz, U., Bernard, H., Werber, D., Böhmer, M.M., Remschmidt, C., Wilking, H., Delere, Y., et al., New England Journal of Medicine, 365 (**2011**) 1763.

Byrne, B., Stack, E., Gilmartin, N. and O'Kennedy, R., Sensors, 9 (**2009**) 4407.

Cademartiri, R., Anany, H., Gross, I., Bhayani, R., Griffiths, M. and Brook, M.A., Biomaterials, 31 (**2010**) 1904.

Carpentar, A.B., in: Manual of Clinical Microbiology, Murray, P.R., Baron, E.J., Landray, M.L., Jorgensen, J.H. and Pfaller, M.A. (Eds), 9th ed. American Society of Microbiology. Washington, D.C., **2007**.

Cavalu, S., Cinta-Pinzaru, S., Leopold, N. and Kieffer, W.C., Biopolymers – Biospectroscopy, 62 (**2001**) 341.

CDC-https://www.cdc.gov/ecoli/index.html, **2019.**

Chaloupka, K., Malam, Y., Alexander M. and Seifalian, A.M., Trends in Biotechnology, 28 (**2010**) 580.

Chou, C., Tsai, Y., Liu, J., Wei, J.C.C., Liao, T., Chen, M. and Liu, L., Journal of Immunological Methods, 255 (**2001**) 15.

Congur, G., Sayar, F., Erdem, A. and Piskin E., Colloid. Surface B: Chemistry, 112 (**2013**) 61.

Cotton, T.M., Kim, J.M. and G.D. Chumanov, G.D., Journal of Raman Spectroscopy, 22 (**1991**) 729.

Croxen, M.A., Law, R.J., Scholz, R., Keeney, K.M., Wlodarska, M. and Finlay, B.B., Clinical Microbiology Reviews, 26 (**2013**) 822.

Csaki, A., Stranik, O. and Fritzsche, W., Expert Review of Molecular Diagnostic, 18 (**2018**) 279.

Dahlin, A., Zäch, M., Rindzevicius, T., Käll, M., Sutherland, D.S. and Höök, F., Journal of the American Chemical Society, 127 (2005) 5043.

Daly, P., Collier, T. and Doyle, S., Letters of Applied Microbiology, 34 (**2002**) 222.

Daniel, M. C. and Astruc, D., Chemical Reviews, 104 (**2004**) 293.

D'Herelle, F., Comptes Rendus Hebdomadaires des Seances de Academia des Sciences D, 165 (**1917**) 373.

D'Herelle, F., Comptes Rendus des Seances de la Societe de Biologie et de ses Filiales, 81(**1918**) 1160.

Dieckmann, R., Helmuth, R., Erhard, M. and Malorny, B., Applied and Environmental Microbiology, 74 (**2008**) 7767.

Dieckmann, R. and Malorny, B., Applied and Environmental Microbiology, 77 (**2011**) 4136.

Dreaden, E.C., Alkilany, A.M., Huang, X., Murphy, C.J. and El-Sayed, M.A., Chemical Society Reviews, 41 (**2012**) 2740.

*E. coli* Facts sheet, CS267331-A September 2016

Eigner, U., Holfelder, M., Oberdorfer, K., Betz-Wild, U., Bertsch, D., and Fahr, A.M., Clinical Laboratory, 55 (**2009**) 289.

Englebienne, P., Analyst, 123 (**1998**) 1599.

Encylopedia Britannica, Inc., - **2016.**

EFSA http://www.efsa.europa.eu/EFSA/efsa_locale1178620753812_121190203 1795. htm, **2009.**

Escherich, T., Reviews of Infectious Diseases, 10 (**1988**) 1220.

Espinal, P., Seifert, H., Dijkshoorn, L., Vila, J. and Roca, I., Clinical Microbiology Infections, 18 (**2011**) 1097.

Fagan, P.K., Hornitzky, M.A., Bettelheim, K.A. and Djordjevic, M. Applied Environmental Microbiology, 65 (**1999**) 868.

Fenn, J.B., Mann, M., Meng, C.K., Wong, S.F. and Whitehouse, C.M., Science, 246 (**1989**) 64.

Ferreira, C., Thiemy, V., Moreira, M., Schippers, D. and Greene, A., Journal of Applied Oral Science, 12 (**2004**) 1.

Fortin, N.Y., Mulchandani, A. and Chen, W., Analytical Biochemistry, 289 (**2001**) 281.

Fratamico, P.M., Bagi, L.K., and Pepe, T., Journal of Food Protection, 63 (**2000**) 1032.

Friedrichs, C., Rodloff, A.C., Chhatwal, G.S., Schellenberger, W. and Eschrich, K., Journal of Clinical Microbiology, 45 (**2007**) 2392.

Garcia, P., Rodriguez, L., Rodriguez, A. and Martinez, B., Trends in Food Science and Technology, 21(**2010**) 373.

Gåserød, O., Smidsrød, O. and Skjåk-Bræk, G., Biomaterials, 19 (**1998**) 1815.

Gauglitz, G. and Vo-Dinh, T., Handbook of Spectroscopy, Wiley-VCH Verlag GmbH & Co. KGaA, Weinheim, **2003.**

Gaus, K., Rösch, P., Petry, R., Peschke, K.D., Ronneberger, O., Burkhardt, H., Baumann, K. and Popp, J., Biopolymers, 82 (**2006**) 286.

Gehring, A.G., Irwin, P.L., Reed, S.A., Tua, S., Anderotti, P.E. and Akhavan-Tafti, H.R.S., Analytical Biochemistry, 258 (**2004**) 293.

Gerba, C.P., Rose, J.B., Haas, C.N. and Crabtree, K.D., Water Research, 30 (**1996**) 2929.

Gervais, L., Gel, M., Allain, B., Tolba, M., Brovko, L., Zourob, M., Mandeville, R.,

Griffiths, M. and Evoy, S., Sensors and Actuators B Chemistry, 125 (**2007**) 615.

Goeller, L.J. and Riley, M.R., Applied Spectroscopy, 6 (**2007**) 679.

Gole, A. and Murphy, C.J., Chemistry of Materials, 16 (**2004**) 3633.

Gomez, T.A., Elias, W.P., Scaletsky, I.C., Guth, B.E., Rodrigues, F.F., Piazza, R.M., Ferreira, L.C. and Martinez, M.B., Journal of Microbiology, 47 (**2016**) 3.

Grosse-Herrenthey, A., Maier, T., Gessler, F., Schaumann, R., Bohnel, H., Kostrzewa, M. and Kruger, M., Anaerobe, 14 (**2008**) 242.

Haes, A. J. and Van Duyne, R. P., Journal of the American Chemical Society, 124 (**2002**) 10596.

Hager, J.W., Rapid Communications in Mass Spectrometry, 16 (**2002**) 512.

Han, X.X., Huang, G.G., Zhao, B. and Ozaki, Y., Analytical Chemistry, 81 (**2009**) 3329.

Handa, H., Gurczynski, S., Jackson, M.P., Auner, G., and Mao, G., Surface Science, 602 (**2008**) 1392.

Handa, H., Gurczynski, S., Jackson, M.P. and Mao, G., Langmuir, 26 (**2010**) 12095.

Hanlon, E.B., Manoharan, R., Koo, T-W., Shafer, K.E., Motz, J.T., Fitzmaurice, M., Kramer, J.R., Itzkan, I., Dasari, R.R. and Feld, M.S., Physics in Medicine and Biology, 45 (**2000)** 1.

Hausler, T., Viruses vs. Superbugs: A Solution to the Antibiotic Crisis?, Palgrave Macmillan, **2006.**

Haynes, C.L., McFarland, A.D. and Van Duyne, R.P., Analytical Chemistry, 77 (**2005**) 338.

Henchal, E.A., Teska, J.D., Ludwig, G.V., Shoemaker, D.R. and Ezzell, J.W., Clinical Microbiology Medicine, 21 (**2001**) 661.

Herne, T.M., Ahern, A.M., and Garrrell, R.L., Journal of American Chemical Society, 113 (**1991**) 846.

Hesari, N., Alum, A., Elzein, M. and Abbaszadegan, M., Enzyme and Microbial Technology, 83 (**2016**) 22.

Holland, J.L., Louie, L., Simor, A.E. and Louie, M., Journal of Clinical Microbiology, 38 (**2000**) 4108.

Holler, J.G., Pedersen, L.K., Calum, H., Nielsen, J.B., Tvede, M., Schonning, K. and Knudsen, J.D., Scandinavian Journal of Infectious Diseases, 43 (**2011**) 234.

Horneffer, V., Forsmann, A., Strupat, K., Hillenkamp, F., Kubitscheck, U., Localization of analyte molecules in MALDI preparations by confocal laser scanning microscopy, Analytical Chemistry, 73 (**2001**) 1016.

Housby, J.N. and Mann, N.H., Drug Discovery Today, 14 (**2009**) 536.

Huang, H., He, C., Zeng, H., Xi, X., Yu, X., Yi, P. and Chen, Z., Biosensors and Bioelectronics, 24 (**2009**) 2255.

Hubner, I., Steinmetz, I., Obst, U., Giebel, D. and Bitter-Suermann, D., Applied and Environmental Microbiology, 58 (**1992**) 3187.

Humphrey, S.B., Stanton, T.B., Jensen, N.S. and Zuerner, R.L., Journal of Bacteriology, 179 (**1997**) 323.

Hutchens, T.W. and Yip, T.T., Rapid Communications in Mass Spectrometry, 7 (**1993**) 576.

Ibekwe, A.M., Watt, P.M., Grieve, C.M., Sharma, V.K. and Lyons, S.R., Applied and Environmental Microbiology, 68 (**2002**) 4853.

Ibekwe, A.M. and Grieve, C.M., Journal of Applied Microbiology, 94 (**2003**) 421.

Ilina, E.N., Borovskaya, A.D., Malakhova, M.M., Vereshchagin, V.A., Kubanova, A.A., Kruglov, A.N., Svistunova, T.S., Gazarian, A.O., Maier, T., Kostrzewa, M. and Govorun, V.M., Journal of Molecular Diagnostics, 11 (**2009**) 75.

Ilina, E.N., Borovskaya, A.D., Serebryakova, M.V., Chelysheva, V.V., Momynaliev, K.T., Maier, T., Kostrzewa, M. and Govorun, V.M., Rapid Communications in Mass Spectrometry, 24 (**2010**) 328.

Italia J.T., Rovira, H.G., Masangkay, J.S., Yoshikawa, Y., Perez, M.T.M., Reyes, A.W.B. and Baticados, W.N., Veterinarski Arhiv, 82 (**2012**) 283.

Jackson, C.R., Tyler, H.L. and Millar, J.J., Journal of Visualized Experiments, 80 (**2013**) 1.

Jarvis, R.M. and Goodacre, R., Analytical Chemistry, 76 (**2004**) 40.

Jarvis, R.M., Brooker, A. and Goodacre, R., Analytical Chemistry, 76 (**2004**) 5198.

Joan, J.W.F. and Slonczewski, L., Microbiology: An Evolving Science. Norton eTextbook, **2017**.

Jung, L.S., Campbell, C.T., Chinowsky, T.M., Mar, M.N. and Yee, S.S., Langmuir**,** 14 (**1998**) 5636.

Kanusaki, H., and Tanji, Y., Applied Genetics and Molecular Biotechnology, 85 (**2015**) 1533.

Kaper, J.B., Nataro, J.P. and Mobley, H.L., National Reviews of Microbiology, 2 (**2004**) 123.

Karas, M. and Hillenkamp, F., Analytical Chemistry, 60 (**1988**) 2299.

Khalil, U., Younus, M., Asghar, N., Siddiqui, f., Gomez-Duarte, O.G. and Bokhari, H., APMIS: Journal of Pathology, Microbiology and Immunulogy, 124 (**2016**) 872.

Kikuchi, A., Kawabuchi, M., Watanabe, A., Sugihara, M., Sakurai, Y. and Okano, T., Journal of Controlled Release, 58 (**1999**) 21.

Kim, J.W., Chou, L.Z., Marguardat, S.H., Forhilch, A.A. and Baidoo, S.K. Journal of Science Food Agriculture, 79 (**1999**) 1513.

Kim, T., Han, J-I., Journal of Environmental Management, 130 (**2013**) 267.

Kneipp, K., Kneipp, H., Manoharan, H., Hanlon, E.B., Itzkan, I. and Desari, R.R., Feld, M.S., Physcal Review, 57 (**1998**) 6281.

Koo, J., DePaola, A. and Marshall, D.L., Journal of Food Protection, 63 (**2000**) 1665.

Kotloff, K.L., Nataro, J.P., Blackwelder, W.C., Nasrin, D., Farag, T.H., Panchalingam, S., Wu, Y., Sow, S.O., Lancet, 382 (**2013**) 209.

Krasaekoopt, W., Bhandari, B. and Deeth, H., International Dairy Journal, 14 (**2004**) 737.

Krieg, N.R., in: Bergey's Manual of Systematic Bacteriology, Brenner, D.J., Krieg, N.R. and Staley, J.T., (Eds). 2$^{nd}$ ed. Vol.2, Springer, New York, **2005**.

Kretzer, J.W., Lehmann, R., Schelcher, M., Banz, M., Kim, K.P., Korn, C. and Loessner, M.J., Applied Environmental Microbiology, 73 (**2007**) 1992.

Kutter, E. and Sulakvelidze, A., Bacteriophages: Biology and Applications, CRC Press, **2004**.

Lakshmanan, R.S., Guntupalli, R., Hu, J., Kim, D.J., Petrenko, V.A., Barbaree, J.M. and Chin, B.A., Journal of Microbiological Methods, 71 (**2007a**) 55.

Lakshmanan, R.S., Guntupalli, R., Hu, J., Petrenko, V.A., Barbaree, J.M. and Chin, B.A., Sensors and Actuators B Chemistry, 126 (**2007b**) 544.

Lam, J.S., Mutharia, L.M. Antigen-antibody reactions. In: Methods for General and Molecular Bacteriology, Murray, R.G.E (Ed), American Society of Microbiology. Washington, D.C., **1994**.

Lan, S., Ping, Z., Da-wei, Z., Yang-jun-qi, W., Ru-gang, Z., Optoelectronics Letters, 11 (**2015**) 157.

Lartigue, M.F., Hery-Arnaud, G., Haguenoer, E., Domelier, A.S., Schmit, P.O., van der Mee-Marquet, N., Lanotte, P., Mereghetti, L., Kostrzewa, M. and Quentin, R., Journal of Clinical Microbiology, 47 (**2009**) 2284.

Lewin, M.M., The Journal of Infectious Diseases, 155 (**1987**) 377.

Li, S., Li, Y., Chen, H., Horikawa, S., Shen, W., Simonian, A. and Chin, B.A., Biosensors and Bioelectronics, 26 (**2010**) 1313.

Li, W. and Drake, M.A., Applied and Environmental Microbiology, 67 (**2001**) 3291.

Lindberg, A.A., Wollin, R., Gemski, P. and Wohlhieter, J.A., Journal of Virology, 27 (**1978**) 38.

Liu, T.T., Lin, Y.H., Hung, C.S., Liu, T.J., Chen, Y., Huang, Y.C., Tsai, T.H., Wang, H.H., Wang, D.W., Wang, J.K., Wang, Y.L. andLin, C.H., PLoS One, 4 (**2009**) 5470.

Liu, X.D., Yu, W.Y., Zhang, Y., Xue, W.M., Yu, W.T., Xiong, Y., Ma, X.J., Chen, Y. and Yuan, Q., Journal of Microencapsulation, 19 (**2002**) 775.

Liu, Y., Ai, K. and Lu, L., Chemical Reviews, 114 (**2014**) 5057.

Liz-Marzan, L.M., Langmuir, 22 (**2006**) 32.

Lu, X.M., Rycenga, M., Skrabalak, S.E., Wiley, B. and Xia, Y.N., Annual Review of Physical Chemistry, 60 (**2009**) 167.

Ma, Y., Pacan, J.C., Wang, Q., Xu, Y., Huang, X., Korenevsky, A. and Sabour, P.M., Applied and Environmental Microbiology, 74 (**2008**) 4799.

Ma, Y., Pacan, J.C., Wang, Q., Sabour, P.M., Huang, X. and Xu, Y., Food Hydrocolloids, 26 (**2012**) 434.

Mackenzie, W.R., Hoxie, N.J., Proctor, M.E., Gradus, M.S., Blair, K.A., Peterson, D.E., Addiss, J.J., Fox, K.R., Rose, J.B. and Davis, J.P., New England Journal of Medicine, 331 (**1994**) 161.

Maki, J.S., Benson, J.A., Collins, M.L.P., Letters in Applied Microbiology, 37 (**2003**) 239.

Malinsky, M.D., Kelly, K.L., Schatz, G.C. and Van Duyne, R.P., Journal of the American Chemical Society**,** 123 (**2001**) 1471.

Marshall, A.G., Hendrickson, C.L. and Jackson, G.S., Mass Spectrometry Reviews, 17 (**1998**) 1.

Martin, S.E., Shabanowitz, J., Hunt, D.F. and Marto, J.A., Analytical Chemistry, 72 (**2000**) 4266.

Martin, S.E., Shabanowitz, J., Hunt, D.F., Marto, J.A., Martiny, D., Dediste, A., Debruyne, L., Vlaes, L., Haddou, N.B., Vandamme, P. and Vandenberg, O., Clinical Microbiology Infection, 17 (**2011**) 1001.

Marvin, L.F., Roberts, M.A. and Faya, L.B., Clinica Chimica Acta, 337 (**2003**) 11.

McFarland, A.D. and Van Duyne, R.P., Nano Letters, 3 (**2003**) 1057.

Meisel, S., Stöckel, S., Elschner, M., Melzer, F., Rösch, P. and Popp, J., Applied and Environmental Microbiology, 78 (**2012**) 5575.

Meisel, S., Stöckel, S., Rösch, P. and Popp, J., Food Microbiology, 38 (**2014**) 36.

Merchant, M., and Weinberger, S.R., Electrophoresis, 21 (**2000**) 1164.

Microbiology Society-www.microbiologysociety.org - **2013.**

Moghtader, F., Saluti, M., Türk, M. and Piskin, E., Artificial Cells, Nanomedicine and Biotechnology, 42 (**2014**) 392.

Moghtader, F., Congür, G., Zareie, H., Erdem, A. and Piskin, E., RSC Advances, 7 (**2017**) 97832.

Moghtader, F., Eğri, S. and Piskin, E., Artificial Cells, Nanomedicine and Biotechnology, 45 (**2017**) 357.

Moghtader, F., Tomak, A., Zareie, H. and Piskin, E., Artificial Cells, Nanomedicine and Biotechnology, (**2018**) DOI: 10.1080/21691401.2018.1452251.

Morris, M.C. and Beinstock, R.J., Spectroscopy of Biological Systems. Wiley, New York, **1986.**

Moskovits, M., Reviews of Modern Physics, 57 (**1985)** 783.

Mothershed, E.A. and Whitney, A.M., Clinical Chimica Acta, 363 (**2006**) 206.

Mullis - (https://en.wikipedia.org/wiki/Kary_Mullis, **2018**.

Murata, Y., Toniwa, S., Miyamoto, E. and Kawashima, S., International Journal of Pharmaceutics, 176 (**1999**) 265.

Myres, G.S.A., Rasko, D.A., Cheung, J.K., Ravel, J., Seshadri, R. and DeBoy, R.T., Genomic Research, 16 (**2006**) 1031.

Naidoo, K. and Lindsay, D., Food Control, 21 (**2010**) 1042.

Nagy, E., Becker, S., Soki, J., Urban, E. and Kostrzewa, M., Journal of Medical Microbiology, 60 (**2011**) 1584.

Naja, G., Bouvrette, P., Hrapovic, S. and Luong, J.H.T., Analyst, 132 (**2007**) 679.

Nanduri, V., Sorokulova, I.B., Samoylov, A.M., Simonian, A.L., Petrenko, V.A. and Vodyanoy, V., Biosensors and Bioelectronics, 22 (**2007**) 986.

Napa Valley- www.napavalley.edu - **2016.**

Narita, A., Takahara, M., Ogino, T., Fukushima, S., Kimura, Y. and Tabata, Y., The Knee, 16 (**2009**) 285.

Nataro, J.P., Bopp, C.A., Fields, P.I., Kaper, J.B., Strockbine, N.A., in Manual of Clinical Microbiology, Murray, P.R., Baron, E.J., Landry, M.L., Jorgensen, J.H. and Pfaller, M.A. (Eds.), 9th ed., American Society of Microbiology, Washington, D.C., **2007.**

Nature-www.nature. com - **2016.**

Nikoobakht, B. and El-Sayed, M.A., Chemistry of Materials, 15 (**2003**) 1957.

Nolte, F.S. and Caliendo, A.M., in Manual of Clinical Microbiology, Murray, P.R., Baron, E.J., Landry, M.L., Jorgensen, J.H. and Pfaller, M.A. (Eds.), 9th ed., American Society of Microbiology, Washington, D.C., **2007.**

Nurliyana, M.R., Sahdan, M.Z., Wibowo, K.M., Muslihati, A., Saim, H., Ahmad, S.A., Sari, Y. and Mansor, Z., Journal of Physics-Conference Series, 995 (**2018**) 1.

Olsen, E.V., Sorokulova, I.B., Petrenko, V.A., Chen, I., Barbaree, J.M. and Vodyanoy, V.J., Biosensors and Bioelectronics, 21 (**2006**) 1434.

Olsvik, O. and Strockbine, N.A., In: Diagnostic Molecular Microbiology: Principles and Applications, Persing, D.H., Smith, T.F., Tenover, F.C. and White, T.J (Eds). American Society for Microbiology, Washington, D.C., **1993.**

O'Sullivan, J., Bolton, D.J., Duffy, G., Baylis, C., Tozzoli, R., Wasteson, Y. and Lofdahl, S. Methods for Detection and Molecular Characterisation of Pathogenic *Escherichia coli,* Booklet, Co-ordination Action Project - FOOD-CT-2006-036256, **2006**.

Ozeki, M. and Tabata, Y., Journal of Biomaterials Science, Polymer Edition, 16 (**2005**) 549.

Panda, A., Kurapati, S., Samantaray, J.C., Myneedu, V.P., Verma, A., Srinivasan, A., Indian Journal of Medical Microbiology, 31 (**2013**) 117.

Panda, A., Kurapati, S., Samantaray, J.C., Srinivasan, A. and Khalil, S., Indian Journal of Medical Research, 140 (**2014**) 770.

Patel, Z.S., Yamamoto, M., Ueda, H., Tabata, Y., Biodegradable gelatin microparticles   as delivery systems for the controlled release of bone morphogenetic protein- 2. Acta Biomaterialia, 4 (**2008**) 1126.

Plaque assay - www.virology.ws/2009/07/ detecting-viruses-the-plaque-assay/, **2018**.

Perelle, S., Dilasser, F., Malorny, B., Grout, J., Hoorfar, J. and Fach, P., Molecular Cellular Probes, 18 (**2004**) 409.

Pignone, M., Greth, K.M., Cooper, J., Emerson, D. and Tang, J., Journal of Clinical Microbiology, 44 (**2006**) 1963.

Pyle, B.H., Broadaway, S.C. and McFeters, G.A., Applied Environmental Microbiology, 65 (**1999**) 1966.

Rådström, P., Knutsson, R., Wolffs, P., Dahlenborg, M. and Löfström, C., Methods

in Molecular Biology, 216 (**2003**) 31.

Raman, C.V. and Krishnan, K.S., Nature, 121 (**1928**) 501.

Rodriguez-Lorenzoa, L., Fabrisb, L. and Alvarez-Pueblaa, R.A., Analytica Chimica Acta, 745 (**2012**) 10.

Rosi, N.L. and Mirkin, C.A., Chemical Reviews, 105 (**2005**) 1547.

Rossen, L., Nørskov, P., Holmstrøm, K., and Rasmussen, O. F., International Journal of Food Microbiology, 17 (**1992**) 37.

Riboh, J. C., Haes, A. J., McFarland, A.D., Ranjit Yonzon, C. and Van Duyne, R.P., The Journal of Physical Chemistry B, 107 (**2003**) 1772.

Qadri, F., Svennerholm, A.M., Faruque, A.S. and Sack, R.B., Clinical Microbiology Reviews, 18 (**2005**) 465.

Sakai, T. and Alexandridis, P., The Journal of Physical Chemistry B, 119 (**2005**) 8457.

Sambrook, J. and Russell, D.W., Molecular Cloning: A Laboratory Manual, 2nd ed., Cold Spring Harbor Laboratory Press, New York, **1989**.

Seng, P., Drancourt, M., Gouriet, F., La, S.B., Fournier, P.E., Rolain, J.M. and Raoult, D., Clinical Infectious Diseases, 49 (**2009**) 543.

Sengupta, A., Mary, L.L. and Davis, E.J., Applied Spectroscopy, 59 (**2005**) 1016.

Sengupta, A., Mirna, M. and Davis, E.J., Analytical Bioanlytical Chemistry, 386 (**2006**) 379.

Sepulveda, B., Angelome, P.C., Lechuga, L.M. and Liz-Marzan, L.M., Nano Today, 4 (**2009**) 244.

Serwer, P. and Hayes, S.J., Electrophoresis, 3 (**1982**) 76.

Shabani, M., Zouro, B., Allain, C.A., Marquette, M.F., Lawrence, R. and Mandeville, S. Analytical Chemistry, 80 (**2008**) 9475.

Shen, W., Lakshmanan, R.S., Mathison, L.C., Petrenko, V.A. and Chin, B.A., Sensors and Actuators B, 137 (**2009**) 501.

Shulman, S.T., Friedman, H.C., Sims, R.H., Clinical Infectious Diseases, 45 (**2007**) 1025.

Sil, S., Mukherjeei R., Kumar, N.S., Aravind, S., Kingston, J. and Singh, U.H., Defence Life Journal, 2 (**2017**) 435.

Singh, A., Glass, N., Tolba, M., Brovko, L., Griffiths, M., Evoy, S., Biosensors and Bioelectronics, 24 (**2009**) 3645.

Singh, A., Arutyunov, D., McDermott, M.T., Szymanski, C.M. and Evoy, S., Analyst, 136 (**2011**) 4780.

Singh, A., Arutyunov, D., Szymanski, C.M. and Evoy, S., Analyst, 137 (**2012**) 3405.

Slide Player-http://slideplayer.com/slide/4683531/ - **2016.**

Slide Share-www.slideshare.net - **2016**.

Singh, A., Poshtiban, S. and Evoy, S., Sensors, 13 (**2013**) 1763.

Smith, D.K. and Korgel, B.A., Langmui*r*, 24 (**2008**) 644.

Sneath, P.H.A., in: Bergey's Manual of Systematic Bacteriology, Brenner, D.J., Krieg, N.R. and Staley, J.T., (Eds). 2$^{nd}$ ed. Vol.2, Springer, New York, **2005**.

Soto-Muñoz, L., Teixidó, N., Usall, J., Viñas, I., Crespo-Sempere, A. and Torres, R., International Journal of Food Microbiology, 180 (**2014**) 49.

Spiro, T.G. and Gaber, B.P., Annular Review of Biochemistry, 46 (**1977**) 533.

Srivastava, S.K., Hamo, H.B., Kushmaro, A., Marks, R.S., Grüner, C., Rauschenbache, B. and Abdulhalima, I., Analyst, 140 (**2015**) 3201.

Stiles, P.L., Dieringer, J.A., Shah, N.C. and Van Duyne, R.P., Annual Review of Analytical Chemistry*,* 1 (**2008**) 601.

Stöckel, S., Meisel, S., Elschner, M., Rösch, P. and Popp, J., Angewandte Chemie International Edition, 51 (**2012a**) 5339.

Stöckel, S., Meisel, S., Elschner, M., Rösch, P. and Popp, J., Analytical Chemistry, 84 (**2012b**) 9873.

Straub, T.M., Chandler, D.P., Journal of Microbiological Methods, 53 (**2003**) 185.

Struelens, M.J., Clinical Microbiology Infections, 12 (**2006**) 23.

Study Blue - www.studyblue.com - **2016**.

Sulakvelidze, A. and Kutter, E., in: Bacteriophages: Biology and Application. Kutter, E., Sulakvelidze, A. (Eds), Boca Raton (FL), CRC Press, **2005**.

Summers, W.C., Annual Reviews Microbiology*,* 55 (**2001**) 437**.**

Sun, W., Brovko, L. and Griffiths, M., Journal of Indian Microbiology and Biotechnology, 2 (**2001**) 126.

Sundaram, J., Park, B., Hinton, A., Lawrence, K.C. and Kwon, Y., Food Measurements, 7 (**2013**) 1.

Tabata, Y., Nagano, A. and Ikada, Y., Tissue Engineering, 5 (**1999**) 127.

Tajima, S. and Tabata, Y., Journal of Tissue Engineering and Regenerative Medicine, 10 (**2013**) 801.

Tajima, S. and Tabata, Y., Regenerative Therapy, 6 (**2017**) 90.

Takahashi, Y., Yamamoto, M. and Tabata, Y., Biomaterials, 26 (**2005**) 3587.

Tanaka, K., Waki, H., Ido, Y., Akita, S., Yoshida, Y., Yoshida, T. and Matsuo, T., Rapid Communication Mass Spectrometry*,* 2 (**1988**) 151.

Tawil, N., Sacher, E., Mandeville, R. and Meunier, M., Biosensors and Bioelectronics, 37 (**2012**) 24.

Tolba, M., Minikh, O., Brovko, L.Y., Evoy, S. and Griffiths, M.W., Applied Environmental Microbiology, 76 (**2010**) 528.

Tomak, A. and Zareie, H.M., RSC Advances, 5 (**2015**) 38842.

Twort, F.W., The Lancet, 186 (**1915**) 1241.

Ueda, H., Nakamura, T., Yamamoto, M., Nagata, N., Fukuda, S., Tabata, Y. and Shimizu, Y., Journal of Controlled Release, 88 (**2003**) 55.

US Pharmacopeia Convention. The United States Pharmacopeia, 27th ed. Rockville (MD): United States Pharmacopeia Convention, 2728. **2004**.

Xi, H.Y., Cai, Q., He, M. and Shi, H.C., Detection of *Escherichia coli* in wastewater based on enzyme immunoassay. 26 (**2005**) 128.

Xue, W.M., Yu, W.T., Liu, X.D., He, X., Wang, W. and Ma, X.J., Chemical Journal of Chinese Universities, 25 (**2004**) 1342.

Vo-Dinh, T., Houck, K. and Stokes, D.L., Analytical Chemistry, 66 (**1994**) 3379.

Wang, N., He, M. and Shi, H.C., Analytical Chimica Acta, 590 (**2007**) 224.

Weadock, K.S., Miller, E.J., Keuffel, E.L. and Dunn, M.G., Journal of Biomedical Materials Research, 32 (**1996**) 221.

Weldon, M.K. and Morris, M.D., Applied Spectroscopy, 54 (**2000**) 124.

Wells, J.G., Davis, B.R., Wachsmuth, I.K., Riley, L.W., Remis, R.S., Sokolow, R., Morris, G.K., Journal of Clinical Microbiology, 18 (**1983**) 512.

WHO. World Health Organization. The evolving threat of antimicrobial resistance. Options for action. World Health Organization, Geneva, Switzerland, **2012**.

WHO. Bulletin of the World Health Organization, 95 (**2017**) 233.

Wildeboer, D., Amirat, L., Price, R.G. and Abuknesha, R.A., Water Research, 44 (**2010**) 2621.

Willets, K.A. and Van Duyne, R.P., Annual Review of Physical Chemistry, 58 (**2007**) 26.

Winter, P.C., Polymerase chain reaction (PCR). Encylopedia of Life Sciences, John Wiley and Sons, Ltd., **2007**.

World Press - Bacteriophageacd. worldpress. com - **2016**a.

World Press - Bioinfo2010.worldpress.com -**2016b**.

Yolken, R.H., Greenberg, H.B., Merson, M.H., Sack, R.B. and Kapikian, A.Z., Journal of Clinical Microbiology, 6 (**1997**) 439.

Yonzon, C.R., Jeoung, E., Zou, S., Schatz, G.C., Mrksich, M. and Van Duyne, R.P., Journal of the American Chemical Society, 126 (**2004**) 12669.

Zeiri, L., Bronk, B.V., Shabtai, Y., Eichler, J. and Efrima, S., Applied Spectroscopy, 58 (**2004**) 33.

Zeiri, L. and Efrima, S., Journal of Raman Spectroscopy, 36 (**2005**) 667.

Zourob, M., Elwary, S. and Turner, A., Principles of Bacterial Detection:

# CIRRICULUM VITAE

**Credential**

Name, Surname : Farzaneh Moghtader

Place of Birth : Maragheh, Iran

Maritial Status : Bachelor

E-mail : farzaneh_moghtader@yahoo.com

Address (home in Iran) : Rajaii Shahr, Phaz 2, Khyabane Rastakhiz,
No:9/1, +989354786179, Karaj, İran,3146916551

Address (work in Turkey) : NanoBMT, Cyberpark, Bilkent, Ankara, Turkey

**Education**

BSc : Zanjan Branch,Islamic Azad University,
Faculty of Basic Medical Sciences,
Microbiology Department, Zanjan,Iran, *June 2008*

MSc : Hacettepe University, Graduate School of Science
and Engineering, Nanotechnology and Nanomedicine
Division (Program), *September 2012*

PhD : Hacettepe University, Graduate School of Science
and Engineering, Nanotechnology and Nanomedicine
Division (Program), *February 2019*

MSc (second) : İstinye University, Institute of Health Sciences, Stem
Cells and Tissue Engineering Program, *started
February 2018 –*

**Languages** : Azerbaijani (Excellent); Turkish (Excellent);
Persian (Excellent); English (good); Arabic (good)

**Work Experience**

: Nikoo group, Texitiles and textile based products
producer, Bolvera Mirdamad, No:139, Tehran, Iran
as the Quality Control Manager and R&D personal
to develop "Nonwoven antibacterial textiles",
*November 2008-December 2009*

: Azerbaijan Embassy, Tehran, as a translator
(about one year)

: NanoBMT: Nanobiyomedtek Biyomedikal ve
Biyoteknoloji San.Tic. Ltd.Şti., Cyberpark, Bilkent,
Ankara, Turkey, as the R&D Manager
*August 2014 - continue*

: University of Kansas, Mechanical Engineering and
Bioengineering, Lawrence, USA

as Visiting Scientist
November 2016 - April 2017

: University of Kyoto, Institute of Frontier Life and
Medical Sciences, Department of Regeneration
Science and Engineering, Laboratory of Biomaterials,
Kyoto, Japan as Visiting Scientist
September 2018 - December 2018

**Areas of Experiences**

: Microbiology; Bacteriophages; Biofilms; Nanoparticles;
Antibacterial Textiles/Materials; Detection of Bacteria;
EIS, SERS, LSPR, MALDI-TOF-MS techniques;
Phage therapy: Phage immobilization and release;
Stem cells/Spheroids and Tissue Engineering

**Projects**

1. A Turkish Scientific and Technological Council Project (TÜBİTAK 1001 -
a two years Project). Entitled: "Polymeric dental implants reinforced with
titanium nanofibers", Atılım University-Hacettepe University, Coordinators:
Dr.J. Park - Prof.E. Pişkin; **Farzaneh Moghtader** was a fulltime research
assistant about nine months from January to September 2012 (completed).

2. An European Commission, FP7- IAPP Project (from November 2011 to
Novermber 2015 - a four years Project). Entitled "NanobacterphageSERS:
Design of novel portable-sensors based on suspension arrays composed of
monoclonal antibody, aptamer and bacteriophage carrying magnetically
loaded nanoparticles and surface enhanced raman spectroscopy",
Hacettepe University-Eliava Institute/Georgia University of Brighton/UK-
Aptares/Germany-University of Bilkent/Turkey - Gate Elektronik/Turkey-
Biyomedtek/Turkey; Coordinator: Prof.E.Pişkin; **Farzaneh Moghtader** was a
partime researcher and a full time Secondee at Eliava Institute,
Tbilisi/Georgia for *about 5 months* (completed).

3. A Turkish Scientific and Technological Council Project (Tübitak 1003 - from
April 2014 to October 2016 - a 30 months Project). Entitled: "Biobased/
Biodegradable films and smart labels carrying bacteriophages and
nanoparticles for food packaging" Coordinator: Prof. E.Pişkin; NanoBMT
was responsible of design and prototype production of several materials and
devices acting as like sub-constructor in five work packages - **Farzaneh
Moghtader** was performing/acting as a fulltime researcher and the R&D
manager of NanoBMT (completed).

4. A KOSGEB (Başkent -Tekmer) supported project run by NanoBMT (from
Nov 2016 to Nov 2018 - a two years project: "Design and prototype
production of portable systems/devices for continuous monitoring of
bacterial contamination in air" - Coordinator: Prof. E. Pişkin; **Farzaneh
Moghtader** is performing/acting as a fulltime researcher and the R&D
manager of NanoBMT (continue). Approximate Budget: 400 000 Turkish
Liras.

5. A Turkish Scientific and Technological Council Project (Tübitak 1511) -
entitled: "Monitoring of Airborne bacterial contaminations in food processing
and development of early detection system; Coordinator: Prof. E. Pişkin;

**Farzaneh Moghtader** will be co-director and performing/acting as a fulltime researcher and the R&D manager of NanoBMT. Approximate Budget: 1.3 Million Turkish Liras (started in January 2018). A 3-year project.

**Projects submitted/under-evaluation:**

6. A Turkish Scientific and Technological Council Project (Tübitak 1511) - entitled: "Development of new nanotechnology based materials for solar cells in use or new generation". The Project will be run by NanoBMT and Safa Tarım A.Ş. (Konya, Turkey) will be the other main partner. Coordinator: Prof. E.Pişkin; **Farzaneh Moghtader** will be performing/acting as a fulltime researcher and the R&D manager of NanoBMT. Approximate Budget: 3 Million Turkish Liras (submitted in August 2016).

7. A Turkish Scientific and Technological Council Project (Tübitak 1511) - entitled: "Development of smart/active packaging materials and Technologies for food packaging". The Project will be run by Safa Tarım A.Ş. (Konya, Turkey) and NanoBMT will be the other main partner. **Farzaneh Moghtader** will be performing/acting as a fulltime researcher and the R&D manager of NanoBMT (submitted). Approximate Budget: 1.5 Million Turkish Liras (submitted in August 2016).

8. A Turkish Scientific and Technological Council Project (Tübitak 1003) - entitled: "Processing of CASEIN and the production of protective packaging materials" - passed the first step; the whole project was prepared for the second step, and recently submitted (24 May 2017). There are two subprojects. The First is about isolation of casein micelles from skim milk by membrane separation coordinated by Yeditepe University (coordinator: Prof.F. Yeşim Ekinci-Kadıpaşaoğlu).The second is related to loading of the casein micelles with active agents and preparation of electrospun matrices that will be used as protective functional labels for fresh food products in plastic packaging. It will be coordinated by NanoBMT (coordinator: **Farzaneh Moghtader** as the R&D manager of NanoBMT). Approximate Budget: 1.9 Million Turkish Liras.

9. A Turkish Scientific and Technological Council Project (Tübitak 1003) Entitled: "Production of NANOCELLULOSE composites with PLLA and their application in food packaging" - passed the first step. The whole project was prepared for the second step, and recently submitted (24 May 2017). There are three subprojects. The first is about isolation of NANOCELLULOSE micelles from wood pulps - coordinated by NanoBMT (coordinator: Prof. Erhan Bişkin). Prof.Bişkin is the coordinator of the whole project and **Farzaneh Moghtader** will be responsible from this subproject. The second is related to packaging film production from PLLA/Nanocomposites. It will be coordinated by Gaziosmanpaşa University (coordinator: Yrd.Prof.Dr. Sinan Eğri. The third is related to LLA relasing PLLA functional labels. Hacettepe University will coordinate this subproject (coordinator: Prof.H.Yavuz Ersan). Approximate Budget: 2.3 Million Turkish Liras.

10. The COST Action Proposal OC-2016-2-21405 " Vacuum Science and Technology for the Advancement of Life Sciences" to the COST Open Call OC-2016-2. M.: Silvan is the coordinator. NanoBMT will be one of the main partners. **Farzaneh Moghtader** will be performing/acting as a

researcher and the R&D manager of NanoBMT Approximate Budget: 200 000 Euro (submitted in December 2016).

11. A Turkish Scientific and Technological Council Project (Tübitak 1003) Entitled: "Development of nanobiomaterials using stem cells/bacterio-phages/antibiotics and application protocols for combined therapy of bacterial infections in skin wounds and tissue regeneration" - passed the first step. The whole project was prepared for the second step, and recently submitted (November 2018). Coordinated by NanoBMT (coordinator: Prof. Erhan Bişkin). Prof.Bişkin is the coordinator of the whole project and **Farzaneh Moghtader** will be co-coordinator. Approximate Budget: 1 Million Turkish Liras.

# 1 Publications

1. **Farzaneh Moghtader,** Mojtaba Saluti, Mustafa Türk, Erhan Piskin, Nanoemulsions and nonwoven fabrics carrying AgNPs: antibacterıal but may be cytotoxic, *Artificial Cells, Nanomedicine and Biotechnology,* 42: 392-399, **2014**.

2. **Farzaneh Moghtader,** Gülşah Congür, Arzum Erdem, Erhan Pişkin, Impedimetric detection of pathogenic bacteria with bacteriophages using gold nanorod deposited graphite electrodes, *RSC Advances*, 6,:97832-97832, **2016**.

3. **Farzaneh Moghtader,** Sinan Eğri, Erhan Piskin, Phages in modified alginate beads, *Artificial Cells, Nanomedicine and Biotechnology,* 45: 357-363, **2017**. http://dx.doi.org/ 10.3109/21691401.2016.1153485

4. **Farzaneh Moghtader,** Aysel Tomak, Hadi Zareie, Erhan Pişkin, Bacterial detection using bacteriophages and gold nanorods by following time-dependent changes in Raman spectral signals, *Artificial Cells, Nanomedicine and Biotechnology,* 2018. DOI: 10.1080/21691401.2018.1452251

5. **Farzaneh Moghtader,** Erhan Pişkin, Bacterial detection of using MALDI-TOF MS by following amplification of bacteriophages, *Rapid Communications in Mass Spectroscopy,* 2018 (in preparation).

6. **Farzaneh Moghtader,** Aytaç Gül, Hadi Zareie, Erhan Pişkin, Detection of pathogenic bacteria with bacteriophages and nanoparticles by LSPR, 2018 (in preparation).

7. Ayça Bal Öztürk, Meltem-Avcı Adalı, **Farzaneh Moghtader,** Fatameh Sharifi, Berivan Çeçen, Gökçen Yaşayan, Emine Alarçın, Current strategies and future persepectives of skin-on-chip platforms: Innovations, technical chalanges and commercial outlook, Current Pharmaceutical Design, 2019 (in press)

**Meetings and Courses Attended**

1. State hospital - Medical microbiology labs (three months in 2003, Karaj, Iran)

2. The Standards Institute of Iran: Quality control - about one week in 2007, Karaj, Iran.

3. Zakir M.O. Rzayev, **Farzaneh Moghtader,** Sevda İsmailova, Kouroush Salimi, Erhan Pişkin, "Polymer-organoclay nanohybrids carrying silver ions: Synthesis and antibacterial properties", Internation Conference on nanostructured polymers and nanocomposites, 24-27 April 2012, Prague, Check Republic.

4. **Farzaneh Moghtader,** Mustafa Türk, Mojtaba Saluti, Erhan Piskin, "Nonwoven dressings carrying silver nanoparticles", 8th Nanoscience and Nanotechnology Congress, 25-29 June 2012, Ankara, Turkey.

5. Araz N.Dizaji, Ayfer Çalış, Erhan Piskin, **Farzaneh Moghtader,** Mustafa Türk, "Properties of silver nanoparticles produced by using rhodopseudomunas palustris", 8th Nanoscience and Nanotechnology Congress, 25-29 June 2012, Ankara, Turkey.

6. Zakir M.O. Rzayev, **Farzaneh Moghtader,** Sevda İsmailova, Kouroush Salimi, Erhan Pişkin, "Polymer-organoclay nanohybrids carrying silver ions: Synthesis and antibacterial properties", IBNC2012: Iran-Belarus International Conference on Modern Nanotechnology, 27-29 June 2012, Minsk, Belarus.

7. **Farzaneh Moghtader,** Mustafa Türk, Mojtaba Salouti, Erhan Piskin, "Nonwoven dressings carrying silver nanoparticles", IBNC2012: Iran-Belarus International Conference on Modern Nanotechnology, 27-29 June 2012, Minsk, Belarus.

8. **Farzaneh Moghtader,** Mustafa Türk, Mojtaba Salouti, Erhan Piskin, "Antibacterial properties and cytotoxicity of nonwoven dressings loaded with silver nanoparicles". Colloids and Nanomedicine 2012, 15-17 July 2012, Amsterdam, The Netherlands.

9. Filiz Sayar, **Farzaneh Moghtader,** Erhan Piskin "Gold nanoprobes carrying single ssODNs for detection of target ssODNs of MTB and GOR in nanoemulsions". Colloids and Nanomedicine 2012, 15-17 July 2012, Amsterdam, The Netherlands.

10. **Farzaneh Moghtader,** Mustafa Türk, Mojtaba Salouti, Erhan Piskin, Biomed 2012, 8-10-September 2012, Tokat, Turkey.

11. **Farzaneh Moghtader,** as an invited competetor with the Project "Silver containing nanowoven textiles", V. International R&D Project Market- UTIB Turkish Textile and Confection Sector, 4-5 April 2013, Merinos, Bursa.

12. **Farzaneh Moghtader,** Nina Chanishvilli, Erhan Piskin, "Viruses/phages: ready to enter/devour", EuroBIOMAT 2013: European Symposium on Biomaterials and Related Area, 23-24 April, 2013, Weimar, Germany.

13. **Farzaneh Moghtader,** as a "Local Organizing Committee Member", TERMIS-EU: "Tissue Engineering and Regenerative Medicine European Chapter Meeting, 17-20 June 2013, İstanbul, Turkey

14. **Farzaneh Moghtader,** Nina Chanishvilli, Erhan Piskin, "AgNPs and materials carrying them: antibacterial but may be cytotoxic", E-MRS Fall 2013: European Materials Research Society, 16-20 September 2013, Warsaw, Poland.

15. **Farzaneh Moghtader,** Nina Chanishvilli, Erhan Piskin, Alginate beads carrying T4 bacteriophages, VI. International Bioengineering Congress, 12-15 November 2013, Kuşadası, Turkey.

16. **Farzaneh Moghtader,** as an invited young investigator with the Project "Silver containing nanowoven textiles", V. International R&D Project Market- UTIB Turkish Textile and Confection Sector, 4-5 April 2013, Merinos, Bursa.

17. **Farzaneh Moghtader,** "Electrospinning of polymers" - practical laboratory work at University of Beira Interior, 24 January-1 February 2014, Covilha, Portugal.

18. **Farzaneh Moghtader,** as participant "Winter School: Recombinant protein synthesis and purification", Gaziosmanpaşa University, Bioengineering Department, 3-8 February 2014, Tokat, Turkey.

19. **Farzaneh Moghtader,** with Young Investigator Award, 3rd Minicircle and DNA Vector Conference, 8-9 May 2014, Bielefeld, Germany.

20. Erhan Piskin and **Farzaneh Moghtader**, "Design and use of nonviral vectors for gene and antisense delivery", 3rd Minicircle and DNA Vector Conference, 8-9 May 2014, Bielefeld, Germany.

21. **Farzaneh Moghtader,** Nina Chanishvilli, Erhan Piskin, "Viruses/phages: ready to enter/devour", EuroBIOMAT 2013: European Symposium on Biomaterials and Related Area, 23-24 April 2014, Weimar, Germany.

22. Erhan Piskin, **Farzaneh Moghtader,** Barbaros Çetin, Gökhan Demirel, "Bacteriophages: Propagation, purification and use in target bacteria detection on a lab-on-a-chip device", BIOSENSORS 2014: 24th World Congress on Biosensors, 27-30 Mayıs 2014, Melbourne, Australia.

23. **Farzaneh Moghtader,** Gülşah Congür, Arzum Erdem, Erhan Piskin, "Electrochemical detection of pathogenic bacteria using bacteriophages at a single-use graphite electrodes modified with gold nanorods", BIOSENSORS 2014: 24th World Congress on Biosensors, 27-30 Mayıs 2014, Melbourne, Australia.

24. **Farzaneh Moghtader,** Öner Okan Ekiz, Erhan Piskin, "Surface enchanced plasmon resonance detection of pathogenic bacteria using bacteriophages on nanostructured platforms", BIOSENSORS 2014: 24th World Congress on Biosensors, 27-30 Mayıs 2014, Melbourne, Australia.

25. **Farzaneh Moghtader**, Gülşah Congur, Arzum Erdem, Erhan Piskin,, "Electrochemical detection of pathogenic bacteria using bacteriophages at a single-use graphite electrodes modified with gold nanorods", BIOMED 2014: 20th International Biomedical Science and Technology Symposium; NanoBioTech 2014: 1th International NanoBioTechnology Symposium; International workshop on Detection of Pathogenic Microorganisms: Probes, Platforms and Detectors, 24-30 August 2014, Köyceğiz, Muğla, Turkey.

26. **Farzaneh Moghtader,** Gülşah Congür, Arzum Erdem, Erhan Piskin, "Detection of pathogeniz bacteria with Electrochemical Impedance Spectroscopy (EIS) using bacteriophages at a single-use graphite electrodes modified with gold nanorods", 3. EuroBioMAT 2015: European Symposium and Exhibition on Biomaterials and Related Areas", 21-22 May 2015, Weimar, Germany

27. **Farzaneh Moghtader** and Erhan Piskin, "Detection of pathogenic bacteria by EIS", NOMAD Symposium, 19 May 2015, Xi'an, China.

28. Arzum Erdem, Erhan Piskin, Filiz Sayar, Gülşah Congür, **Farzaneh Moghtader,** "Gold nanorods modified electrochemical biosensors", NANOMED 2015: 4th Nanomedicine World Congress; NANOBIOTECH 2015: 2nd International NanoBioTechnology Symposium Focusing on Nanomedicine", 8-12 September 2015, Köycegiz, Muğla, Turkey.

29. Frederico Nogueira, Luiza Granadeiro, Claudia Mouro, **Farzaneh Moghtader,** Erhan Piskin, Isabel Gouveia, "Comparison of two strategies to obtain antimicrobial and antioxidant properties onto silk-fibroin (Sf)-L-Cystein conjugates for skin disease management", NANOMED 2015: 4th Nanomedicine World Congress; NANOBIOTECH 2015: 2nd International NanoBioTechnology Symposium Focusing on Nanomedicine", 8-12 September 2015, Köycegiz, Muğla, Turkey.

30. **Farzaneh Moghtader,** Hadi M. Zareie, Mustafa Türk, Erhan Piskin, "Immobilization of AgNPs on cotton nonwoven matrices for antibacterial activity", NANOMED 2015: 4th Nanomedicine World Congress; NANOBIOTECH 2015: 2nd International NanoBioTechnology Symposium Focusing on Nanomedicine", 8-12 September 2015, Köycegiz, Muğla, Turkey.

31. Aliakbar Ebrahimi, '**Farzaneh Moghtader,** F. Yeşim Ekinci, Erhan Piskin, "Electrospun matrices made of polycaprolactone and oligocaprolactone grafted chitosan blends carrying bacteriophages as antibacterial materials", International Symposium on Advanced Polymeric Materials (ISAPM 2016), 16-19 May 2016, Kuala Lumpur, Malaysia

32. **Farzaneh Moghtader, "**Antibacterial nonwoven/electrospun matrices carrying silver nanoparticles and bacteriophages", 3rd iPROMEDAI S&T Schedule: Antimicrobial Material & Surface, Greece, 9-12 October, 2016, Kuşadası, Turkey & Samos.

33. **Farzaneh Moghtader,** Special/invited scientific visit - Prof. G. Marletta, Catania University, 15-24 January 2017, Catania, Italy.

34. **Farzaneh Moghtader**, iPROMEDAI - MC and S&T meeting, 18-20 April 2017, Malta.

35. **Farzaneh Moghtader,** Aliakbar Ebrahimi, Tülin Kutsal, F.Yeşim Ekinci, O. Erdem Haberal, Erhan Pişkin, "Electrospun matrices made of polycapro-lactone and oligocaprolactone grafted chitosan blends carrying bacteriophages as antibacterial materials", Fifth International Conference on Natural Polymers, Bio-Polymers, Bio-Materials, their Composites, Nanocomposites, Blends, IPNs, Polyelectrolytes and Gels: Macro to Nano Scales (ICNP 2017 Rio), 7-9 June 2017, Rio de Janeiro, Brazil.

36. **Farzaneh Moghtader,** Sinan Eğri, Erhan Pişkin, "Polyelectrolyte gels as carriers for phages in GIT for sustained delivery", Fifth International Conference on Natural Polymers, Bio-Polymers, Bio- Materials, their

Composites, Nanocomposites, Blends, IPNs, Polyelectrolytes and Gels: Macro to Nano Scales (ICNP 2017 Rio), 7-9 June 2017, Rio de Janeiro, Brazil.

37. Erhan Piskin, **Farzaneh Moghtader,** O. Erdem Haberal, "Bacteriophages with or without plasmonic nanoparticles are potential active agents for diagnosis and therapy of bacterial infections/contaminations", 14th International Conference on Nanoscience & Nanotechnologies, 4-7 July 2017, Thessaloniki, Greece (invited talk).

38. **Farzaneh Moghtader**, Aysel Tomak, Hadi M. Zareie, Erhan Piskin, "Bacterial detection using gold nanorods with or without bacteriophages by SERS", ESB 2017, 4-8 September 2017, Athens, Greece (poster presentation-accepted)

39. **Farzaneh Moghtader,** O.Erdem Haberal, Aysel Tomak, Hadi M. Zareie, Erhan Piskin, "Bacterial detection by SERS using nanoparticles and bacteriophages", V ISNS Nanomedicine World Congress, 13-15 November 2017, Montreal, Canada.

40. **Farzaneh Moghtader,** "Using bacteriophages for therapy of bacterial infections and detection of bacteria with bavteriophages and gold-nanorods, 10 May 2018, Invited Lecture, Catania University Catania, Italy

41. **Farzaneh Moghtader,** Orhan Erdem Haberal, Erhan Piskin, Detection of bacteria in air by using an air sampler carrying phages and gold nanoparticles by raman probe, 5thWorld Congress on Targeting Infectious Diseases-Targeting Phage and Antibiotic Resistance – Phage Therapy and Innovative Ideas, 17-18 May, 2018, Florence, Italy.

42. **Farzaneh Moghtader,** Sinan Eğri, Erhan Piskin, Safe and active - sustained release of phages in GIT, 5thWorld Congress on Targeting Infectious Diseases -Targeting Phage and Antibiotic Resistance – Phage Therapy and Innovative Ideas, 17-18 May, 2018, Florence, Italy.

43. **Farzaneh Moghtader,** Ahmad Salmanogli, M.Hadi Zareie, Erhan Piskin, Detection of bacteria by SERS using phages and gold nanorods: Experimental and theoretical analysis, BIOSENSORS 2018, 28th Anniversary World Congress on Biosensors, June 12-15, 2018, Miami, USA

44. Ahmad Salmanogli, **Farzaneh Moghtader,** Erhan Piskin, Plasmonic nanosensor for image resolution enhancing, BIOSENSORS 2018, 28th Anniversary World Congress on Biosensors, June 12-15, 2018, Miami, USA

45. **Farzaneh Moghtader**, Hakan Darici, Aliakbar Ebrahimi, Erdal Karaöz, Erhan Piskin, Spheroid formation and culture on electrospun matrices, TERMIS 2018, 5th World Congress of Tissue Engineering and Regenerative Medicine – International Society, September 4-7, 2018, Kyoto, Japan

46. Erhan Piskin, **Farzaneh Moghtader**, O. Erdem Haberal, Ahmad Salmanogli, Raman spectral analysis and imaging of biological cells and

tissue, TERMIS 2018, 5th World Congress of Tissue Engineering and Regenerative Medicine – International Society, September 4-7, 2018, Kyoto, Japan

47. **Farzaneh Moghtader**, Erhan Piskin, Yasuhiko Tabata, Bacteriophages and MSCs aggregates in/on alginate-gelatin microgels. ISNSCON 2018: 6th World Congress on Nanomedical Sciences, January 7-10, 2019, Delhi, India.

48. Erhan Piskin, **Farzaneh Moghtader**, Yasuhiko Tabata, Treatment strategies for infected wounds: Bacteriophages and/or stem cells. ISNSCON 2018: 6th World Congress on Nanomedical Sciences, January 7-10, 2019, Delhi, India.

# HACETTEPE ÜNİVERSİTESİ
## FEN BİLİMLERİ ENSTİTÜSÜ
### YÜKSEK LİSANS/DOKTORA TEZ ÇALIŞMASI ORJİNALLİK RAPORU

HACETTEPE ÜNİVERSİTESİ
FEN BİLİMLER ENSTİTÜSÜ
BİYOMÜHENDİSLİK ANABİLİM DALI BAŞKANLIĞI'NA

Tarih: 04/02/2019

Tez Başlığı / Konusu: SERS İle Bakteri Tanısında NanoBiyo-Yaklaşımlar

Yukarıda başlığı/konusu gösterilen tez çalışmamın a) Kapak sayfası, b) Giriş, c) Ana bölümler d) Sonuç kısımlarından oluşan toplam 135 sayfalık kısmına ilişkin, 04/02/2019 tarihinde tez danışmanım tarafından *Turnitin* adlı intihal tespit programından aşağıda belirtilen filtrelemeler uygulanarak alınmış olan orijinallik raporuna göre, tezimin benzerlik oranı % 10'dur.

Uygulanan filtrelemeler:
1- Kaynakça hariç
2- Alıntılar hariç
3- 5 kelimeden daha az örtüşme içeren metin kısımları hariç

Hacettepe Üniversitesi Fen Bilimleri Enstitüsü Tez Çalışması Orjinallik Raporu Alınması ve Kullanılması Uygulama Esasları'nı inceledim ve bu Uygulama Esasları'nda belirtilen azami benzerlik oranlarına göre tez çalışmamın herhangi bir intihal içermediğini; aksinin tespit edileceği muhtemel durumda doğabilecek her türlü hukuki sorumluluğu kabul ettiğimi ve yukarıda vermiş olduğum bilgilerin doğru olduğunu beyan ederim.

Gereğini saygılarımla arz ederim.

04/02/2019

| | |
|---|---|
| **Adı Soyadı:** | Farzaneh Moghtader |
| **Öğrenci No:** | N12141848 |
| **Anabilim Dalı:** | Nanoteknoloji ve Nanotıp |
| **Programı:** | Doktora |
| **Statüsü:** | ☐ Y.Lisans  ☒ Doktora  ☐ Bütünleşik Dr. |

**DANIŞMAN ONAYI**

UYGUNDUR

Prof. Dr. Erhan Bişkin

# HACETTEPE UNIVERSITY
## GRADUATE SCHOOL OF SCIENCE AND ENGINEERING
## THESIS/DISSERTATION ORIGINALITY REPORT

**HACETTEPE UNIVERSITY**
**GRADUATE SCHOOL OF SCIENCE AND ENGINEERING**
**TO THE DIVISION OF BIOENGINEERING**

Date: 04/02/2019

Thesis Title / Topic: NanoBio-Approaches for Detection of Bacterias by SERS

According to the originality report obtained by myself/my thesis advisor by using the *Turnitin* plagiarism detection software and by applying the filtering options stated below on 04/02/2019 for the total of 135 pages including the a) Title Page, b) Introduction, c) Main Chapters, d) Conclusion sections of my thesis entitled as above, the similarity index of my thesis is 10%.

Filtering options applied:
1. Bibliography/Works Cited excluded
2. Quotes excluded
3. Match size up to 5 words excluded

I declare that I have carefully read Hacettepe University Graduate School of Sciene and Engineering Guidelines for Obtaining and Using Thesis Originality Reports; that according to the maximum similarity index values specified in the Guidelines, my thesis does not include any form of plagiarism; that in any future detection of possible infringement of the regulations I accept all legal responsibility; and that all the information I have provided is correct to the best of my knowledge.

I respectfully submit this for approval.

04/02/2019

| | |
|---|---|
| **Name Surname:** | Farzaneh Moghtader |
| **Student No:** | N12141848 |
| **Department:** | Nanotechnology and Nanomedicine |
| **Program:** | Doctorate |
| **Status:** | ☐ Masters  ☒ Ph.D.  ☐ Integrated Ph.D. |

## ADVISOR APPROVAL

APPROVED

Prof. Dr. Erhan Bişkin